University of Pavia

Department of Earth and Environmental Sciences

UNIVERSITÀ
DI PAVIA

PhD Program in Earth and Environmental Sciences

(XXXIII cycle)

Integrative assessment of Badland erosion dynamics in the Oltrepo area

Supervisor: Prof. Michael Maerker

PhD: Alberto Bosino

Student I.D.: 460630

"…La campagna che mi pareva di aver visto arrivando, non si vedeva più; e da ogni parte non c'erano che precipizi di argilla bianca, su cui le case stavano come librate nell'aria; e d'ognintorno altra argilla bianca, senz'alberi e senz'erba, scavata dalle acque in buche, coni, piagge di aspetto maligno, come un paesaggio lunare…"

Carlo Levi - 'Cristo si è fermato a Eboli'

Index

-Abstract 7

-Introduction 10

-CHAPTER I: "Study Area" (Paper I) 18

Abstract

Introduction

Geological setting

Geology of the study area

Tectonic features of the study area

Methods

Results

Conclusion

Acknowledgment

References

-CHAPTER II: "I calanchi" (Paper II) 42

Abstract

Introduction

Study area

Methods

Results and discussion

Conclusion

Acknowledgment

References

-CHAPTER III: "Geostatistics" (Paper III) 76

Abstract

Introduction

Study area

Material and Methods

Results

Discussion

Conclusion

Acknowledgment

References

-CHAPTER IV: "Field measurements" (Paper IV) 123

Abstract

Introduction

Material and Methods

Results

Discussion

Conclusion

Acknowledgment

References

-Summary of results and discussion 159

-Conclusion and future research needs 166

-References 170

-Appendix 181

-Acknowledgement 184

ABSTRACT

The present work is the result of three years of investigations on soil erosion forms and features in the Oltrepo Pavese, Northern Apennines, Italy. The aim of the work is to review from a modern and scientific point of view the badlands which crop out in the study area as well as to improve methodologies to study the sediment dynamics in badland areas. Badlands are the result of a complex interaction between sub-surface and surface runoff soil erosion processes and are a hotspot for biodiversity and geodiversity. In addition, badlands have always been a fundamental environment for soil erosion investigations.

This work is based on the following four principal steps: i) the geological and structural characterisation of the study area, ii) the description of badland forms and features, iii) a probabilistic approach to determine soil erosion susceptible areas in the Oltrepo Pavese and iv) the assessment of suspended sediment dynamics at catchment scale. This study highlights a complex geological and structural sector of the Northern Apennines characterised by soft sedimentary bedrock materials that are prone to be eroded by running water. Initially, a litho-structural map was assembled, and the geological formations of the study area were grouped according to their lithology. The map represents a homogeneous base of information to classify from lithological point of view the badlands of the study area and will become a raster-base for spatial multilayer analysis. Subsequently, a geological, geomorphological and morphometrical classification of the badlands which crop out in the study area was performed though field survey and detailed terrain analysis based on Digital Terrain Models (DTM). The Oltrepo Pavese badlands were classified in type A and B according to their morphology and vegetation conditions. The badlands show high heterogeneity and can be closely related with melange bedrock, claystone and interstratified rocks. Furthermore, the badlands show the typical characteristics of Apennine badlands even if certain morphological differences were noted. This study also highlights the importance of the rainfall characteristics and land use changes playing

an important role in the development and stabilisation of the badland forms and features. The land use change induced by planting operations (afforestation) and the reduction of agricultural activities in the area, as well as the reduction of the precipitation amount leads to a shrinking of badlands. Though a detailed terrain analysis and the application of the Maximum Entropy model (MaxEnt) three susceptibility maps were generated for the badland and rill-interrill erosion forms. The predictor analysis has highlighted that the more important predictors (i.e. lithology, land use, elevation) can significantly explain the diversity between calanchi type A and B. However, less significant predictors e.g. Vertical Distance to Channel Network, Valley Depth and Catchment Area are fundamental to understand the development of the two morphotypes. Finally, the study reveals for the first time, the dynamics between precipitation, discharge and suspended sediment transport in a small watershed basin sited in the Northern Apennines. A laser diffraction instrument was installed at the outlet of a small watershed basin deeply interested by aquatic erosion and the sediment diameter and concentration was evaluated with respect to rainfall. The initial moisture condition, hydrophobicity, vegetation cover, and physical conditions of the basin play a fundamental role in the assessment of sediment dynamics. Finally, the study reveals the importance of a correct land management to reduce badland erosion in the Apennine region.

INTRODUCTION

Soil erosion was widely studied in the last two centuries in the Mediterranean region. Especially in Italy a large scientific background is the result of years of investigations on the dominant soil erosion landforms such as rill-interrill erosion, gullies, tunnelling, badlands, and shallow landslides.

This thesis focuses on soil erosion forms and features present in the Oltrepo Pavese study area, which is sited in the Northern Apennines (Italy) (Figure 1). Especially shallow landslides are the source of severe geo-engineering problems in the area causing severe damage to roads and buildings. The landslides expose the bedrock, favouring runoff processes and triggering laminar and concentrated water erosion. While shallow landslides were broadly studied in the Oltrepo Pavese (e.g. Meisina et al., 2013; Zizioli et al., 2013; Bordoni et al., 2018), the surface- and subsurface runoff related forms and features after the first studies of Bucciante (1922) in the 1920s have never been considered under a modern and scientific point of view.

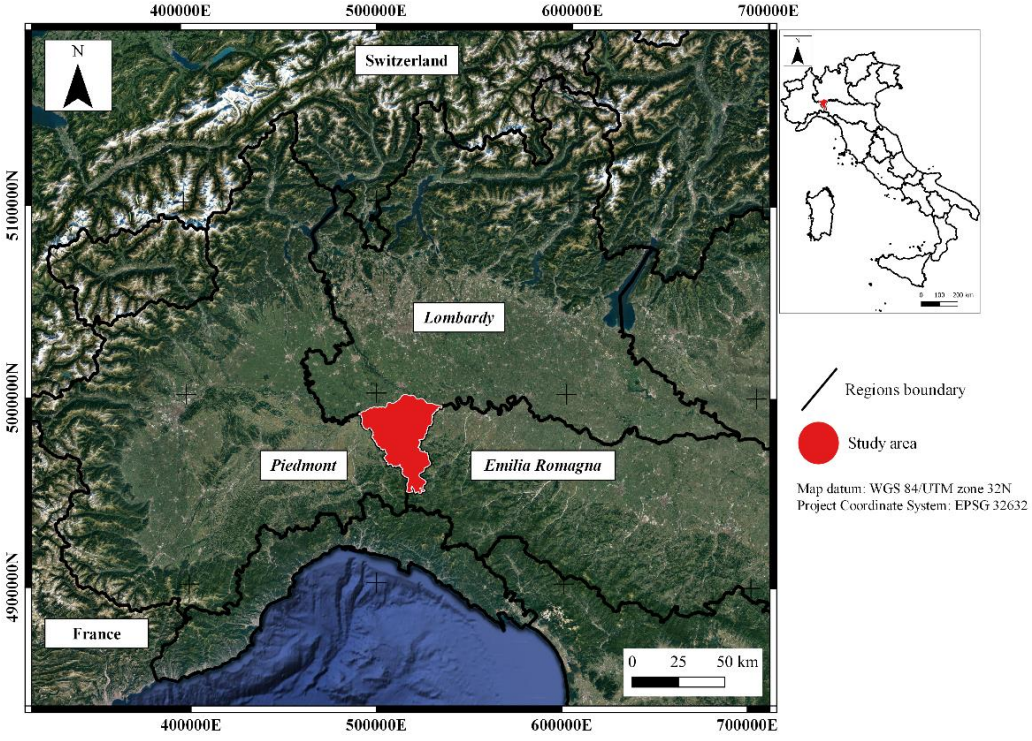

Figure 1: Study area.

Especially badlands represent a complex interaction between several subsurface and surface runoff processes as well as mass movements. The Badlands can be seen as a heterogeneous system composed by the above-mentioned forms and features (Figure 2).

$$Badland = \sum splash + \frac{rill}{interrill} erosion + tunneling + gully + shallow\ landslide$$

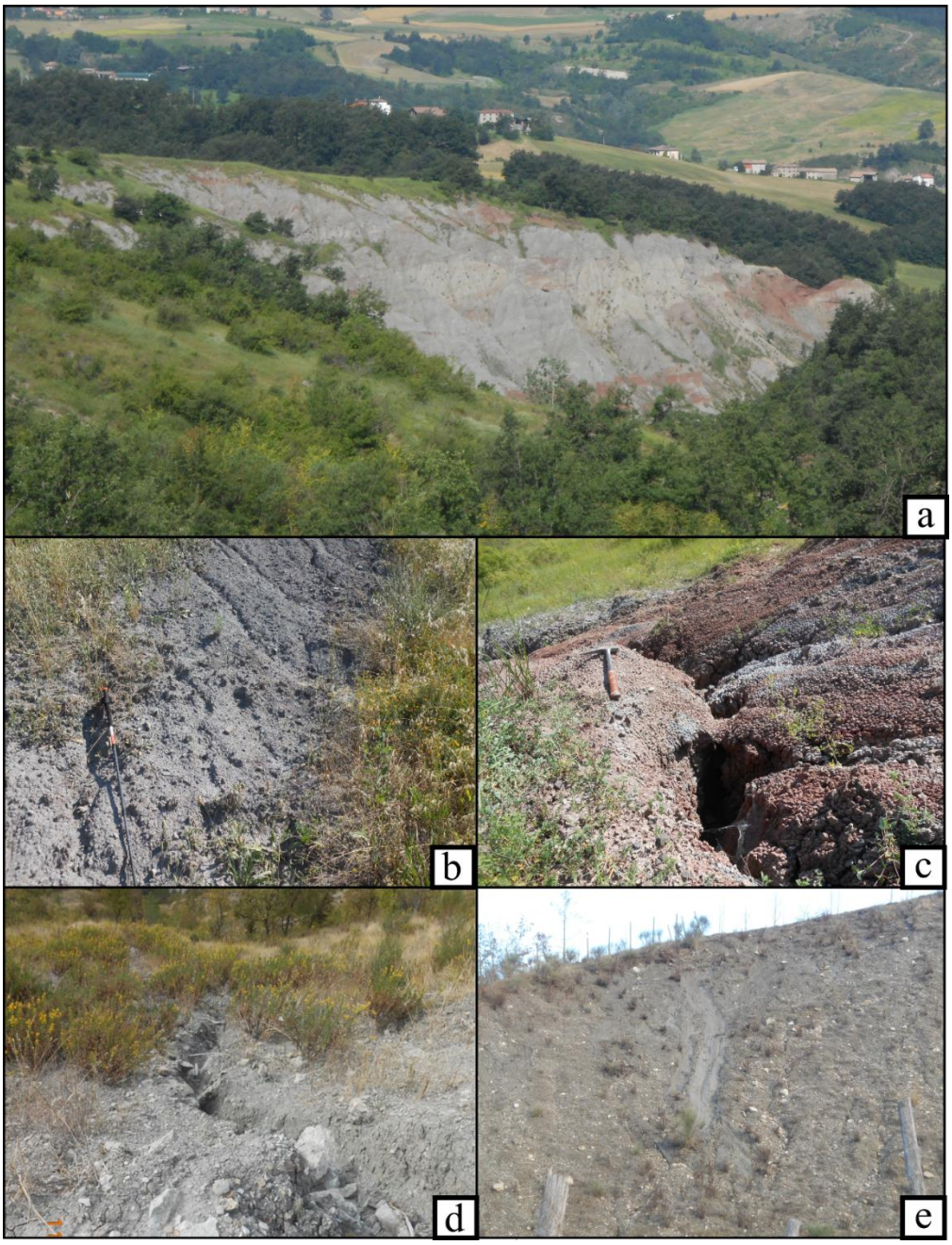

Figure 2. Soil erosion forms and features in the study area. a) Badlands. b) Rill-interrill. c) Tunnelling. d) Small gully. e) Slump in badland.

In Italy badlands are called “calanchi”, an Italian term meaning slowly falling or slumping down (Bucciante, 1922). Calanchi are defined as ‘intensely dissected natural landscapes where vegetation is sparse or absent and which are useless for agriculture’ (Bryan and Yair, 1982).

The first qualitative studies regarding the Italian calanchi are attributed to Bombicci, 1881; Amici, 1898; Bruzzo, 1908; Bucciante, 1922. During the following decades numerous studies on calanchi landforms were conducted at national scale (e.g. Castiglioni, 1933; Alexander, 1980, 1982; Phillips, 1998; Brandolini et al., 2018) as well as at catchment scale (e.g. Buccolini and Coco 2010; Battaglia et al., 2011; Aucelli et al., 2016; Caraballo-Arias and Ferro, 2017). The calanchi identification was historically performed through classic cartographic approaches (e.g. Farabegoli and Agostini 2000; Battaglia, 2011; De Waele et al., 2012), as well as based on remotely sensing data (e.g. Alatorre and Beguería, 2009; Liberti et al., 2009). Especially in the last 20 years, the spatial analysis of Digital Elevation Models (DEM) have allowed a spatial and temporal investigation of calanchi processes and landforms (e.g. Buccolini et al., 2007; Buccolini and Coco, 2010, 2013; Castaldi and Chiocchini, 2012; Caraballo-Arias et al., 2014, 2015; Cappadonia et al., 2016; D’Intino et al., 2020). In many Italian regions the calanchi are directly associated with the soft unconsolidated, poorly consolidated sedimentary marine clays of Plio-Pleistocene age significantly erodible by water (e.g. Phillips, 1998; Gallart et al., 2002; Piccarreta et al., 2006; Phillips and Dudik, 2008; Vergari et al., 2013). Other authors relate the calanchi formation with the lithological, mineralogical, geochemical and pedological properties of the clay deposits (e.g. Alexander 1982; Faulkner and Agostini, 2000; Summa et al., 2007; Battaglia et al., 2002; Pulice et al., 2013; Vergari et al., 2013; Grubin, 2013; Grubin et al., 2018). A holistic morphological description of calanchi was done by Moretti and Rodolfi (2000) who classify the calanchi in type A which are characterised by knife-shape slopes, sparse vegetation, and without gravitational processes, and Type B that are characterised by a smooth morphology with diffuse vegetation and/or landslide processes. Furthermore, Ciccacci et al.,

2008 have extended the morphological definition by adding a Type C that is characterised by intense gravitative processes with numerous small scattered landslides, which almost completely destroy the calanchi ridges and fill up the bottom of the small valleys with the eroded material. Moreover, several authors correlate the calanchi formation and evolution with the climate and vegetation conditions (e.g. Gallart et al., 2002; Biondi and Pesaresi, 2004; Loppi et al., 2004; Tosi et al., 2007; Maccherini et al., 2011; Bollati et al., 2012; Castaldi and Chiocchini, 2012; García-Ruiz et al., 2013; Pulice et al., 2013; Nadal-Romero et al., 2014; Grubin, 2018) as well as with the human impact (e.g. Buccolini et al., 2007; Capolongo et al., 2008; Castaldi and Chiocchini, 2012; Gallart et al., 2013; Torri et al., 2013) that may significantly contribute to the evolution and stabilisation or destabilization of calanchi areas. Other authors presented morphological and topographic descriptions of forms and features (e.g. Calzolari and Ungaro, 1998; Buccolini et al., 2012; Gallart et al., 2013; Cappadonia et al., 2016; Caraballo-Arias et al., 2017) in relation to the drainage network and river basin shape (Caraballo-Arias and Ferro, 2017). The topographic indices extrapolated from high-resolution DEMs were utilised to assess sediment connectivity at basin scale (e.g. Caraballo-Arias et al., 2015; Di Stefano and Ferro, 2019). Furthermore, the scientific community was involved in the evaluation of sediment dynamics, connectivity, and denudation rates at catchment scale (e.g. Faulkner, 2008; Maerker et al., 2012; Vergari et al., 2015; Di Stefano and Ferro, 2019). In addition, different techniques were applied in Italy and in other Mediterranean areas to estimate quantitatively calanchi erosion processes (e.g. Sirvent et al., 1997; Clarke and Rendell, 2006; Ciccacci et al., 2008). Cappadonia et al. (2011) evaluated the erosion rates through pin measurements. Saez et al. (2011) and Corona et al. (2011) used root exposure analysis, or Licciardello et al. (2019) measurements of suspended sediment concentration. Nadal-Romero et al. (2008) and Vergari et al. (2015) utilized turbidimeter analysis and runoff sampling. Regüés and Nadal-Romero (2013), applied back-scattering infrared techniques. Brakensiek et

al. (1979) and Cantón et al. (2001) operated with H-flume gauging approaches. Furthermore Benito et al. (1992) and Sirvent et al. (1997) performed profilometer measurements. De Poley and Gabriels, (1980), Sirvent et al. (1997), Buccolini et al. (2012) and Kropáček et al. (2016) derived from remotely sensed data volumetric measurements and morphometric derivations and finally Tarolli, (2014); Krenz and Khun, (2018); Llena, (2020) applied hight resolution topographic survey methods.

In the last few years, thanks to the development of dedicated software and GIS tools, several studies have been conducted on susceptibility modelling of calanchi and other landforms (i.e gully or rill-interrill erosion) at local or basin scale (e.g. Phillips and Dudik 2008; Vergari, 2015; Bianchini et al., 2016; Maerker et al., 2020).

Finally, a wide literature refers to regional studies on calanchi forms and features in Southern Italy (e.g. Piccarreta et al., 2005, 2006; Summa et al., 2007; Liberti et al., 2009; Cappadonia et al., 2011; Pulice et al., 2012, 2013; Caraballo-Arias et al., 2014, 2015, 2017a; Cappadonia et al., 2016) as well as in central Italy (e.g., Dramis et al., 1982; Mazzanti and Rodolfi, 1988; Moretti and Rodolfi, 2000; Battaglia et al., 2002, 2011; Farifteh and Soaters, 2006; Buccolini et al., 2007; Della Seta et al., 2009; Ciccacci et al., 2008, 2009; Buccolini and Coco, 2010, 2013; Bollati et al., 2012; Castaldi and Chioccini, 2012; Vergari et al., 2013, 2019; Cocco et al., 2015; Aucelli et al., 2016; Del Monte et al., 2017; D'Intino et al., 2020) and finally in Northern Italy with the first work of Bucciante 1922, and subsequently, Farabegoli and Agostini, (2000), Castaldini et al., (2005), De Waele et al., (2012), and Vergari et al., (2015) who identified the calanchi in the Emilia-Romagna region. More recently Maerker et al. (2020) conducted a morphological description of calanchi and through the application of probabilistic methods (MaxEnt model applicated on calanchi and rill-interrill erosion forms and features) the triggering factors of Ligurian calanchi were identified.

From the literature review clearly appears that the calanchi in the Northern Apennines in general, and in Oltrepo Pavese area in particular, were only scarcely studied. The Oltrepo Pavese calanchi have been firstly recognized by Bucciante (1922) who presented a qualitative description of the calanchi in the Staffora, Schizzola, Coppa and Tidone valleys. In the following years, these landforms were not considered in scientific publications and/or in integrated studies on soil erosion processes and dynamics conducted in the region.

Therefore, the research questions of this thesis can be summarised as follows:

- Which lithotypes crop out in the Oltrepo Pavese study area and how are they distributed and related to soil erosion forms and features?

  The Oltrepo Pavese is only partially covered by modern geological maps (SERVIZIO GEOLOGICO D'ITALIA, 2005 and 2014). However, a complete basis of information is a prerequisite to assess earth surface processes causing soil erosion. Thus, the first aim of this thesis is to obtain a lithological and structural description of the entire study area through a comprehensive litho-structural map. The study area appears to be characterised by soft sedimentary bedrock prone to be eroded by surface and subsurface runoff. Eleven lithotypes were identified from field survey and existing published maps. In addition, structural lineaments were obtained starting from detailed DTM. All the results were summarised in chapter I

- How are calanchi forms and features spatially and temporally distributed in the Oltrepo Pavese and what are their environmental characteristics?

  After a detailed field survey, the inventory of the Oltrepo Pavese calanchi was compiled. Moreover, a detailed morphological, geological, morphometric, and temporal characterisation of calanchi forms and features was carried out. As highlighted by this study the Oltrepo Pavese calanchi present common characteristics with other calanchi of the Apennine chain (i.e. morphometric characteristics and morphology), with

significant differences regarding the temporal evolution over longer periods. The morphological classification of the calanchi was done following Moretti and Rodolfi, 2000. Most of the Oltrepo Pavese calanchi display the typical characteristics of type B calanchi, i.e. bland morphology with diffuse vegetation and/or landslide processes. This is essentially due to the Melange bedrock, rainfall conditions and the evolutionary history of the form itself. The multitemporal analysis conducted over a period of 40 years highlighted a reduction of the badlands surface area. These data are partially in accordance with other Italian case studies. In fact, land use change, reduction of agricultural activities and decrease of precipitation resulted in shrinking of the Oltrepo Pavese calanchi. The results were illustrated in chapter II.

- Which are the main environmental factors that influence calanchi and rill-interrill erosion processes?

  The previous cited works about susceptibilities to calanchi and rill-interrill erosion focuses only on small to medium size catchments or slope systems. We successfully applied a stochastic approach to derive a susceptibility map of the Oltrepo Pavese study area based on the dominant independent variables. The results indicate that the land use, lithology, and elevation play a major role in the development of calanchi. However, minor predictors which are often not considered can significantly contribute to the development of both calanchi type A and B. The study shows that a wide portion of the Oltrepo Pavese is potentially affected by rill-interrill as well as calanchi erosion and good agriculture practice can reduce or prevent soil erosion in the area. All the results were presented in chapter III.

- What is the intensity of the processes related to calanchi erosion and are these processes correlated with precipitation, discharge, and sediment dynamics? The sediment dynamics was assessed based on the analysis of suspended sediments in the drainage

system of a small test basin. The study shows in detail the dynamics related to the Suspended Sediment volume Concentration and the Sauter Mean Diameter of the eroded sediments. Moreover, it is highlighted that sediment dynamics in calanchi areas are affected by the initial soil conditions (moisture, as well as vegetation). The results were described and discussed in chapter IV.

Considering the highlighted research needs this thesis wants to contribute to the understanding of soil erosion forms and features in a portion of the Northern Apennines scarcely studied up to now. Furthermore, a new methodology to assess the sediment dynamics at basin scale was tested. As already stated by authors like e.g. Gallart et al. (2013); Caraballo-Arias and Ferro, (2016) there are remaining various future research needs and numerous research questions regarding soil erosion especially in the complex calanchi landscapes. In the final section of the thesis I will resume the salient future prospective and calanchi research needs.

CHAPTER I: STUDY AREA

Bosino Alberto, Pellegrini Luisa, Omran Adel, Bordoni Massimiliano, Meisina Claudia, and Maerker Michael (2019). Litho-structure of the Oltrepo Pavese, Northern Apennines (Italy)

Journal of Maps, 15(2), 382–392.

Map available at: https://www.tandfonline.com/doi/full/10.1080/17445647.2019.1604438

Abstract

In this article we present a detailed litho-structural map of the Oltrepo Pavese, a sector of the Northern Apennines, Southern Lombardy, Italy. Lithology and geological structures are an important basis for different disciplines of Earth Sciences. In particular, for the assessment of earth surface processes such as soil erosion, mass movements, flooding, etc. The Oltrepo Pavese is characterised by a complex geology and related tectonic settings. In this study, we conducted a comprehensive lithological mapping approach considering existing geological maps, and detailed field surveys. The lithotypes have been subdivided into 11 classes based on the dominant outcropping lithologies. Integrating bibliographic data and a detailed Digital Terrain Analysis of a high-resolution DTM (5 m) we detected faults, folds and tectonic lineaments in the study area. The final result is represented by a litho-structural map of the Oltrepo Pavese-area, consisting in two shape files elaborated in an open source GIS environment.

1. Introduction

The Oltrepo Pavese area is located in the Northern Apennines and is belonging to the southern part of Lombardy, Italy (Figure 1a). The Oltrepo Pavese covers about 1110 km^2 dominated by a hilly landscape. The elevation ranges from 60 m.a.s.l. close to the Po River up to 1724 m.a.s.l. at the top of Monte Lesima (Figure 1b). The region is characterised by a typical agricultural land use (Figure 1c) consisting in permanent grassland (12.4%), bushes (12.45%), broad-leave forests, vineyards (13.65%), simple agricultural fields (14.54%) and, bushes in abandoned agricultural areas (14.55%). The Oltrepo Pavese area is one of the most important agricultural and vine-growing regions of Italy (DUSAF, 2015 from GEOPORTALE DELLA LOMBARDIA available at http://www.geoportale.regione.lombardia.it/). From the geological

point of view the study area is a mosaic of different Mesozoic and Cenozoic sedimentary formations. The geology of the Oltrepo Pavese has been studied and mapped by several authors in the past (e.g. Bellinzona et al., 1971; Boni, 1967; Braga et al., 1985; Di Dio et al., 2005; Marroni et al., 2010; Meisina et al., 2006; Panini et al., 2002; SERVIZIO GEOLOGICO D'ITALIA, 1965; SERVIZIO GEOLOGICO D'ITALIA, 1969; SERVIZIO GEOLOGICO D'ITALIA, 2005; SERVIZIO GEOLOGICO D'ITALIA, 2010; SERVIZIO GEOLOGICO D'ITALIA, 2014; Taramelli, 1882; Vercesi et al., 2014). However, there is no accurate and homogeneous subdivision of lithologic formations available or a comprehensive regional litho-structural map for further geological assessments and modelling approaches. Generally, litho-structural maps yield information on different rock types as well as geological structures and play a fundamental role in understanding the history of the study region (Ali and Ali, 2013). Therefore, we generated a new litho-structural map of the Oltrepo Pavese. The Main Map was developed based on historical maps, field surveys and DTM analysis, and represents 11 lithologies as well as the main faults, folds, thrust and tectonic lineament systems present in the study area. Finally, the litho-structural map gives important information about the lithology of the substrates and the structural setting of the study area. Thus, this map provides basic information for the assessment of processes i.e. flooding, soil erosion etc. and features i.e. gully, Badlands etc. related to earth sciences.

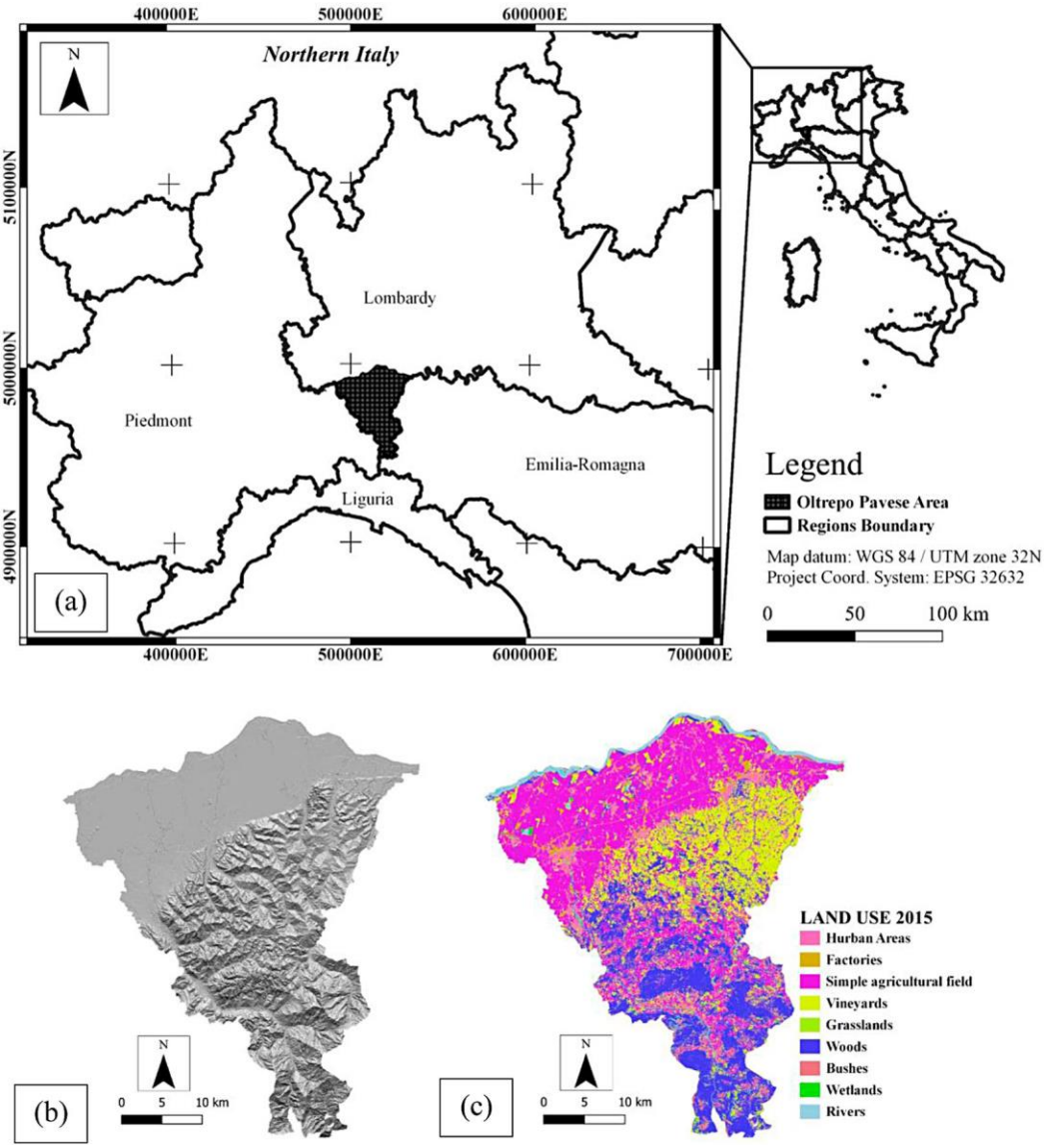

Figure 1. (a) Setting of the Oltrepo Pavese study area. (b) Hillshading of the study area. (c) Land Use of the Oltrepo Pavese, according to CORINE 2015.

2. Geological Setting

2.1. Geology of the study area

The Oltrepo Pavese is located in the northern parts of the Apennines and shows typical features of a foldthrust belt landscape structure (Carmignani et al., 2004; Cibin et al., 2001; Toscani et al., 2006). Several authors (e.g. Ciarapica and Passeri, 1998; Decarlis et al., 2014; Finetti et al., 2001; Maino et al., 2013) link the evolution of the Apennines with the formation of the Balearic basin. According to this theory the opening of the basin, caused by the anticlockwise rotation

of the Corsica-Sardina blocks, is setting up the Apennines orogen (Maino et al., 2012, 2013). The origin of the Apennines can be associated with two main accretionary steps: (i) the initial Cretaceous western subduction, of the Ligurian Piemonte Ocean, under the European Plate – Eoalpine Phase and (ii) the Eocenic collision between Europe and the Adriatic microplate – Mesoalpine Phase. During these phases the chain acquired its dominant eastward vergence. Finally, during the Oligocene the formation of a double vergence accretionary wedge occurs, which is related to the late eastward subduction of the Adria region (Vercesi et al., 2014).

Several authors (e.g. Ciarapica and Passeri, 1998; Decarlis et al., 2014; Finetti et al., 2001; Maino et al., 2013) link the evolution of the Apennines with the formation of the Balearic basin. According to this theory the opening of the basin, caused by the anticlockwise rotation of the Corsica-Sardinia blocks, is setting up the Apennines orogen (Maino et al., 2012, 2013). The origin of the Apennines can be associated with two main accretionary steps: (i) the initial Cretaceous western subduction, of the Ligurian Piemonte Ocean, under the European Plate – Eoalpine Phase and (ii) the Eocenic collision between Europe and the Adriatic microplate – Mesoalpine Phase. During these phases the chain acquired its dominant eastward vergence. Finally, during the Oligocene the formation of a double vergence accretionary wedge occurs, which is related to the late eastward subduction of the Adria region (Vercesi et al., 2014).

The Northern Apennines is historically subdivided in several tectono-stratigraphic Units belonging to the two continents (Adria and Europe) and the ocean between them. From the base to the top the relevant Units are structured as follows: Tuscan-Umbrian, Subligurian, Ligurian, and Epiligurian (e.g. Elter, 1975; Elter et al., 2003; Piazza et al., 2016). In the study area different allochthonous units crop out such as the Subligurian (SUB) and Ligurian Units (LIG), that are often covered by Epiligurian Units (EPI). These, in turn, are sealed by post-Messinian deposits (PMess) and finally covered by Quaternary alluvial deposits (Q). The Subligurian Units represent the interface between the External Ligurian domain and the Tuscan domain. In

the Oltrepo Pavese the Subligurian Units are characterised by the Monte Penice Flysch as well as interstratified limestones; the so called Canetolo clay- and limestones. These Units lay on the thinned boundary of the Adriatic Continent. From a lithological point of view, they are composed by turbiditic deposits of interstratified and massive limestones. Above the Subligurian Units the Ligurian Units crop out (Elter et al., 1966). The latter units were historically subdivided in Internal and External Units. The External Units are widely distributed in Oltrepo Pavese area and are characterised by the presence of resedimented ophiolites. They are considered fragments of the Ligurian-Piemonte ocean (Elter and Marroni, 1991; Molli et al., 2010). The Unit is represented by flysch, terrigenous interstratified rocks and claystones that were deposited between the Adriatic plate and the Ligurian-Piemonte Ocean. The Internal Ligurian Units do not crop out in the Oltrepo Pavese. They are distinguished from the External Ligurian Units by the presence of ophiolites still in their original stratigraphic position with an Upper Jurassic/ Lower Cretaceous sedimentary cover (Molli et al., 2010). The Epiligurian Units, deposited on the top of the Ligurian Units, represent sedimentary depositions in thrust-top basins (Ricci Lucchi and Ori, 1985). These Units are related to the erosion and sedimentation of the Ligurian Units during the Eocene-Miocene uplift phases of the Apennines belt. The synorogenetic deposition of the Epiligurian Units causes the quite complex geology of the area, bringing these Epiligurian Units in stratigraphic and unconformable contact with the Ligurian Units. Subsequently, during the Oligo-Miocene rising phases of the Apennines, the Epiligurian Untis acted like preferential path in the overtrusting bringing the Ligurian Unit in tectonic contact with the Epiligurian one (Figure 2a).

From a lithological point of view the Epiligurian formations are very heterogeneous (Panini et al., 2002). In fact, they are mainly composed by:

- Melange: i.e. Brecce Argillose di Baiso representing submarine landslides.
- Marls: i.e. Monte Piano Marls pelagic sediments.

- Interstratified rocks: i.e. Ranzano Formation, clastic turbidit formations.
- Sandstones: i.e. Monte Vallassa Sandstone, platform deposits.

Furthermore, in the Oltrepo Pavese area the sedimentary formations of the Tertiary Piedmont Basin (BTP) crop out. The BTP is an episutural basin like initially described by Bally and Snelson (1980) covering both the Alpine and Apennines Units. These formations are represented by continental and marine rocks consisting of conglomerates, sandstones, flysch and hemipelagic deposits. Moreover, evaporitic, and terrigenous formations were deposited during the Messinian in small shallow marine basins. Finally, the area is characterised by Quaternary alluvial, colluvial and landslide deposits. From a geomorphological point of view the area is highly influenced by shallow landslide, in unconsolidated or weakly consolidated substrates. Moreover, Badlands (Calanchi) landforms are present in the soft sedimentary formations and show certain relation to tectonic lineaments.

2.2. Tectonic features of the study area

From a tectonic point of view the Oltrepo Pavese is a very complex mosaic of tectonic units. During the middle Eocene-late Miocene emplacement phases of the Apennines chain the Internal Ligurian Units were thrusted on the External ones and during the same time sin-tectonic deposits, i.e. turbiditic sequences and submarine landslides, were deposited on the underlying Ligurian Units generating the Epiligurian Units. Even if the Oltrepo Pavese represents a delimited study area, it is very difficult to observe directly the above-mentioned sequences in open sections.

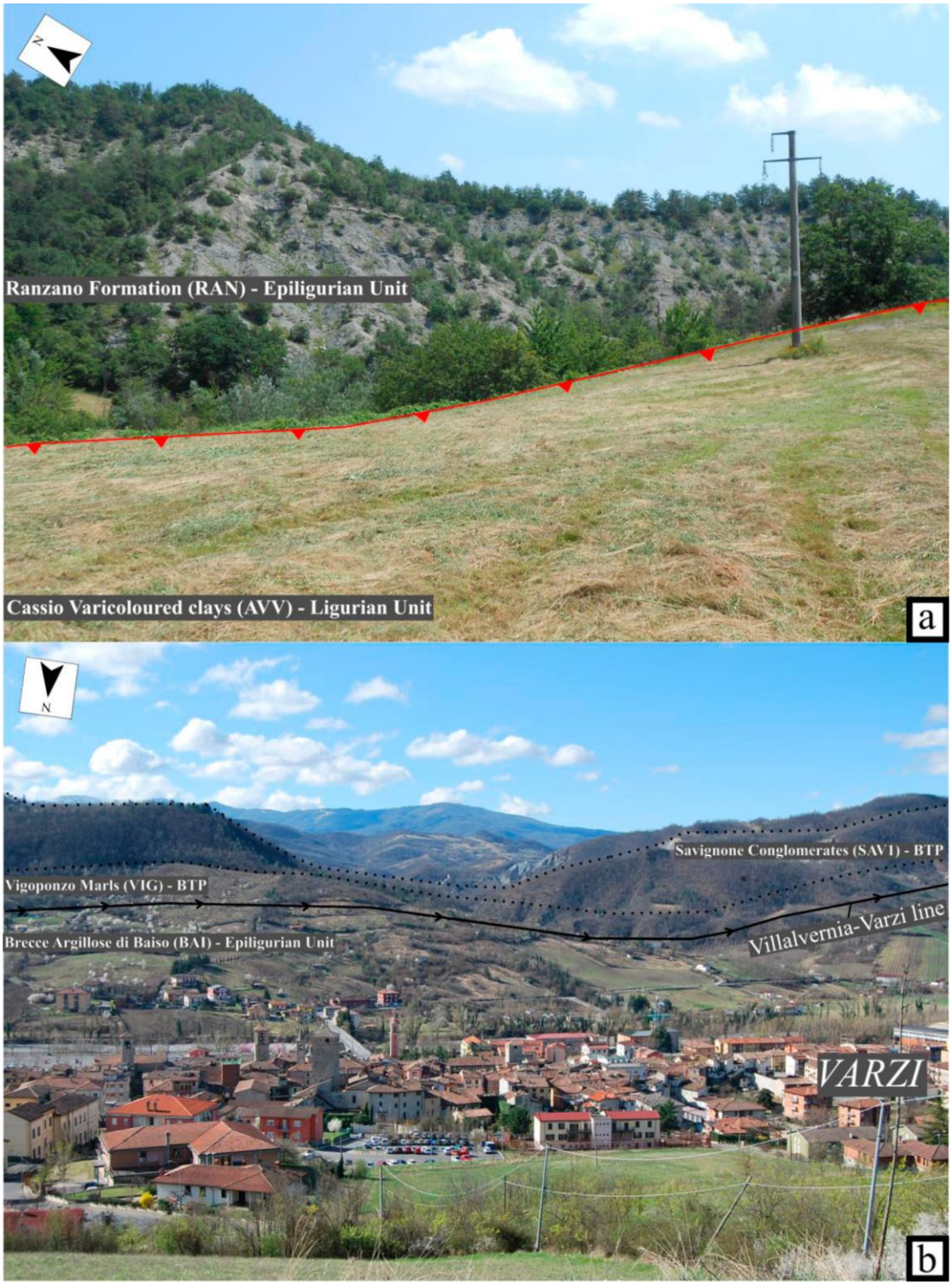

Figure 2. (a) Boundary between the soft Cassio Varicoloured clays (AVV) belonging to the Ligurian Units and the Epiligurian Unit of the more resistive Ranzano Formation (RAN). The Ligurian Units are overthrusting on the Epiligurian ones (44°54'25.26"N - 9° 16'38.60"E). (b) Villalvernia-Varzi fault line close to the town of Varzi separating the Epiligurian Units – Breccie Argillose di Baiso (BAI) from the BTP Formations -Vigoponzo Marls (VIG) and the Savignone Conglomerates (SAV1).

Thus, especially the available described outcrops reveal important tectonic information. The faults and tectonic lineaments detected in the field fit to three main directions as defined by Panini et al. (2002): (i) NW/SE directions: defined as 'Apenninic direction' which frequently juxtapose the Epiligurian Units with the Ligurian ones. In other words, these tectonic lineaments follow the direction of the overlapping Apennines strata; (ii) NE/SW directions: defined as 'Anti-Apennines direction' that is orthogonal to the Apennines lineaments and interrupt the lateral continuity of the tectonic Units; and (iii) N/S directions: usually represented by left lateral strike-slip faults. The main fault of the study area is the Villalvernia- Varzi Line (VVL). The fault is an east-west oriented strike-slip fault (Bellinzona et al., 1971; Cerrina Feroni et al., 2002; Festa et al., 2015; Meisina and Piccio, 2003; Panini et al., 2002) and separates the BTP formations on the Epiligurian Units (Figure 2b).

3. Methods

The detection and identification of the sedimentary formations is a complex task since only a few outcrops are available in the study area. This is caused by the hilly landscape and the rolling morphology, which makes it difficult to observe directly the bedrocks. Furthermore, the bushy vegetation cover does not allow the direct analysis to extract the lithology, such as classic remote sensing i.e. mineral mapping using ASTER data (i.e. Omran et al., 2012). However, a complete lithological and structural map is a prerequisite to assess surface earth processes and to simulate these processes through models at local and regional scales. To carry out the litho-structural map of the Oltrepo Pavese we followed subsequent steps, (Figure 3).

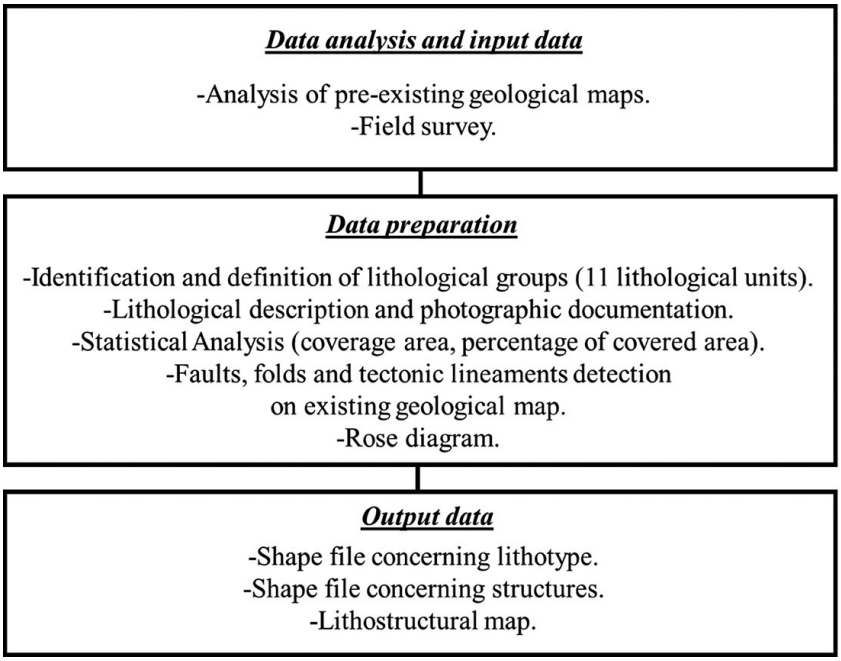

Figure 3. Flow chart of the applied methodology.

To discriminate the lithologies outcropping in the study area we analysed and combined available geological maps covering different parts of the Oltrepo Pavese.

The following maps were used: 1:50.000 geological map (SERVIZIO GEOLOGICO D'ITALIA, 2005; SERVIZIO GEOLOGICO D'ITALIA, 2014), 1:100.000 geological maps (SERVIZIO GEOLOGICO D'ITALIA, 1965; SERVIZIO GEOLOGICO D'ITALIA, 1969), as well as more local information provided by Vercesi and Scagni (1984), Braga et al. (1985), Meisina et al. (2006). Moreover, we mapped areas of the Oltrepo Pavese not covered or that have a too coarse scale, (e.g. areas covered by the old 1:100.000 scale sheets). The geological formations were grouped in 11 classes (Table 1) according to their lithological characteristics and their behaviour in the respects of the processes of degradation. The lithological Units were elaborated in QGIS generating a shapefile with the extent of the Oltrepo Pavese area. Each lithological unit was described and photo-documented (Figure 4). Moreover, for the 11 lithological classes the coverage area and the percentage of the covered area was determined through statistical analysis.

Finally, faults, thrust, folds and tectonic lineament systems were added to the Main Map. The tectonic elements are based on the bibliography following SERVIZIO GEOLOGICO D'ITALIA (1965), Marchetti et al. (1978), Marchetti et al. (1979), Boccaletti and Coli (1982), Scagni and Vercesi (1987), Pellegrini and Vercesi (1995), Pellegrini and Arzani (1997), Mantelli and Vercesi (2000), as well as the SERVIZIO GEOLOGICO D'ITALIA (2014). Moreover, we conducted a detailed DTM analysis followed by a visual and semi-automatic elaboration to extract lineaments. The DTM data with 5 m cell size (Regional Topographical Data Base) was downloaded from the geoportal of the Lombardy region (http://www.geoportale.regione.lombardia.it/).

The DTM was pre-processed and four hillshadings were generated in a SAGA GIS environment.

Lineaments are defined as 'simple or composite linear features of a surface, whose parts are aligned in a rectilinear or slightly curvilinear way, which differs distinctly from the pattern of adjacent features and presumably reflect a subsurface phenomenon' (O'Leary et al., 1976). However, tectonic lineaments are often represented by linear features of the earth surface usually connected with zones of structural weakness. Moreover, scarps, linear ridges, joints, and faults etc. can be interpreted as lineaments (Pandian et al., 2016). Lineaments were traditionally identified and extracted from topographic maps using a visual procedure (Zhumabek et al., 2017). Despite traditional methods an automatic lineament extraction can be used to identify lineaments, especially at broader scales.

The semi-automatic extraction of lineaments was carried out using the PCI Geomatica software package (PCI Geomatics Ltd., 2017). The combination of the semi-automatic extraction was refined with a visual interpretation and lineament identification. Initially, the DTM is pre-processed and clipped to the extent of the Oltrepo Pavese study area. The pre-processing was performed with SAGA GIS and consists in the application of a simple filter and fill sink

algorithm (Planchon and Darboux, 2002) to correct the DEM hydrologically and to eliminate major artefacts. Furthermore, four hillshadings were generated using four illumination angles (0°, 45°, 90°, 135°) and a vertical exaggeration of 4. We chose the following parameter setting for the PCI analysis: Filter Radius = 20; Edge Gradient Threshold = 200; Curve length Threshold = 10; Line fitting Error threshold = 3; Angular difference threshold = 30; and Linking Distance Threshold = 20. Subsequently, a rose diagram of faults and tectonic lineaments was derived using GeoRose (version 0.5.0). The final step consists in the QGIS elaboration of the main map.

Table 1. Lithological and geological subdivision.

ID	Formation/abbreviation	Units
(1) Alluvial Deposits	Voghera Synthem (VOH)	Q
	Rivazza Synthem (RVX)	Q
	Rivanazzano Unit (URV)	Q
	Torretta Unit (TTS)	Q
	Varzi Unit (VRZ)	Q
	Ardivestra Unit (ADV)	Q
	Nizza Unit (NIZ)	Q
	Other alluvium South of the Po River (ALL)	Q
(2) River Terrace Deposits	Cà D'Andrino Group (GD)	Q
	Codevilla Unit (LLX)	Q
	Torrazza Coste Group (TZ)	Q
	Diluvium (Q1m), (Q1a), (Q1b)	Q
(3) Colluvial Deposits	Retorbido Group (RE)	Q
	Other colluvial deposits (COL)	Q
(4) Landslide Deposits	Po Syntem (POI)	Q
	Other gravitational deposits (POI1)	Q
(5) Conglomerates	Bagnaria Conglomerates (UBG)	Q
	Cassano Spinola Conglomerates (CCS)	Pmess
	Argille Azzurre, Mondondone Conglomerates (FAAa)	Pmess
	Salti del Diavolo Conglomerates (AVV1)	LIG
(6) Melange	Brecce Argillose di Baiso (BAI)	EPI
	Brecce Argillose della Val Tiepido Canossa (MVT)	EPI
	Brecce Argillose di Costa Pelata (BPE)	EPI
	Palombini Claystone (Ap)	LIG
	Serpentinites (Sr)	LIG
(7) Sandstones	Cassano Spinola Conglomerates, Member of Monte Arzolo Sandstone (CCS1, aA)	PMess
	Corvino S. Quirico Formation (fQ)	PMess
	Asti sand (AST)	PMess
	Martinasca Formation (fM)	PMess
	Gremiasco Formation, Member of Nivione (GEM2a)	BTP
	Monte Vallassa Sandstone (AVL)	EPI
	Montù Beccaria Formation (fB)	EPI
(8) Claystones	Argille Azzurre (FAA)	Pmess
	Sparano Formation (fS)	Pmess
	Cassio Varicoloured clays (AVV)	LIG
	Montoggio claystone (MGG)	LIG
(9) Interstr. Rocks	Monastero Formation (MST)	BTP
	Castagnola Formation (FCA)	BTP
	Savignone Conglomerates, Monte Rivalta Member (SAV1)	BTP
	Ranzano Formation (RAN)	EPI
	Scabiazza Sandstone (SCB) Val Luretta Formation, Poviago Member (VLU1) and Monteventano Member (VLU2)	LIG LIG
	Monte Ragola Complex (MRA)	LIG
(10) Interstr. Limestones and Limestones	Dernice Formation (DRN)	BTP
	Pietra dei Giorgi Limestone (cG)	EPI
	Monte Antola Formation (FAN)	LIG
	Flysch di Bettola (BET)	LIG
	Flysch di Monte Cassio (MCS)	LIG
	Flysch di Monte Penice (PEN)	SUB
	Canetolo Clay and Limestone (ACQ)	SUB
(11) Interstr. Marls and Marls	Sapigno Formation (GNO)	PMess
	Gessoso Solfifera Formation (fgs)	PMEss
	Monte Brugi Marls (BGU)	BTP
	Vigoponzo Marls (VIG)	BTP
	Gremiasco Formation, Nivione Member (GEM2c)	BTP
	Monastero Formation (MSTd)	BTP
	S. Agata Fossil Marls (SAF, mA)	EPI
	Contignaco Formation (CTG)	EPI
	Monte Piano Marls (MMP)	EPI
	Antognola Formation (ANT)	EPI
	Val Luretta Formation, Genepreto Member (VLU3)	LIG

Notes: (SUB): Subligurian Units. (LIG): Ligurian Units. (EPI): Epiligurian Units. (BTP): Tertiary Piedmont Basin. (PMess): Post Messinian Units. (Q): Quaternary deposits.

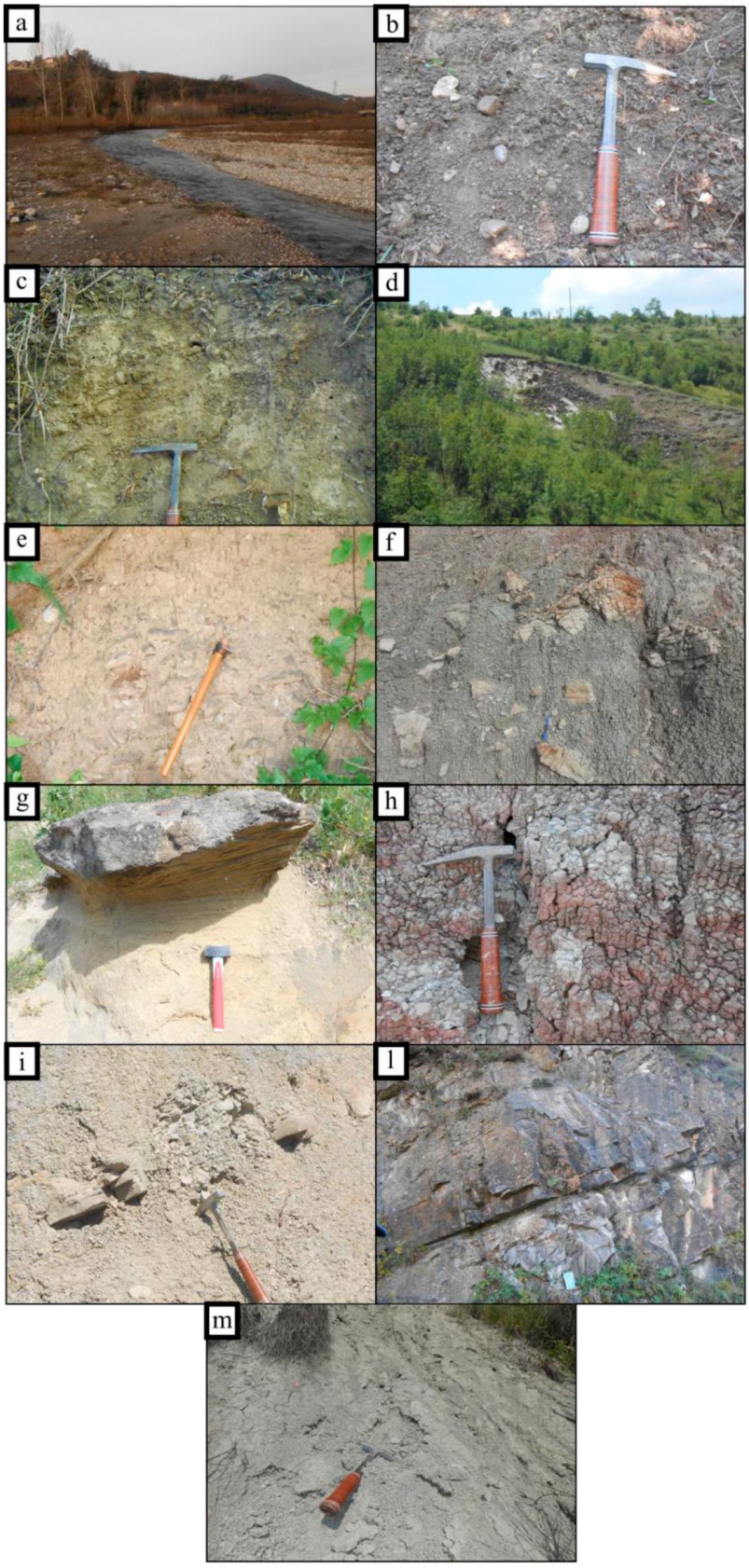

Figure 4. Examples of lithological units. (a) Alluvial Deposits Staffora River. (b) River Terrace Deposits. (c) Colluvial Deposits. (d) Landslide Deposits. (e) Conglomerates. (f) Melange. (g) Sandstones. (h) Claystones. (i) Interstratified rocks. (l) Interstratified limestones and limestones. (m) Marls and interstratified marls.

4. Results

We identified, homogenised and classified the main formations outcropping in the Oltrepo Pavese based on the different lithotypes. The main geological formations are illustrated in (Table 1). They are described with the common abbreviations and the geological Units they belong to, as reported in Boni (1967), Di Dio et al. (2005), Marroni et al. (2010), and Vercesi et al. (2014). In total 11 lithological units were identified, documented and described as follows:

(1) Alluvial Deposits (Figure 4a): The unit is lithologically composed by rounded gravel, sand, silt, and clay deposited by the Po river and its tributaries. It consists in rounded gravel in a sandy matrix and is often orientated.

(2) River Terrace Deposits (Figure 4b): The unit is lithologically composed by flat and rounded centimetric pebbles scattered in a brown silt, sandy silt and clay silt matrix. Usually gravel layers are found at the base of the group or layers of red fine sediments. Pedogenetic processes occurred generating a sandy clay loam texture. The average colour is defined by a Munsell soil colour chart of 2.5Y4/3. This deposit can be associated to river terrace deposits, from local river system at the margins of the Apennines.

(3) Colluvial Deposits (Figure 4c): The unit is lithologically composed by sandy silt, silt and clay silt deposits. The parental material is already pedogenetically modified. In outcrops diffuse planar layers are visible. The average Munsell soil colour range between 7.5YR and 10YR (e.g. 10YR5/4 represented in Figure 3l). This deposit can be associated with colluvial and mass flow processes.

(4) Landslide Deposits (Figure 4d): The unit is lithologically composed by unlithified deposits generated by landslides and denudation processes. The unit is characterised by incoherent material without stratification, metric and centimetric blocks in fine matrix.

(5) Conglomerates (Figure 4e): The unit is lithologically composed by rounded centimetric pebbles, usually orientated (imbricated) often interbedded

with grey/light grey sand and silt lens. In outcrops two main types of conglomerates are found: (i) grain dominated conglomerates (Orthoconglomerate) and (ii) matrix dominated conglomerates (Paraconglomerate) characterised by a sandy/silty matrix. The pebbles are mainly composed by limestones and sandstones with variable size, from sub centimetric to centimetric size. These deposits represent the river sediments.

(6) Melange (Figure 4f): The unit is lithologically composed by centimetric to metric chaotic blocks in a fine grey or reddish clay matrix. The blocks are mainly composed by sandstone, limestone and conglomerates, corresponding to the Ligurian and Epiligurian Formations. The smectite clay matrix comprises minerals like montmorillonite, and illite. Moreover, low percentages of fine silt are present. The texture appears chaotic without stratifications. These deposits represent submarine landslides (Olistrostroms).

(7) Sandstones (Figure 4g): The unit is lithologically composed by stratified or massive deposits of yellow to grey bioclastic sandstones, biocalcarenites, rich in fossils (i.e. foraminifers and platform dweller). These rocks are more or less cemented and represent platform deposits. The fluvial sandstones of this group occasionally are interbedded with silty claystones usually characterised by cross beddings or a poorly defined stratification.

(8) Claystones (Figure 4h): The unit is lithologically composed by dark red, dark grey, grey and violet claystones, with subordinated siltstones and sandstones. In outcrops usually, pop-corn structures appear or other desiccation forms like mud cracks. Generally, typical characteristics of run off processes are present. In outcrops alternated bands of coloured clays are often visible, representing a zonal change in chemical composition. In general, the inherited stratification is not preserved due to the high tectonic deformation and shrinking-swelling phenomena of active layer clays. These rocks represent ocean floor sediments.

(9) Interstratified rocks (Figure 4i): The unit is lithologically composed by an alternation of conglomerates, sandstones and pelites in variable proportions. In general, we found

centimetric to sub-metric grey or light brown sandstones interbedded with grey silty marly siltstones. Groove cast, flute cast and sparse bioturbation on the top of the strata can be observed. Run off processes are evident in the outcrops characterised by thick fine-grained strata interbedded with thin sandstone layers. These rocks might crop out in a folded and deformed way due to tectonic activity. These deposits can be associated with terrigenous turbiditic sediment deposited in small basins.

(10) Interstratified limestones and limestones (Figure 4l): The unit is lithologically composed by yellow or white massive limestone, and limestone interbedded with calcareous marls and pelites. Centimetric and metric strata of limestone are observed occasionally with sandstone layers at the base. Ripple and flute cast rarely occur. This unit can be associated with calcareous turbiditic sediments deposited in small basins.

(11) Marls and Interstratified Marls (Figure 4m): The unit is lithologically composed by grey, light blue to greenish marls, chalky marl, marls interbedded with silty marls, flint, pelites and clayey marls. The lithology crops out with a typical conchoid or flaked fracturing. On the exposed surface weathering processes and runoff features are presents. Usually scarce bioturbations are evident.

These deposits represent pelagic sediments deposited regularly in shallow basins, often combining the marine sedimentation with evaporitic conditions.

Once the lithological units were classified, we determined the coverage area and the percentage of coverage area for each lithological unit (see Table 2). The final map (Main Map) was completed adding the faults, folds and tectonic lineaments. Even though faults and folds have been reported in bibliography we identified the tectonic lineaments with a combination of visual (DTM interpretation) and semi-automatic procedures (analysis PCI output). The PCI output was combined with a classic visual method modifying the lineaments in QGIS in order to extract only the major tectonic lineaments. The direction of the main faults and tectonic

lineaments is represented in a rose diagram. Basically, two main directions: NW/SE-NE/SW and N/S are highlighted in the rose diagram. These directions correspond to the main Apennines and anti-Apennines directions. Moreover, a N/S direction typically represents strike-slip faults (Figure 5). Finally, the main map was elaborated in QGIS joining lithology and structural elements.

Table 2. Coverage area and percentage of coverage area of the Oltrepo Pavese lithologies.

ID	Coverage area (Km^2)	Percentage of coverage area (%)
(1) Alluvial Deposits	423	38
(2) River Terrace Deposits	36	3
(3) Colluvial Deposits	33	3
(4) Landslide Deposits	66	6
(5) Conglomerates	9	1
(6) Melange	67	6
(7) Sandstones	53	5
(8) Claystones	35	3
(9) Interstr. Rocks	151	13
(10) Interstr. Limestones and Limestones	84	8
(11) Interstr. Marls and Marls	153	14

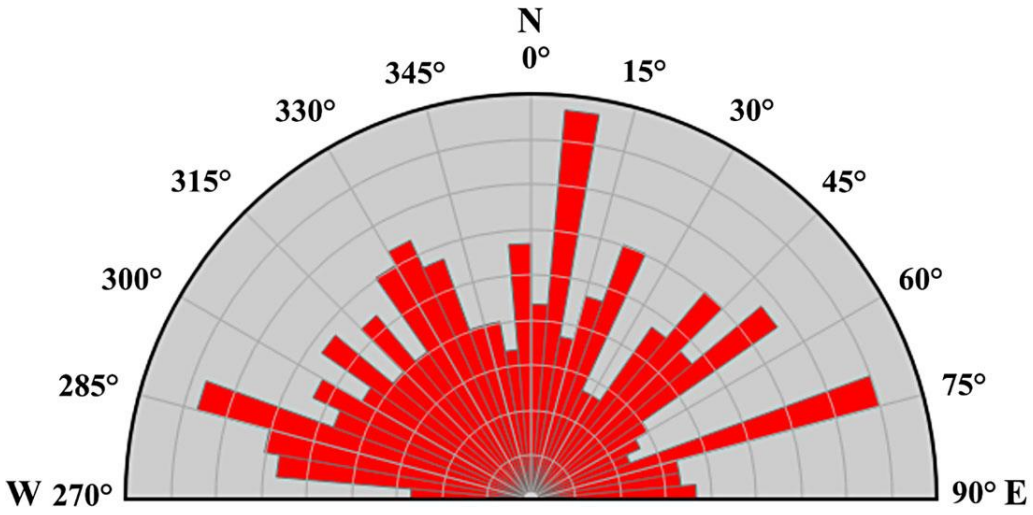

Figure 5. Rose diagram show the main direction of faults and tectonic lineaments.

5. Conclusions

In the complex landscape of the study area, characterised by a dense vegetation cover, a consistent lithologic classification was not existing and hence, also a corresponding homogeneous map was missing so far. Thus, in this paper we present a litho-structural map of the Oltrepo Pavese area. The main lithologies were obtained combining bibliographic information and own field surveys. The lithologies are grouped in 11 representative classes based on their intrinsic characteristics. The map is enhanced with the main structural elements (faults, folds and tectonic lineaments) present in the study area. The latter were derived with a combination of a semi-automatic GIS-based method and a traditional visual method. The lineaments extracted can be associated with faults and disturbance zones. The final map (Main Map) represents the litho-structure of the study area. Moreover, we provide two vector files characterising the lithology and the linear structures for the Oltrepo Pavese. This study provides basic information for further assessment of earth surface processes in the Oltrepo Pavese Area.

Software

The maps were generated and realised using open source GIS (QGIS 3.0). The DTM was elaborated with SAGA GIS and PCI Geomatica. The Rose diagram was generated with GeoRose (version 0.5.0). The statistical analysis has been conducted in Microsoft Excel.

Acknowledgements

The authors are grateful to Prof. Pier Luigi Vercesi for the valuable comments and support.

References

Ali, S. A., and Ali, U. 2013. Litho-structural mapping of sind catchment (Kashmir basin), NW Himalaya, using remote sensing and GIS techniques. International Journal of Science and Research (IJSR), 4(7), 1325–1330.

Bally, A. W., and Snelson, S. 1980. Realms of subsidence. In A. D. Miall (Ed.), Factors and Principles of world petroleum occurrence (Vol. 6, pp. 9–75). Calgary: Can. Soc. Petrl. Geol. Mem.

Bellinzona, G., Boni, A., Braga, G., and Marchetti, G. 1971. Note Illustrative della Carta Geologica D'Italia in scala 1:100,000 – Foglio 71 Voghera (p. 121). Roma: Serv. Geol. d'It.

Boccaletti, M., and Coli, M. 1982. Carta Strutturale dell'appennino Settentrionale. Firenze: P.F.G. -Sottoprogetto 5 - Modello Strutturale, 4 Tavv. Selca.

Boni, A.1967. Note Illustrative della Carta Geologica D'Italia in scala 1:100,000 – Foglio 59 Pavia (p. 68). Roma: Serv. Geol. d'It.

Braga, G., Brasschi, G., Calculli, S., Caucia, F., Cerro, A., Colleselli, F.,…Veniale, F. 1985. I fenomeni franosi nell'Oltrepo Pavese: tipologie e cause. Geologia Applicata e Idrogeologia. Volume XX Parte II.

Carmignani, L., Conti, P., Cornamusini, G., and Meccheri, M. 2004. The internal Northern Apennines, the Northern Tyrrhenian sea and the Sardinia- Corsica Block. Special Volume of the Italian Geological Society for the IGC 32 Florence.

Cerrina Feroni, A., Ottria, G., Martinelli, P., and Martelli, L. 2002. Carta geologico-strutturale dell'Appennino emiliano – romagnolo alla scala 1:250.000. Firenze: Regione Emilia-Romagna, C.N.R., Ed. S.EL.CA.

Ciarapica, G., and Passeri, L. 1998. Evoluzione paleogeografica degli Appennini. Atti Ticinensi di Scienze delle Terra, 40, 233–290.

Cibin, U., Spadafora, E., Zuffa, G. G., and Castellarin, A. 2001. Continental collision history from arenites of episutural basin in the Northern Apennines, Italy. Geological Society of America Bulletin, 113(1), 4–19.

Decarlis, A., Maino, M., Dallagiovanna, G., Lualdi, A., Masini, E., Toscani, G., and Seno, S. 2014. Salt tectonics in the SW Alps (Italy–France): From rifting to the inversion of the European continental margin in a context of oblique convergence. Tectonophysics, 636, 293–314.

Di Dio, G., Piccin, A., and Vercesi, P. L. 2005. Carta Geologica d'Italia alla scala 1:50,000. Foglio 179 'Ponte dell'Olio' (p. 108). Roma: APAT – Dipartimento Difesa Del Suolo - Servizio Geologico D'Italia.

Elter, G., Elter, P., Sturani, C., and Weidmann, M. 1966. Sur la prolongation du domaine ligure de l'Apennin dans le Monferrat et les Alpes et sur l'origine de la Nappe de la Simme s.l. des Prealpes romandes et chablaisiennes. Arch. Sciences de Geneve, 19/3, 279–378. Geneve.

Elter, P. 1975. Introduction a la geologie de l'Apennin Septentrional. Bulletin de la Societe Geologique de France, 17, 956–962. Paris.

Elter, P., Grasso, M., Parrotto, M., and Vezzani, L. (2003). Structural setting of the Apennines-Maghrebian thrust belt. Episodes, 26, 205–211.

Elter, P., and Marroni, M. 1991. Le unità Liguri Dell'Appennino Settentrionale: sintesi dei dati e nuove interpretazioni. Mem. Descr. Carta Geol. D'It, XLVI, 121–138.

Festa, A., Fioraso, G., Bissacca, E., and Petrizzo, M. R. 2015. Geology of the Villalvernia – Varzi Line between Scrivia and Curone valleys (NW Italy). Journal of Maps, 11(1), 39–55.

Finetti, I. R., Boccaletti, M., Bonini, M., Del Ben, A., Geletti, R., Pipan, M., and Sani, F. 2001. Crustal section based on CROP seismic data across the North Tyrrhenian–Northern Apennines–Adriatic Sea. Tectonophysics, 343 (2001), 135–163.

Maino, M., Dallagiovanna, G., Gaggero, L., Seno, S., andTiepolo, M. 2012. U-Pb zircon geochronological and petrographic constraints on late to post-collisional Variscan magmatism and metamorphism in the Ligurian Alps, Italy. Geological Journal, 47(6), 632–652.

Maino, M., Decarlis, A., Felletti, F., and Seno, S. 2013. Tectono-sedimentary evolution of the Tertiary Piedmont basin (NW Italy) within the Oligo-Miocene central Mediterranean geodynamics. Tectonics, 32(3), 593–619.

Mantelli, L., and Vercesi, P. L. (2000). Evoluzione Morfostrutturale Recente del Pedeappennino Vogherese-Tortonese. Atti Ticinensi di Scienze della Terra, 41, 49–58.

Marchetti, G., Papani, G., and Sgavetti, M. 1978. Evidence of Neotectonics in the North-West Apennines-Po side. In H. Closs, D. M. Order e K. L. Shmidt (Eds.), Alps, Apennines, Hellenide-Geodynamic investigations along Geotraverses by an International Group of Geoscientis. Stuttgard.

Marchetti, G., Pellegrini, L., Perotti, C., and Vercesi, P. L. 1979. L'evoluzione morfo-strutturale dell'Appennino piacentino: proposta di uno schema interpretativo. C.N.R. Estratto da:

Contributi preliminari alla realizzazione della Carta Neotettonica d'Italia, Pubbl. n. 251 del Progetto Finalizzato Geodinamica, pp. 449–461.

Marroni, M., Ottria, G., and Pandolfi, L. 2010. Note illustrative della Geologica d'Italia alla scala 1:50,000. Foglio 196 'Cabella Ligure'. ISPRA, Istituto Superiore per la Protezione e la Ricerca Ambientale.

Meisina, C., and Piccio, A. 2003. River dynamics and slope processes along a sector of the Villalvernia-Varzi Line (Northern Italy). Quaternary International, 101–102, 179–190.

Meisina, C., Zucca, F., Fossati, D., Ceriani, M., and Allievi, J. 2006. Ground deformation monitoring by using the permanent scatterers technique: The example of the Oltrepo Pavese (Lombardia, Italy). Engineering Geology, 88, 240–259.

Molli, G., Crispini, L., Malusà, M., Mosca, P., Piana, F., and Federico, L. 2010. Geology of the Western Alps- Northern Apennine junction area: A regional review. Journal of the Virtual Explorer, 36, paper 9.

O'Leary, D. W., Friedman, J. D., and Pohn, H. A. 1976. Lineament, linear, lineation: Some proposed new standards for old terms. Geological Society of America Bulletin, 87, 1463–1469.

Omran, A., Hahn, M., Hochschild, V., El-Rayes, A. H., and Geriesh, M. 2012. Lithological mapping of Dahab Basin, South Sinai, Egypt, using ASTER Data. Geoinformation 6/2012.

Pandian, M., Shruthi, N., and Pavithra, K. 2016. A Geomatics approach – structural mapping and automatic lineament extraction in parts of central Tamil Nadu. International Journal of Geology and Earth Sciences, 2(4), 11–18.

Panini, F., Fioroni, C., Fregni, P., and Bonacci, M. 2002. Le rocce caotiche dell'Oltrepo pavese: Note illustrative della carta geologica dell'Appennino Vogherese tra Borgo Priolo e Ruino. Atti Ticinensi di Scienze delle Terra, 43, 83–109.

PCI Geomatics Ltd. 2017. https://www.pcigeomatics.com/.

Pellegrini, L., and Arzani, C. 1997. Evoluzione morfoneotettonica nel basso Appennino Pavese-Piacentino: l'esempio del T. Gualdora, affluente del T. Tidone (Piacenza, Italia Settentrionale). Italian Journal of Quaternary Sciences, 10(2), 603–608.

Pellegrini, L., and Vercesi, P. L. 1995. Considerazioni morfoneotettoniche sulla zona a sud del Po tra Voghera (PV) e Sarmato (PC). Atti Ticinensi di Scienze delle Terra, 38, 95–118.

Piazza, A., Artoni, A., and Ogata, K. 2016. The Epiligurian wedge top succession in the Enza Valley (Northern Apennines): evidence of a syn-depositional transpressive system.

Planchon, O., and Darboux, F. 2002. A fast, simple and versatilealgorithm to fill the depressions of digital elevation models. Catena, 46, 159–176.

Ricci Lucchi, F., and Ori, G. G. 1985. Syn-orogenic deposits of migrating basin systems in the NW Adriatic Foreland. In P. Allen and P. Homewood (Eds.), "Foreland Basins Symp. Excursion Guidebook", IAS, pp. 137–176.

Scagni, G., and Vercesi, P. L. 1987. Il messiniano tra la Valle Versa e la Valle Staffora (Appennino pavese-vogherese) Considerazioni Paleogeografiche. Atti Ticinensi di Scienze delle Terra, 31, 1–20.

SERVIZIO GEOLOGICO D'ITALIA. (1965). Carta Geologica d'Italia alla scala 1:100.000, Foglio 59 Pavia, II edizione. Roma.

SERVIZIO GEOLOGICO D'ITALIA. 1969. Carta Geologica d'Italia alla scala 1:100.000, Foglio 71 Voghera, II edizione. Roma.

SERVIZIO GEOLOGICO D'ITALIA. 2005. Carta Geologica d'Italia alla scala 1:50.000, Foglio 179 Ponte dell'Olio. Roma.

SERVIZIO GEOLOGICO D'ITALIA. 2010. Carta Geologica d'Italia alla scala 1:50.000, Foglio 178 Cabella Ligure. Roma.

SERVIZIO GEOLOGICO D'ITALIA. 2014. Carta Geologica d'Italia alla scala 1:50.000, Foglio 178 Voghera. Roma.

Taramelli, T. 1882. Descrizione geologica della Provincia di Pavia, con annessa Carta Geologica. Stab. Civelli G., 1–163. Milano.

Toscani, G., Seno, S., Fantoni, R., and Rogledi, S. 2006. Geometry and timing of deformation inside a structural arc; the case of the western Emilian folds (Northern Apennine front, Italy). Bollettino Della Società Geologica Italiana, 125(1), 59–65.

Vercesi, P. L., Falletti, P., Pasquini, C., Perotti, C., Tucci, G., and Papani, L. 2014. Carta Geologica d'Italia alla scala 1:50,000. Foglio 178 'Voghera', note illustrative InfoCartoGrafiche – Piacenza. ISPRA, Istituto Superiore per la Protezione e la Ricerca Ambientale.

Vercesi, P. L., and Scagni, G. 1984. Osservazioni sui depositi conglomeratici dello sperone collinare di Stradella. Rend. Soc. Geol. It., 7, 23–26.

Zhumabek, Z., Assylkhan, B., Alexandr, F., Dinara, T., and Altynay, K. 2017. Automated lineament analysis to assess the geodynamic activity areas. Procedia Computer Science, 121, 699–706.

CHAPTER II: "I calanchi"

Bosino Alberto, Omran Adel, Maerker Michael (2019). Identification, characterisation and analysis of the Oltrepo Pavese calanchi in the Northern Apennines (Italy)

Geomorphology, 340, 53-66

Abstract

Badlands are characteristic erosional forms distributed along the entire Apennines. In the Italian context Badlands areas are called “calanchi”, the plural of the word “calanco”. In this paper we present the first calanchi inventory map of the Oltrepo Pavese area, Northern Apennines (Italy). In total 263 calanchi were mapped using remote sensing techniques like Orthophotos, Google Earth images, as well as field recognition. Moreover, calanchi were characterised from a geomorphologic, geologic and a morphometric point of view. The calanchi of the Oltrepo Pavese have been categorised in two geomorphological classes based on process related morphologies. In the study area calanchi mainly occur in soft sedimentary bedrock materials such as melanges, marls, claystones, and interstratified rocks. The results show that calanchi formations are often related to faults and tectonic lineaments present in the study area. Moreover, we analyse a 5m cell size Digital Terrain Model to detect correlations between calanchi and morphometric indices. The calanchi, defined and categorised for the first time in the study area, show typical morphometric characteristics of Apennine calanchi forms and features. In particular, they occur on concave south-facing slopes on soft bedrock formations. Finally, a multitemporal air photo interpretation over a 40 years period indicated a general decrease in calanchi areas. The area reduction is mainly correlated to intensive land use changes combined with variations of precipitation pattern. The revegetation trend was also confirmed by NDVI analysis based on Landsat satellites images. The calanchi were digitized and stored in a GIS database providing the information for future quantitative modelling assessments.

1. Introduction

Badland formations consist of a range of erosional forms and processes such as rill–interrill, piping, mass movements, as well as gullying, mud- and debris flows (Alexander, 1980, 1982). Badlands are considered as areas endangering agricultural activities though they have important ecological functions and are hotspot areas of biodiversity i.e. Bollati et al. (2016). Thus, Badlands can be seen as sensitive indicators of global change effects. Generally, Badlands are characterised by steep slopes, high relief and unconsolidated material (Torri et al., 2000).

However, humans play a key role in triggering the process dynamics leading to Badlands formation. Human impacts can be traced back to Roman times and in some areas up to the Neolithic revolution (e.g., Buccolini et al., 2007; Del Monte, 2017). Human activity influences the composition of flora and fauna (land use) as well as soils (irrigation, fertilization, erosion) and potentially indices on the regional climate (global warming). In the Italian context Badlands areas are called "calanchi" derived from the Latin verb "chalare" meaning slowly falling or slumping down (Bucciante, 1922). The identification, characterisation and temporal assessment of spatial variations in calanchi areas was studied in Italy since the beginning of the last century (e.g., Bucciante, 1922; Castiglioni, 1933; Biancotti and Cortemiglia, 1982; Farabegoli and Agostini, 2000; Calzolari and Ungaro, 1998; Moretti and Rodolfi, 2000; Battaglia et al., 2002; Buccolini and Coco, 2010, 2013; Bollati et al., 2012; Caraballo-Arias et al., 2014, 2015; Coco et al., 2015; Bianchini et al., 2016; Bollati et al., 2016; Cappadonia et al., 2016; Caraballo-Arias and Ferro, 2016, 2017; Del Monte, 2017; Brandolini et al., 2018). The formation of calanchi is mainly related to accelerated erosional processes (e.g., Battaglia et al., 2002) due to surface and subsurface runoff in soils often characterised by low permeability. The erosion of the substrates and soils highly depends on the presence/absence of vegetation and should therefore be accounted for in assessments of landscape degradation and/or recovery (Molina et al., 2009). Over the long term, vegetation can increase soil organic matter, improve soil physical properties

and reduce soil erodibility, as well as runoff and erosion to a safe level (Zhang et al., 2015). Furthermore, the physical and chemical properties of the parent material are important factors in the development of rills and pipes (Hodges and Bryan, 1982; Faulkner et al., 2004; Vergari et al., 2013; Bollati et al., 2016). Moreover, the smectite rich soils favour shrinks and swell phenomena facilitating in dry periods preferential infiltration and piping whereas in wet periods overland flow and rill erosion prevail (Picarreta et al., 2006).

However, as mentioned above, investigations on calanchi processes and forms are mainly concentrating in central and southern parts of Italy. In the north-western Apennines the phenomena were studied by Bucciante (1922) as well as Biancotti and Cortemiglia (1982). A part of these case studies, no recent and systematic work have been conducted. Thus, the purpose of this study is aimed at a systematic assessment of the spatial-temporal distribution of Badlands in the Oltrepo Pavese (Figure 1). Figure 2 illustrates a comparison between four Italian calanchi maps evidencing that the calanchi of the Oltrepo Pavese have been revealed in Bucciante (1922), (Figure 2a) but they are not mentioned in subsequent works e.g., Alexander (1980) (Figure 2b); Alexander (1982) (Figure 2c); Phillips (1998) (Figure 2d). Moreover, in this study we want to characterise the calanchi forms and processes in terms of their environmental characteristics such as climate, geology and substrates, vegetation, topographic aspects and human induced land use changes to detect the related driving factors.

Since calanchi areas are important hotspots for biodiversity and geodiversity (Della Seta et al., 2009; Maccherini et al., 2011; Gallart et al., 2013) the knowledge of the spatial distribution and temporal dynamics are important for regional planning and ecosystem conservation.

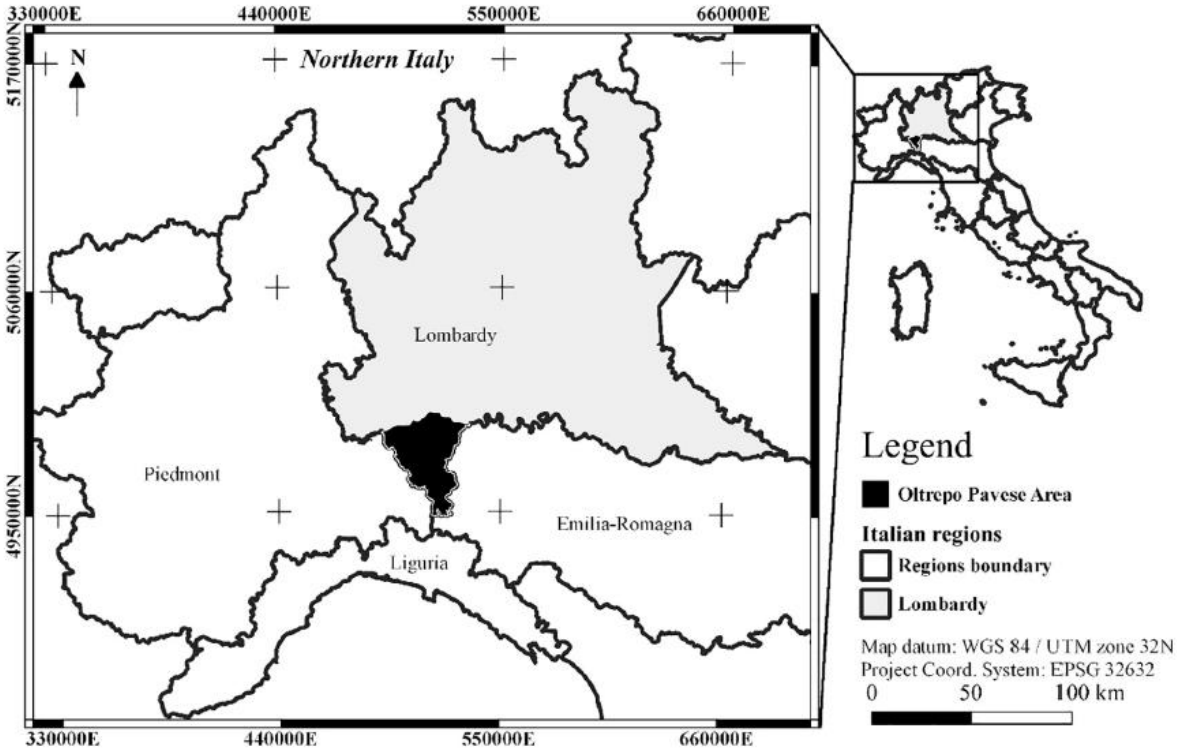

Figure 1. Study area.

2. Study area

The study area (Figure 1) covers approximately 1110 km^2 and comprise the southern part of the Lombardy Region located in Pavia province, South of the Po River. The Oltrepo Pavese is characterised by medium to high relief ranging between 60 m.a.s.l. close the Po River, up to 1724 m.a.s.l. at the top of Monte Lesima. The climate of the Oltrepo Pavese is defined as temperate (Ardenghi and Polani, 2016) belonging to a temperate oceanic climate (Cfb) following the Köppen climate classification (Kottek et al., 2006). The precipitation ranges between 400 mm/year close to the Po plain and 1600 mm/year in the southern mountainous parts (ARPA Lombardia; Rossetti and Ottone, 1979). The study area is characterised by four major geological Units namely Subligurian, Ligurian, Tertiary Piedmont Basin (TPB) and Epiligurian Units. These Units overthrusted each other during the Apennine formation generating a very complex geological and tectonic framework (Vercesi et al., 2014).

Figure 2. Comparison between calanchi maps: (a) modified from Bucciante (1922); (b) modified from Alexander (1980); (c) modified from Alexander (1982); (d) modified from Phillips (1998).

The geological Units are composed by different formations characterised by a variety of lithologies, mainly represented by soft sedimentary rocks. Bosino et al. (2019) evidence that the dominant lithotypes are composed of soft sedimentary marls, melanges, claystones, sandstones and interstratified rocks (Figure 3). The main structural element of the study area is represented by the Villalvernia-Varzi line, an east strike slip fault, which juxtapose the TDB formation with the Epiligurian Units (i.e. Bellinzona et al., 1971; Meisina and Piccio, 2003; Festa et al., 2015). Moreover, the Northern Apennines are also characterised by a set of faults and tectonic lineaments, which follow three main directions identified by Panini et al. (2002); i) NW/ SE defined as 'Apennines direction', ii) NE/SW defined as 'Anti Apennines direction'

as well as iii) the N/S and E/W directions mainly representing strike-slip faults (Panini et al., 2002).

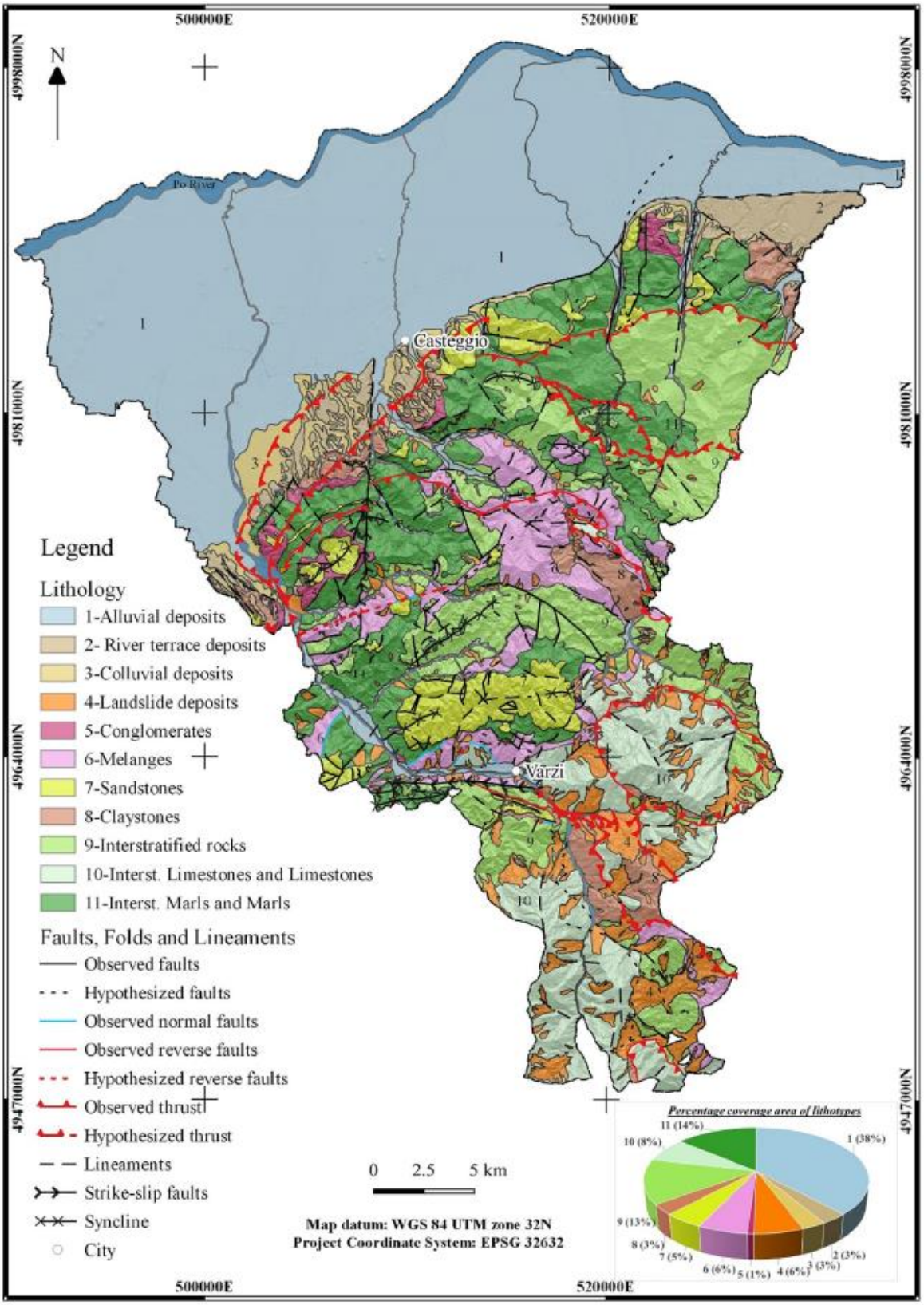

Figure 3. Litho-structural map of the Oltrepo Pavese. (Modified from Bosino et al. (2019).)

From a geomorphological point of view, the area is largely controlled by lithological and structural conditions (Pellegrini and Vercesi, 2017). The distribution of the lithological Units causes variations in surface processes and hence, in landscape evolution. In the southern sector of the study area the dominant outcrops are represented by interstratified limestones and carbonate rocks, which are related to the mountainous landscape, characterised by highly relief energy and "V" shaped valleys. In the central part of the Oltrepo Pavese high erodible rocks are prevailing such as claystones, melanges, marls and interstratified rocks, related to a hilly landscape. In the northern part of the Oltrepo Pavese alluvial deposits of the Po river and of its tributaries generated vast deposition cones and alluvial lowlands (Bosino et al., 2019). In addition, faults and tectonic lineaments play and important role in the landform evolution acting as preferential interference lines in a complex geological setting. The main geomorphological processes and related forms are associated to surface and subsurface runoff as well as mass movements (Figure 4).

Figure 4. Water-related erosion forms and processes of the Oltrepo Pavese. (a) Rill-Interrill erosion and depositional area; (b) Gullying; (c) Piping; (d) Shallow landslides.

The main forms and features related to the above cited processes can be subdivided in:

- Rill-Interrill erosion forms: consisting of i) interrill erosion that is based on laminar flow and the respective soil particle detachment and transport. Instead, rill erosion is the removal of soil by concentrated water running through little streamlets on unvegetated or semi-vegetated slopes. Rills are defined by Nearing et al. (1997) as "ephemeral concentrated flow paths", usually with dimensions in the order of some centimetres (Figure 4a).
- Gully erosion forms: Gully erosion is the removal of soil by concentrated water running through streamlets and channels (Figure 4b). The gullies are also defined as "erosional channels that are too large to be removed easily with standard tillage equipment" (Hassett and Banwart, 1992).
- Piping forms: Piping erosion is caused by sub-surface water flow. Soil particles are detached by hypodermic (interflow) water fluxes causing topsoil collapse and the formation of discontinuous gullies (Jones, 2004; Verachtert et al., 2013) (Figure 4c).
- Landslides: Denudation processes due to shallow landslides, mass flow, and other gravitative processes (Figure 4d). In the study area the dominant processes are represented by shallow landslides which are triggered by extreme rainfall events (Zizioli et al., 2013; Bordoni et al., 2015).

As stated above, the aim of the study is the spatial temporal assessment of the calanchi of the Oltrepo Pavese representing the complex interaction of the above cited processes.

3. Methods

The calanchi characterisation consists in different steps illustrated by the flow chart (Figure 5) and described below.

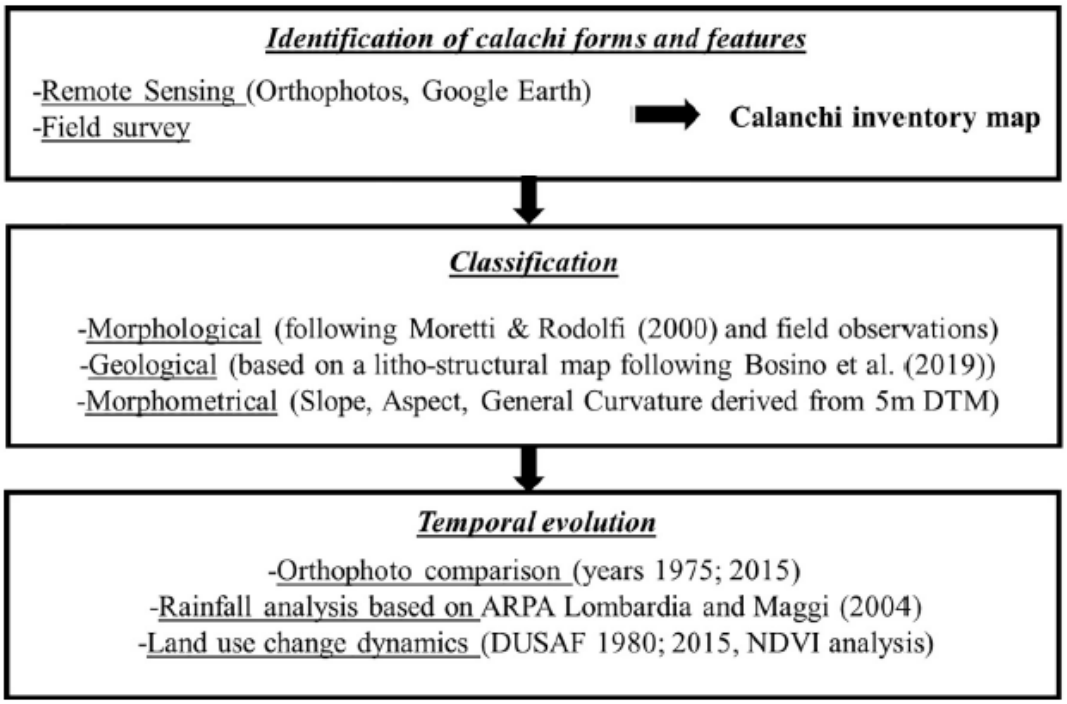

Figure 5. Flow chart illustrating the calanchi assessment approach.

3.1. Identification of calanchi forms and features

Calanchi areas were identified and mapped through orthophotos provided by the 'Geoportale della Regione Lombardia' (http://www.geoportale.regione.lombardia.it/) taking into account the years 1975, 2015, Google Earth Images (different sources from 1999 to 2015) and field surveys. The mapped areas were digitized and reported in a shape file format using QGIS (QGIS, 2018). Subsequently, attribute information was added to the vectorized objects (id, type, surface area). Finally, a calanchi inventory map of the study area was generated (Figure 6a).

3.2. Classification

An initial morphological classification of calanchi forms and features was performed starting from the direct observation of the forms in the field and following the classification developed by Moretti and Rodolfi (2000). Thus, calanchi were divided in Type A (Figure 6b) which can be described as having knife-shape slopes, sparse vegetation, high drainage pattern and no

gravitational process, and Type B (Figure 6c) that, conversely represents soft morphologies with diffuse vegetation and/or landslide processes.

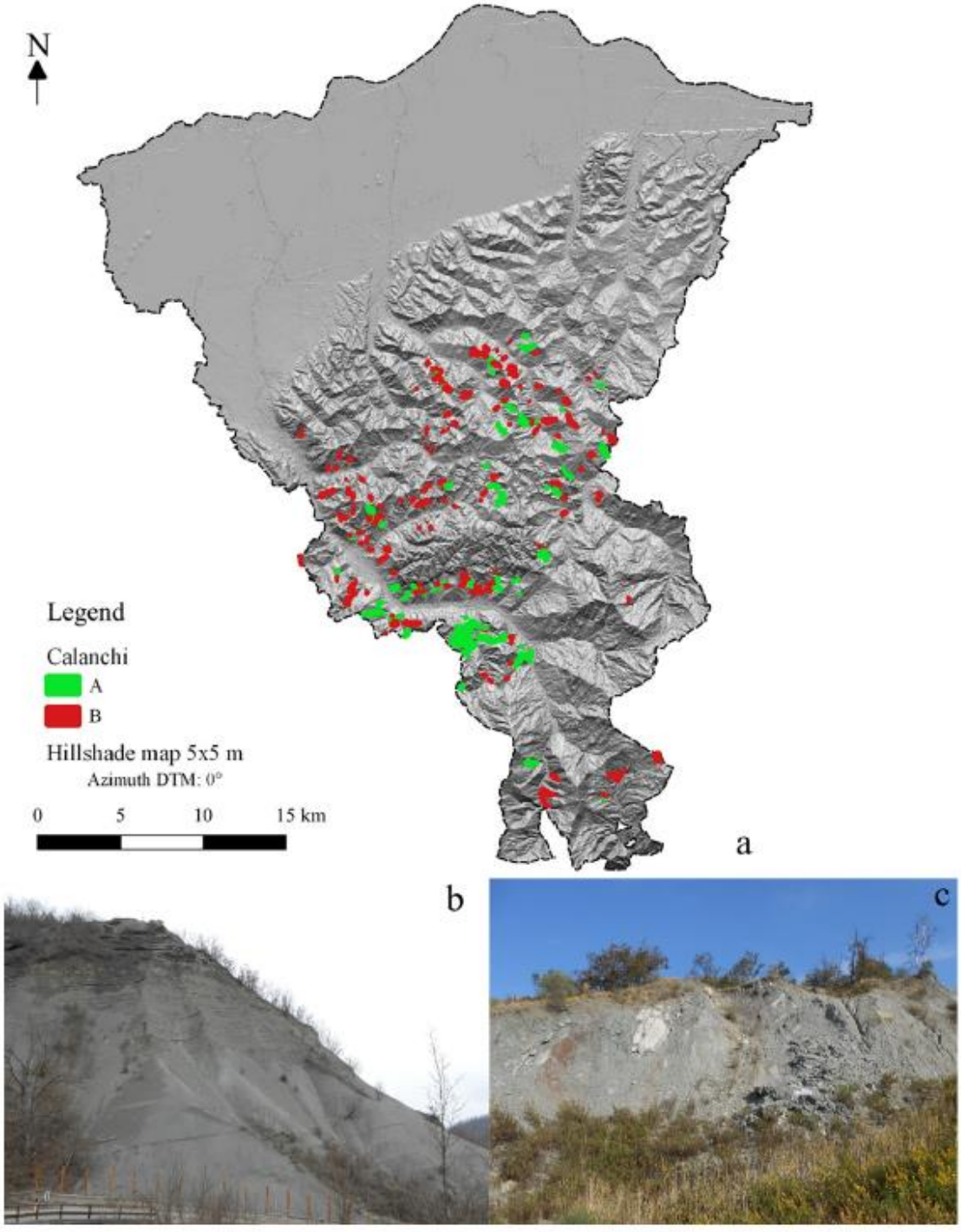

Figure 6. (a) Calanchi inventory map; (b) example of calanchi type A; (c) example of calanchi type B.

Type C calanchi that have been proposed by Ciccacci et al. (2008) are not present in the study area. Indeed, the observations in the Radicofani area (Tuscany) cannot be confirmed. In the

Oltrepo Pavese area mass movements seemto be the initial triggering process of calanchi development. In our work we define calanchi in terms of the total area, so we do not refer to every little horse-shoe type hydrographic unit. However, in our study a calanchi area is represented by only one calanchi type (A or B). Moreover, the calanchi were classified from a lithological point of view employing the 1:50.000 scale litho-structural map of the Oltrepo Pavese (Bosino et al., 2019) in order to find correlations between morphology and lithology. Since many calanchi develop on the boundary between different geological formations, each calanco was rasterized using a 5 m cell size and converted into a point cloud attributing the lithology type. In addition, the study area is characterised by several faults, folds and tectonic lineaments. These elements can be considered as local weak zones inducing or favouring erosional processes. In order to find a correlation between geological structures and calanchi forms and features the distances between each calanco and the surrounding structures were calculated (Bollati et al., 2019).

Furthermore, the morphometric indices such as slope, aspect and general curvature were automatically derived from a Digital Terrain Model (DTM) with 5 m cell size. The DTM was provided by the Geoportale della Lombardia (http://www.geoportale.regione.lombardia.it/). We use SAGA GIS (Conrad et al., 2015) to delineate the three morphometric indices. The DTM was hydrologically corrected to eliminate sinks using the algorithm proposed by Wang and Liu (2006). Following Bianchini et al. (2016), the slopes ranging between 0° and 90° were split in 8 classes, the aspect ranging from 0° to 360° was divided in 9 classes and the general curvature which ranges between −1 and +1 was divided into 3 classes (−1 to −0.002 concave slopes, −0.002 to 0.002 plan slopes, and 0.002 to 1 convex slopes), (Figure 9). These indices have been attributed to the point cloud of the calanchi dataset and the average result for each single calanco was statistically assessed and plotted using R.

3.3. Temporal evolution

To assess the temporal evolution of calanchi in terms of their spatial extent, we compared in detail two pairs of orthophotos of the years 1975 (autumn) and 2015 (late summer) that have an appropriate scale of 1:15.000. Subsequently, we investigated the changes and causes of the area variation through field survey, field observations of the vegetation and land use as well as through a detailed analysis of the rainfall dataset.

Even if the pluviometric data are fragmented in the study area two measuring stations located at Varzi and Torre degli Alberi were taken into consideration. The dataset covers the period 1951–2017 and was obtained merging the results of Maggi (2004) and data provided from ARPA Lombardia (http://www.arpalombardia.it/Pages/Informativa-Privacy.aspx#). We examined the pluviometric trend over a period of 40 years by plotting the average annual rainfall. Finally, the pluviometric trend was analysed comparing the average precipitation trend for the decades 1965–1975 and 2005–2015.

Furthermore, two land use datasets, DUSAF 1980 and 2015 provided by the Geoportale della Lombardia (http://www.geoportale.regione.lombardia.it/) were investigated and the percentages of the major land use classes were calculated. Vegetation cover monitoring gives valuable information about the impact of climate change on erosion processes in the study area. Satellite data and derived vegetation indices like the Normalized Difference Vegetation Index (NDVI) provide information on the spatial distribution of green biomass that in turn deliver insights into the effect of the green cover on soil erosion and the evolution of the calanchi forms. The spatio-temporal variations are assessed through the comparison of three multispectral medium resolution images recorded between 1975 and 2014 for the Oltrepo Pavese area.

For the derivation of the NDVI we used the red and near-infrared spectral bands, from the longest available multi sensor time series. The image selection was based on the following

criteria: i) synchronicity, ii) lowest cloud cover as catalogued by USGS (2019) and iii) a visual inspection of the images.

The series include three images recorded from different earth observation satellite platforms over a 40-years period. We acquired images from the Landsat 2 (L)-4 Multispectral Scanner (MSS) (August 1975), L-5 Thematic Mapper (TM) (June 1994) and Landsat 8 of August 2014. All the acquired images have been pre-georeferenced to UTM zone 32, WGS 84 and ortho-rectified using the DTM (see above). The radiometrically and geometrically corrected images are processed in this study using Envi Software Version 4.5.

The NDVI computed from the near-infrared and red bands of the calibrated images of each year provided a representation of the green vegetation cover distribution. We used the following bands for the NDVI calculation provided by the different platforms: a) band 4 (red) and band 6 (near infrared) from the Landsat 2- MSS image b) band 3 (red) and band 4 (near infrared) from the Landsat 5 image while c) for the Landsat 8 band 4 (red) and band 5 (near infrared) were selected. The NDVI images were classified into ordinal categories representing the vegetation cover of the study area according to Weier and Herring (2000): i) no vegetation for values <0.1, ii) medium vegetation between 0.1 and 0.3 and iii) dense vegetation cover with values >0.3. However, classes 2 and 3 are changing according to the Landsat platforms used as follows: from 0.2 to 0.7 for Landsat 2 (MMS), from 0.3 to 1 for Landsat 5 while Landsat 8 ranges from 0.3 to 1. These intervals were used to compare the images and to understand the evolution of the vegetation within last 40 years in the Oltrepo Pavese.

4. Results and discussion

The main result of this study is represented by the first inventory map of the calanchi forms and features located in the Oltrepo Pavese. Subsequently, we assessed their geomorphological, geological and temporal characteristics and the related driving factors.

In total 263 calanchi were digitized based on the orthophotos of 2015 and the available Google Earth Images. Moreover, the database was validated and refined by an extensive field survey. The calanchi cover and area of 6.9 km2. Based on their forms and features as well as on the respective set of processes, calanchi were classified in Type A and B. In total 32% of the calanchi belong to Type A and cover an area of 3.5 km^2 and 68% belong to Type B covering an area of 3.4 km2. Type B calanchi are described as complex erosional forms showing rill-interrill erosion, gullying, piping, and often are affected by mass movements. Observing the distribution of the calanchi we find a high concentration in the central part of the study area where the soft sedimentary formations crop out. In order to characterise the calanchi forms and features from a geological point of view the inventory dataset was rasterised (5 m cell size) and subsequently converted into a point cloud format. To each point, the lithology was assigned. Finally, we plotted the calanchi point cloud against the lithotype (Figure 7a) and also single calanchi against the lithotype (Figure 7b). The results show a correlation between lithotype and geomorphological characteristics of calanchi forms and features. The Type A are predominantly related to interstratified rocks, which are represented by terrigenous turbiditic deposits of the Northern Apennines. The combination of layers with different geological characteristics, such as centimetric massive strata of sandstone and metric layers of weak fine sediments, allows the formation of well-developed calanchi (Figure 6b). However, the Type A evolves also in fine calcareous sandstones, marls and interstratified marls, melanges and claystone deposits. The fine textured and homogeneous lithotypes generate high surface runoff and generate well defined calanchi.

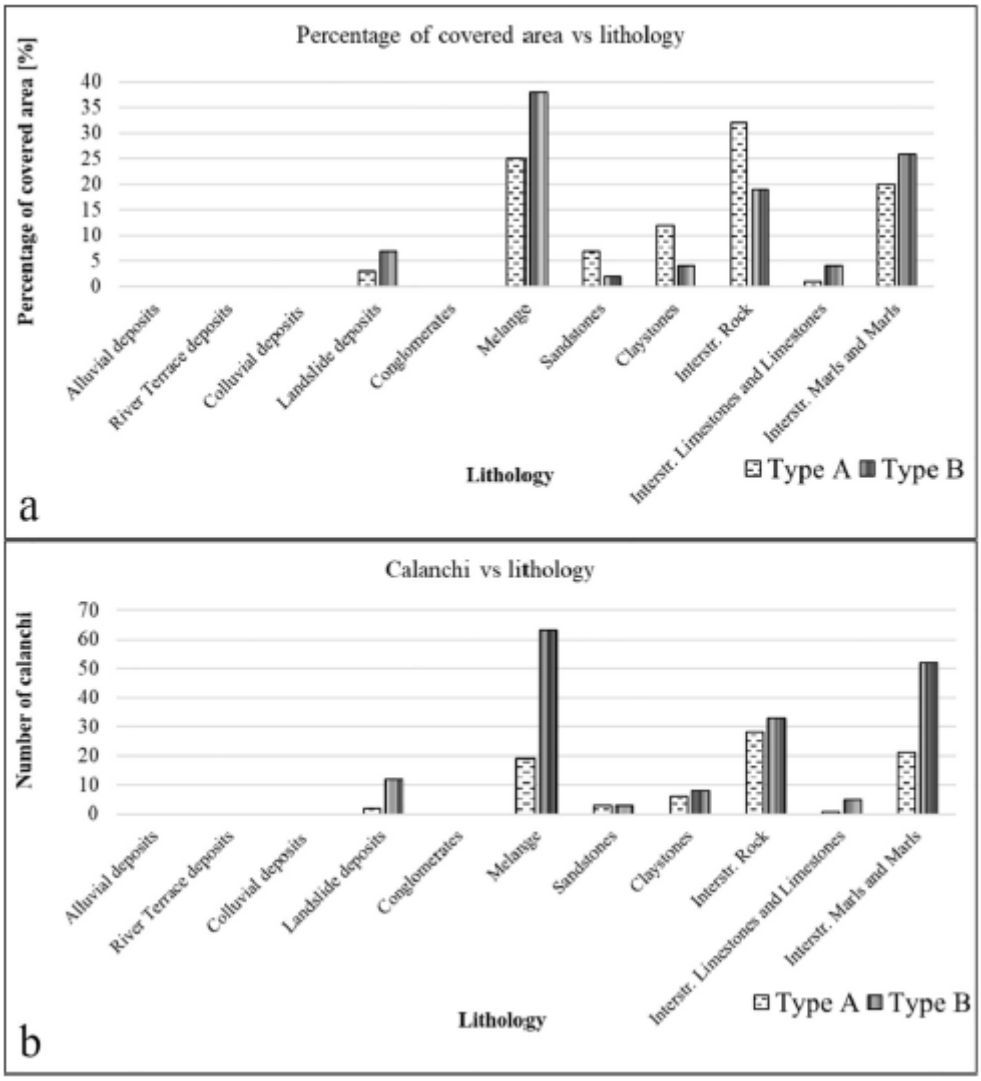

Figure 7. Calanchi Type A and Type B versus the lithotype of the Oltrepo Pavese (a) shows the relation lithology-point cloud and (b) the relation lithology-single calanco. The lithotypes reported are the 11-lithologies following the 1:50.000 litho-structural map of the Oltrepo Pavese, Bosino et al. (2019).

Conversely, the Type B is mainly dominant in the melange formations. The classic melanges, also called "Complessi di Base", are represented by chaotic blocks in a fine clayey matrix (Panini et al., 2002). Weathering and erosional processes yield block falls which are incorporated into the melanges. Moreover, the fine and heterogeneous matrix is susceptible to mud and mass flows causing complex calanchi shapes. Furthermore, landslides contribute substantially to the evolution, or the formation of calanchi in the study area. Generally, landslides, usually triggered by intense precipitation events, induce the exposure of bedrock in which water-driven erosional processes take place forming initially rills, gullies and finally

calanchi forms and features. Moreover, type B calanchi are characterised also by interstratified marls and marls, interstratified rocks, claystone and sandstone. Finally, the geomorphological and geological characterisation indicate that: Type A calanchi represent relatively active forms and features, where the modelling processes are still ongoing. On the other hand, Type B calanchi are characterised by smooth topography and substrates and generally show a much slower development. However, we have no clear evidence that Type A calanchi might be younger than Type B calanchi.

Furthermore, we studied the correlation between erosional forms and tectonic elements characterising the study area. Therefore, the distance from each calanco to the nearest tectonic element was calculated (Bollati et al., 2019).

Figure 8a shows a close-up window of the Oltrepo Pavese where the calanchi are in close contact to the main tectonic elements and allineated with the principal lineaments reported on the litho-structural map of the Oltrepo Pavese (Bosino et al., 2019). Figure 8b shows the resulting histogram evidencing a correlation between geological structures and calanchi.

Finally, we took in consideration three morphometric indices derived from the DTM. The average values of slope, aspect and general curvature were calculated asmean value for each calanco area and plotted in R. The results show that 88.4% of calanchi belong to slope classes between 10 and 40°, are exposed mainly to southern directions (90–270°) and have prevalently convex slopes (from 0.002 to 1) (Figure 9). These results are partially in accordance with Della Seta et al. (2009). In fact, the calanchi of the Oltrepo Pavese are in average more steep than the ones in Southern Tuscany. Regarding aspect and general curvature of the Oltrepo Pavese calanchi our study is in line with Della Seta et al. (2009) mainly manifesting convex south-facing slopes. Concerning the temporal evolution of the calanchi a comparison between two sets of orthophotos was conducted. Figure 10 shows the area variation between the calanchi in 1975 and 2015. Over a 40 years period we observe that 73% of calanchi show a decrease in

average area of ca. 34% and intensified revegetation processes, documented by NDVI values that increase from 0.26 in 1975 to 0.38 in 2014.

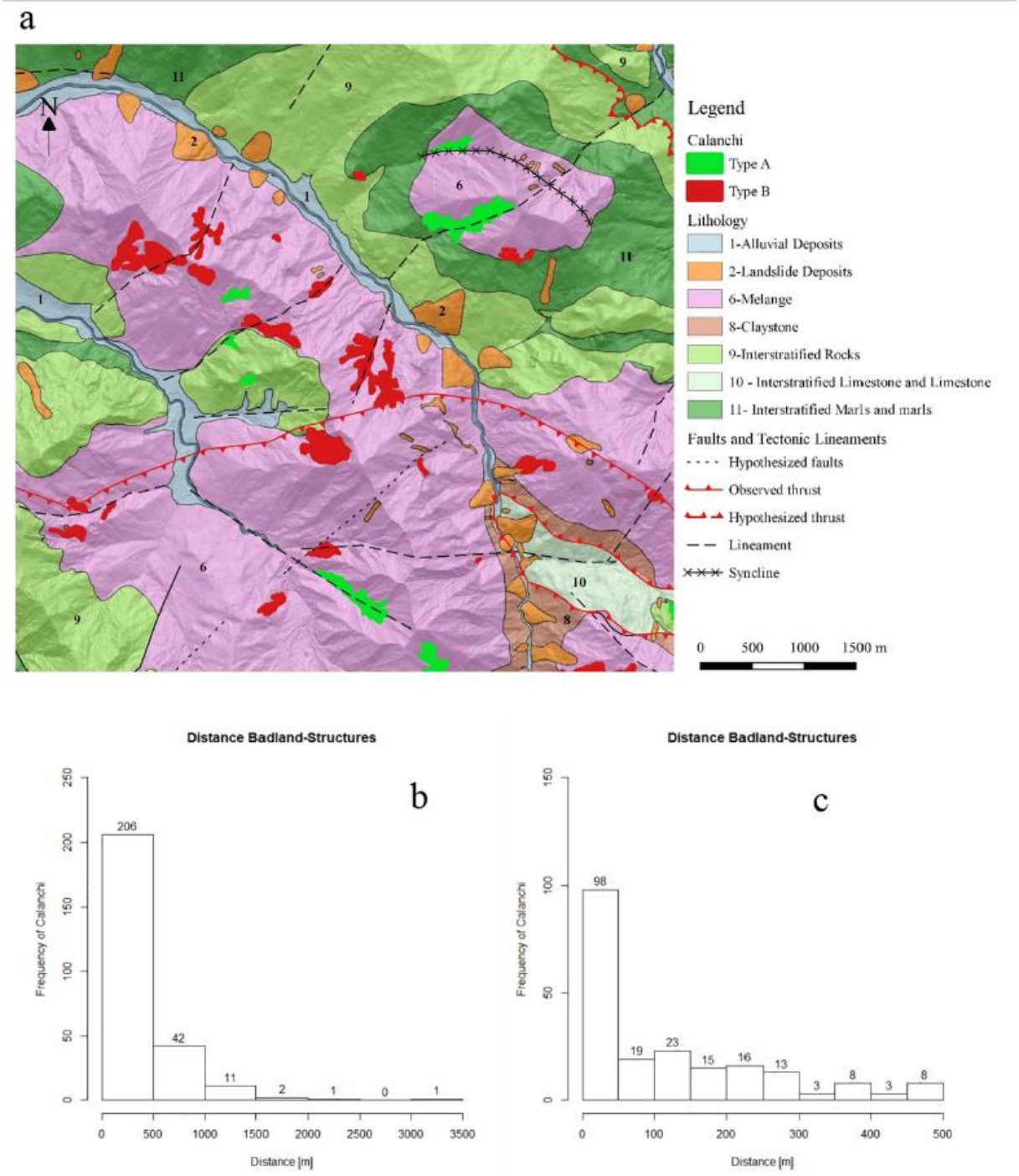

Figure 8. (a) Calanchi type A and B and their correlation with structural elements according to Bosino et al. (2019). (b) Histogram showing distance of calanchi to structural elements. (c) Close up of the calanchi distance to structural elements within a range of 500 m.

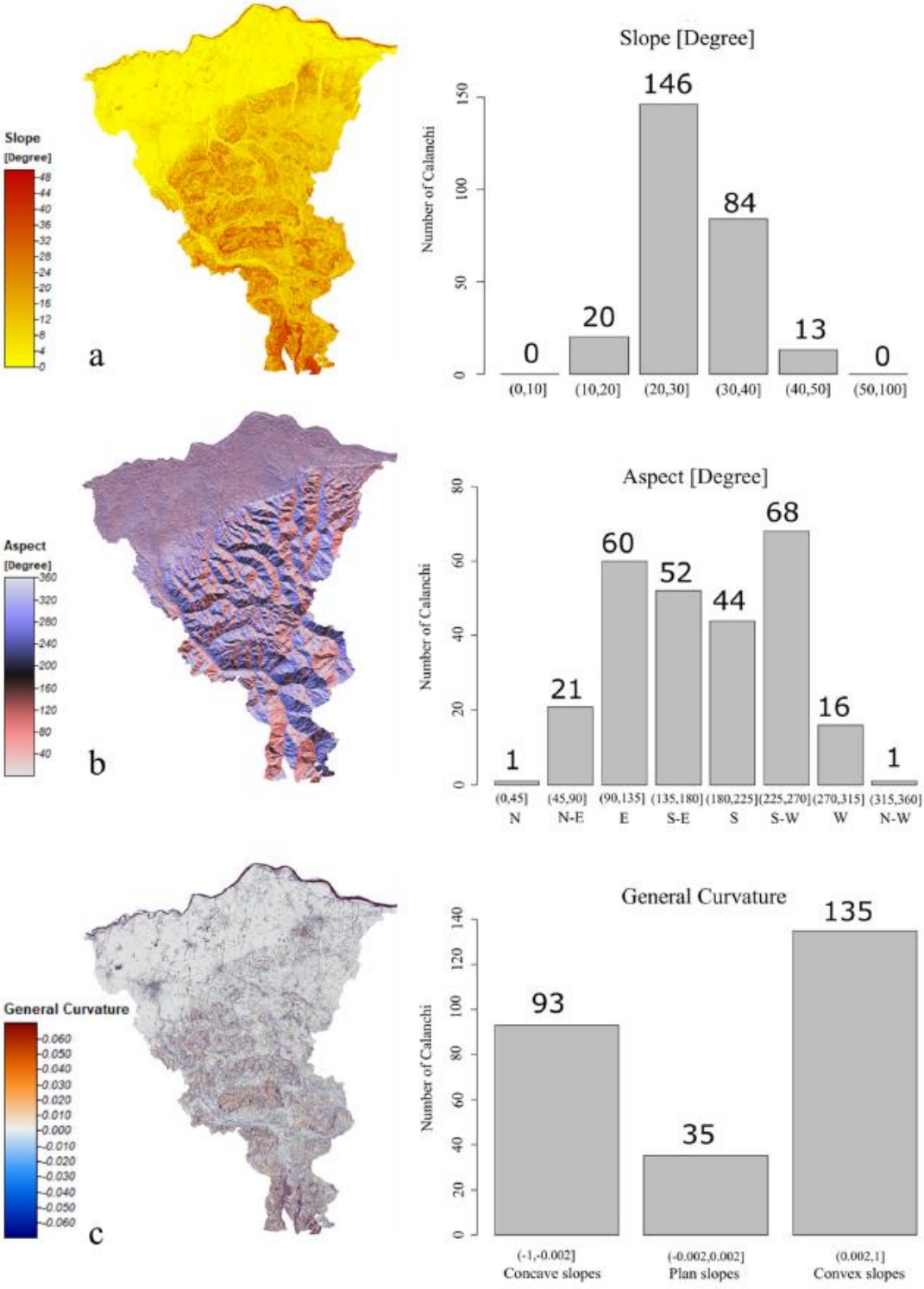

Figure 9. Morphometric parameters calculated as mean value from the point cloud of each calanco; (a) Slope, (b) Aspect, (c) General Curvature.

Observing the orthophoto of 1975 (Figure 10a) we identified rows of trees planted around the calanchi. Typically, associations of Fraxinus excelsior L, Fraxinus ornus L. and Pinus nigra were identified by field survey (Figure 11 a and b respectively).

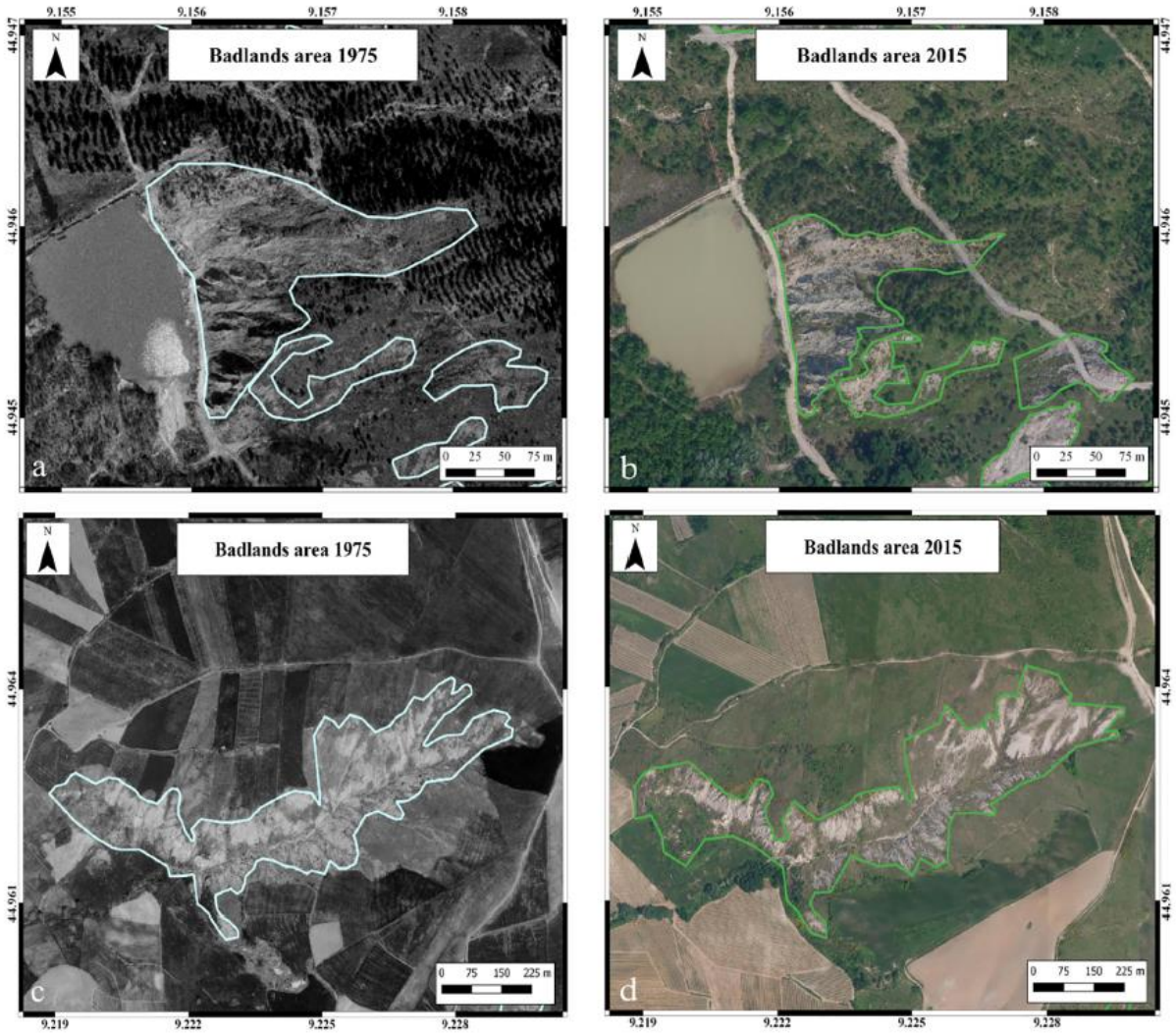

Figure 10. Example of area variation over a 40 years period. SRWGS 84 EPSG 4326. (a-c) Orthophotos of the year 1975 and (b-d) Orthophotos of the year 2015.

Where planting operations were performed 40 years ago (Figure 10a) the area of the calanchi significantly decreased i.e. 51% as shown in Figure 10a/b. Conversely where planting operation was not done (Figure 10c) the calanchi developed further in terms of the classic retrogressive processes (Figure 10d) and hence, the area was increasing. The material eroded from the calanchi areas is usually deposited in the interfluves or at the base of each calanco. In general, these deposits are less sloping and are characterised by more silty-sandy textures compared to

the clayey bedrock (Figs. 8, 9 and 11). The combination of low slopes and more silty textured sediments in the interfluves allows the infiltration of water and permits the vegetation to establish and grow up (Figure 11c) causing in turn a reduction in the calanco area.

Figure 11. Vegetation on calanchi. (a) Fraxinus excelsior L. (b) Pinus nigra. (c) Revegetation in the accumulation zone.

However, the area variation is the result of natural and anthropic factors, which trigger vegetation growth and erosional processes. Major drivers for vegetation growth and soil erosion is the precipitation intensity and duration, as well as land use changes. As specified by Gallart et al. (2002) calanchi can develop in different climatic conditions. Gallart et al. distinguish the

calanchi occurring in arid (precipitation b200 mm), semiarid (precipitation 200–700 mm) and humid climates (precipitation N700 mm). Consequently, the amount of vegetation is controlled by the climate conditions. In fact, in arid conditions the vegetation does not play a significant role on water erosion control. Conversely in semiarid conditions the annual rainfall partially controls the vegetation cover and the erosion rates. However, also exposition and bedrock type are fundamental parameters for vegetation growth. Finally, in humid conditions, a dense vegetation cover contrasts the erosional rate fixing the soils and substrates (e.g., Richard and Mathys, 1999). The Oltrepo Pavese ranges between semiarid and humid conditions (Figure 12). Figure 12 shows a sinusoidal trend of the precipitations for two climate stations (Varzi and Torre degli Alberi) during the period 1951 to 2017. As reported in several studies the average annual precipitation trend is decreasing in amplitude i.e. Buffoni et al. (1999); Brunetti et al. (2006) even though the precipitation intensity is increasing during the last 50 years (Brunetti et al., 2001). These considerations can be adopted also for the Oltrepo Pavese. As shown by the trend lines reported in Figure 12, the average annual amount of rainfall is decreasing.

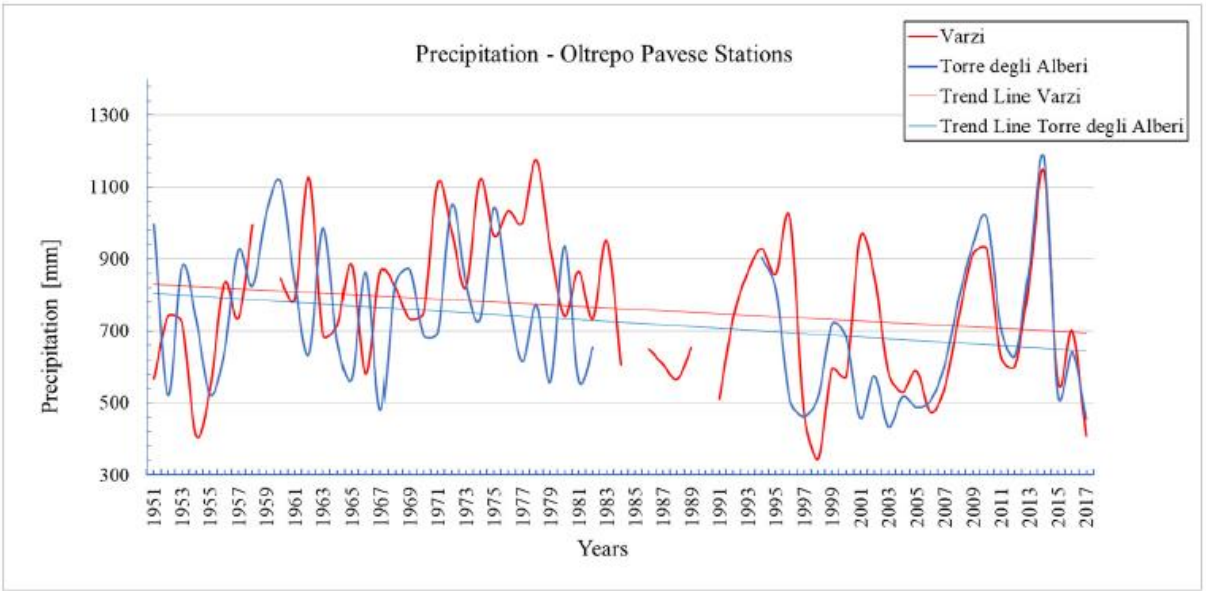

Figure 12. Annual mean precipitation in time for the Varzi and Torre degli Alberi stations.

We analysed the average annual precipitation over two 10 years periods, from 1965 to 1975 and from 2005 to 2015. The average annual precipitation decreases from 875 mm/yr to 723

mm/yr (17%) for the Varzi station and from 787 mm/yr to 751 mm/yr (4%) for the Torre degli Alberi station.

The decreasing precipitation leads to revegetation processes around calanchi areas, due to less surface runoff and thus, erosion processes. This point was confirmed by the NDVI analysis. NDVI values document an increase in vegetation from 51% to 78% from 1975 to 2014 (Figure 13).

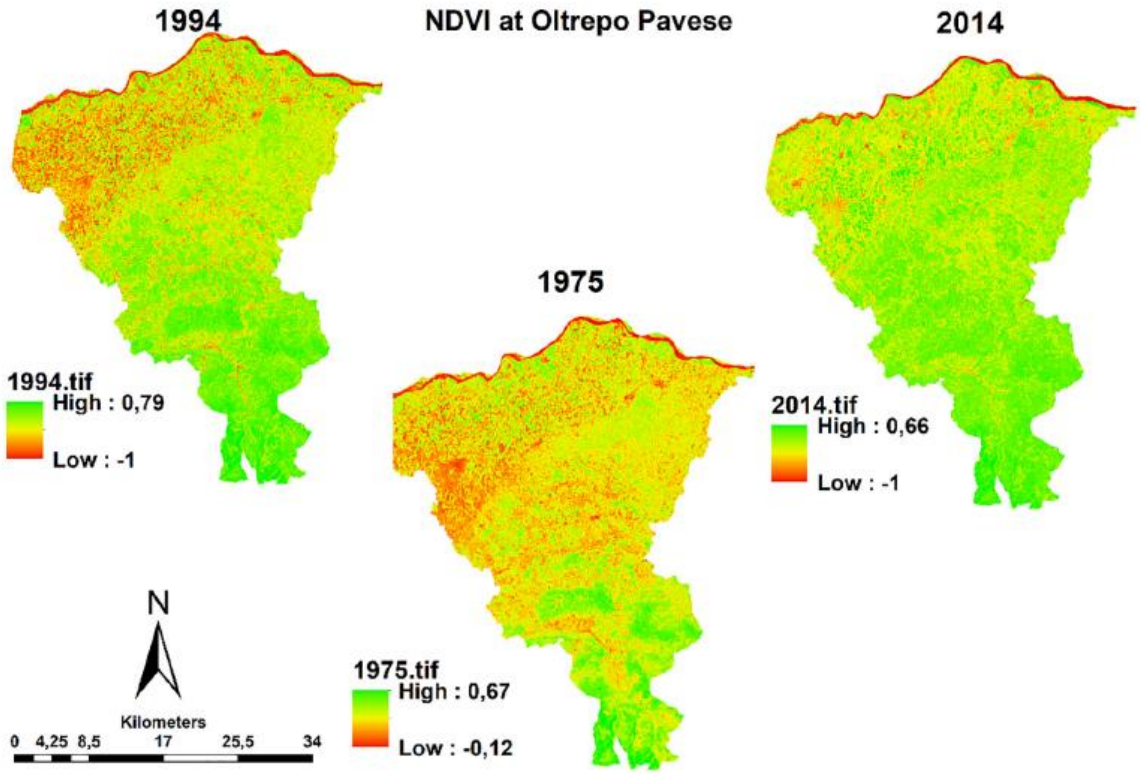

Figure 13. Spatial distribution of NDVI values for different time steps in the Oltrepo Pavese.

Moreover, the spatial extent of green cover in the entire study area increased from 570 km^2 in 1975 to 858 km^2 in 2014. While the dense vegetation cover (class iii) increased in the calanchi areas from 1,7 km^2 (24% of the total calanchi area) in 1975 to 4.9 km^2 (72% of the total calanchi area) in 2014 (Figure 13). The increase of the vegetation cover confirms a stabilisation of the study area and hence, less intensive soil erosion process dynamics. This trend is coming along with profound land use changes (Table 1) that stabilises the areas around the calanchi. In fact,

the differences in land use types between 1980 and 2015 show a decrease of vineyards, orchards, and agricultural fields and an increase of forests and other natural green covers.

Table 1
Land use change in the period 1980–2015 in Oltrepo Pavese (from DUSAF 1980–2015).

ID	Area 1980 [km^2]	Area 2015 [km^2]	Δ [%]
11-Urban area	22	58.9	+167.7
12-Industry	8.3	26.2	+215.6
13-Waste areas	1.6	2.91	+81.8
14-Green urban areas	0.1	6.6	+6500
21-Agricultural fields	572	416	−27
22-Vineyards and orchards	202.2	173.1	−14.5
23-Meadows	44.7	46.2	+3.4
31-Forests	197.8	280	+41.5
32-Bushes	32.2	68.6	+113
33-Sparse vegetation	11.3	13.6	+20.3
51-Water	20.2	20.2	0

In the study area the forest cover increases about 41.5% from 197.8 km^2 in 1980 to 280 km^2 in 2015. On the one hand a decrease of agricultural activity (especially vineyards) favours revegetation and especially an increases of bush and forest covers. Moreover, also the artificial planting actions around the calanchi contributed to the stabilisation of the calanchi area. However, this trend in calanchi area reduction is not in line with research carried out in the same climatic condition in central Italy (see e.g., Ciccacci et al., 2009; Vergari et al., 2013) as well as in the hot Mediterranean climate (Köppen Csa) of Southern Italy (e.g., Capolongo et al., 2008). In both cases the intensification of erosion rates as well as an increase of their area is documented.

This means also, that according to our study, the Northern Apennine calanchi are as must be seen in a different way. The decrease in calanchi areas is mainly due to a general revegetation trend that in turn is driven by profound land use changes and afforestation operations. Concerning the precipitation amount and intensities, the revegetation trend seems to be sustained or at least the effects of precipitation changes are less impacting than the land use changes.

5. Conclusion

In this study we detect and classify for the first time the calanchi of the Oltrepo Pavese area. In total 263 calanchi, covering an area of 6.9 km^2, were identified. The calanchi were classified both from a geomorphological and a geological point of view. We found a dominance of type B calanchi, that are complex Badlands consisting of several erosional processes and related landslides. Type B calanchi prevail in the soft sedimentary bedrocks, that characterise large parts of the Oltrepo Pavese (melanges, claystone, interstratified rocks etc.). They are often associated with faults and tectonic lineaments present in the study area. We extracted three main morphometric indices from the DTM (5 m) and show that calanchi preferentially occur on slopes between 10° and 40°, they have convex slopes and are exposed to Southern directions. In the last 40 years, 73% of calanchi of the Oltrepo Pavese significantly reduce their size (ca. 34% in average) and they show a trend to stabilisation. Several studies regarding the erosional rates on the Badlands of the central and Southern Apennines (e.g., Capolongo et al., 2008; Vergari et al., 2013) as well as in central Mediterranean regions (e.g., Faulkner et al., 2003; Romero-Díaz et al., 2007; Lesschen et al., 2008) show an increase of erosion rates due to cropland abandonment. Also, on the long term there seems to be a trend of a badland increase as shown by Ciccacci et al. (2009) studying the Badlands of Tuscany over a period of 50 years. However, in the Northern Apennines there are no studies or published data concerning area variation or erosion rate changes in Badlands areas. In the Oltrepo Pavese the area reduction of the calanchi was mainly caused by a combination of natural and anthropic processes. On the one hand the average annual precipitation decreases although the precipitation amount still remains within the humid and/or semiarid classes following Gallart et al. (2002). Thus, the study area shows a decrease in surface runoff and related erosion processes and hence, favoured revegetation processes. On the other hand, land use changes cause a reduction of calanchi area. Exposed and more susceptible land use types decrease such as agricultural fields (−27%),

vineyard and orchards (−14.5%), whereas more protective landuse types increase such as forests (+41.5%), sparse vegetation (+20.3%) and bushes (+113). Moreover, planting operations performed with Pinus nigra and Fraxinus excelsior L, around the Badlands areas also contribute to an area reduction of Badlands.

Acknowledgements

This research was conducted with financial support of the Earth and Environmental Sciences PhD program of University of Pavia, Department of Earth and Environmental Sciences.

References

Alexander, D.E. 1980. I Calanchi — accelerated erosion in Italy. Geography 65, 95–100.

Alexander, D.E. 1982. Differences between “Calanchi” and “biancane” Calanchi in Italy. In: Bryan, R., Yair, A. (Eds.), Badland Geomorphology and Piping. Geo Books Norwich, pp. 71–87.

Ardenghi, N.M.G., Polani, F. 2016. La flora della provincia di Pavia (Lombardia, Italia settentrionale). 1. L'Oltrepò Pavese. Natural History Sciences. Atti Soc. it. Sci. nat. Museo civ. Stor. Nat. Milano 3(2), 51–79.

ARPA Lombardia, http://www.arpalombardia.it/siti/arpalombardia/meteo/richiestadati-misurati/Pagine/RichiestaDatiMisurati.aspx.

Battaglia, S., Leoni, L., Sartori, F. 2002. Mineralogical and grain size composition of clays developing Calanchi and biancane erosional landforms. Geomorphology, 49, 153–170.

Bellinzona, G., Boni, A., Braga, G., Marchetti, G. 1971. Note Illustrative della Carta Geologica D'Italia in scala 1:100,000 – Foglio 71 Voghera. Serv. Geol. d'It. 121, Roma.

Bianchini, S., Del Soldato, M., Solari, L., Nolesini, T., Pratesi, F., Moretti, S. 2016. Badland susceptibility assessment in Volterra municipality (Tuscany, Italy) by means of GIS and statistical analysis. Environ. Earth Sci., 75, 889.

Biancotti, A., Cortemiglia, G.C. 1982. Morphogenetic evolution of the river system of south piedemont (Italy). Geogr. Fis. Dinam. Quat., 5. 10–13.

Bollati, I., Della Seta, M., Pelfini, M., Del Monte, M., Fredi, P., Palmieri, E.L. 2012. Dendrochronological and geomorphological investigations to assess water erosion and mass wasting processes in the Apennines of Southern Tuscany (Italy). Catena, 90, 1–17.

Bollati, I., Vergari, F., Del Monte, M., Pelfini, M. 2016. Multitemporal dendrogeomorphological analysis of slope instability in upper Orcia Valley (Southern Tuscany, Italy). Geogr. Fis. Din. Quat., 39, 105–120.

Bollati, I.M., Masseroli, A., Mortara, G., Pelfini, M., Trombino, L. 2019. Alpine gullies system evolution: erosion drivers and control factors. Two examples from the western Italian Alps. Geomorphology, 327, 248–263.

Bordoni, M., Meisina, C., Valentino, R., Bittelli, M., Chersich, S. 2015. Site-specific to local scale shallow landslides triggering zones assessment using TRIGRS. Nat. Hazards Earth Syst. Sci., 15, 1025–1050.

Bosino, A., Pellegrini, L., Omran, A., Bordoni, M., Meisina, C., Maerker, M., 2019. Litho-structure of the Oltrepo Pavese, Northern Apennines (Italy). Journal of Maps, 15(2), 382–392.

Brandolini, P., Pepe, G., Capolongo, D., Cappadonia, C., Cevasco, A., Conoscenti, C., Marsico, A., Vergari, F., Del Monte, M. 2018. Hillslope degradation in representative Italian areas: just soil erosion risk or opportunity for development? Land Degrad. Dev., 29, 3050–3068.

Brunetti, M., Colacino, M., Maugeri, M., Nanni, T. 2001. Trends in the daily intensity of precipitation in Italy from 1951 to 1996. Int. J. Climatol., 21, 299–316.

Brunetti, M., Maugeri, M., Monti, F., Nanni, T. 2006. Temperature and precipitation variability in Italy in the last two centuries from homogenised instrumental time series. Int. J. Climatol. 26, 345–381.

Bucciante, M. 1922. Sulla distribuzione geografica dei Calanchi in Italia. L'universo. 38, 585–605.

Buccolini, M., Coco, L. 2010. The role of the hillside in determining the morphometric characteristics of “Calanchi”: the example of Adriatic central Italy. Geomorphology, 123, 200–210.

Buccolini, M., Coco, L. 2013. MSI (morphometric slope index) for analysing activation and evolution of Calanchi in Italy. Geomorphology, 191, 142–149.

Buccolini, M., Gentili, B., Materazzi, M., Aringoli, D., Pambianchi, G., Piacentini, T. 2007. Human impact and slope dynamics evolutionary trends in the monoclinal relief of Adriatic area of central Italy. Catena, 71, 96–109.

Buffoni, L., Maugeri, M., Nanni, T. 1999. Precipitation in Italy from 1833–1996. Theor. Appl. Climatol., 63, 33–40.

Calzolari, C., and Ungaro, F. 1998. Geomorphic features of a badland (biancane) area (Central Italy): characterisation, distribution and qualitative spatial analysis. Catena, 31, 237–256.

Capolongo, D., Pennetta, L., Picarreta, M., Fallacara, G., Boenzi, F. 2008. Spatial and temporal variations in soil erosion and deposition due to land-levelling in a semi-arid area of Basilicata (Southern Italy). Earth Surf. Process. Landforms, 233, 364–379.

Cappadonia, C., Coco, L., Buccolini, M., Rotigliano, E. 2016. From slope morphometry to morphogenetic processes: an integrated approach of field survey, geographic

information system morphometric analysisis and statistics in italian Calanchi. Land Degrad. Develop. 27, 851–862.

Caraballo-Arias, N.A., Ferro, V. 2016. Assessing, measuring and modelling erosion in Calanchi areas: a review. Journal of Agricultural Engineering XLVII 573, 181–190.

Caraballo-Arias, N.A., Ferro, V. 2017. Are calanco landforms similar to river basins? Sci. Total Environ. 603-604, 244–255.

Caraballo-Arias, N.A., Conoscenti, C., Di Stefano, C., Ferro, V. 2014. Testing GIS-morphometric analysis of some Sicilian Calanchi. Catena, 113, 370–376.

Caraballo-Arias, N.A., Conoscenti, C., Di Stefano, C., Ferro, V. 2015. A new empirical model for estimating Calanchi Erosion in Sicily, Italy. Geomorphology, 231, 292–300.

Castiglioni, B. 1933. Osservazioni sui Calanchi appenninici. Estr. da: Boll. Della Soc. Geologica Ital. 52, 1933, fasc.2.

Ciccacci, S., Galiano, M., Roma, M.A., Salvatore, M.C. 2008. Morphological analysis and erosion rate evaluation in badlands of Radicofani area (Southern Tuscany — Italy). Catena, 74, 87–97.

Ciccacci, S., Galiano, M., Roma, M.A., Salvatore, M.C. 2009. Morphodynamics and morphological changes of the last 50 years in a Badlands sample area of Southern Tuscany (Italy). Z. Geomorphol., 53(3), 273–297.

Coco, S., Brecciaroli, G., Agnelli, A., Weindorf, D., Corti, G. 2015. Soil genesis and evolution on Calanchi (badland-like landform) of central Italy. Geomorphology, 248, 33–46.

Conrad, O., Bechtel, B., Bock, M., Dietrich, H., Fischer, E., Gerlitz, L., Wehberg, J., Wichmann, V., Böhner, J. 2015. System for Automated Geoscientific Analyses (SAGA) v. 2.1.4. Geosci. Model Dev., 8, 1991–2007.

Del Monte, M. 2017. The Typical Badlands Landscape Between the Tyrrhenian Sea and the Tiber River. © Springer International Publishing AG 2017 M. Soldati and M. Marchetti

(eds.), Landscapes and Landforms of Italy. World Geomorphological Landscapes. 281–291.

Della Seta, M., Del Monte, M., Fredi, P., Palmieri, E.L. 2009. Space-time variability of denudation rates at the catchment and hillslope scales on the Tyrrhenian side of Central Italy. Geomorphology, 107 (3–4), 161–177.

Farabegoli, E., Agostini, C. 2000. Identification of calanco, a badland landform in the Northern Apennines, Italy. Earth Surf. Process. Landform, 25, 307–318.

Faulkner, H., Alexander, R., Wilson, B.R. 2003. Changes to the dispersive characteristics of soils along an evolutionary slope sequence in the Vera Badlands, southeast Spain: implications for site stabilization. Catena, 50, 243–254.

Faulkner, H., Alexander, R., Teeuw, R., Zukowskyj, P. 2004. Variations in soil dispersivity across a gully head displaying shallow sub-surface pipes, and the role of shallow pipes in rill initiation. Earth Surf. Process. Landforms., 29 (1143), 1160.

Festa, A., Fioraso, G., Bissacca, E., Petrizzo, M.R. 2015. Geology of the Villalvernia – Varzi Line between Scrivia and Curone valleys (NW Italy). Journal of Maps, 11(1), 39–55.

Gallart, F., Solè, A., Puigdefàbregas, J., Lázaro, R. 2002. Calanchi System in the Mediterranean. -in: BULL, L.J. and M.J. Kirkby (eds): Dryland Rivers: Hydrology and Geomorphology of Semi-Arid Channels. -Chichester: John Wiley and Sons Ltd. 299–326.

Gallart, F., Marignani, M., Pérez-Gallego, N., Santi, E., Maccherini, S. 2013. Thirty years of studies on badlands, from physical to vegetational approaches. A succinct review. Catena, 106, 4–11.

Hassett, J.J., Banwart, W.L. 1992. Soils and Their Environment. vol. 424. Prentice-Hall, Englewood Cliffs, NJ. Hodges, W.K., Bryan, R.B., 1982. The influence of material

behaviour on runoff initiation in the Dinosaur Badlands, Canada. In: Bryan, R., Yair, A. (Eds.), Badland Geomorphology and Piping. Geo Books Norwich England, pp. 13–46.

Jones, J.A.A. 2004. Pipe and piping. Goudie AS (Eds) Encyclopedia of Geomorphology Routledge, pp. 784–788.

Kottek, M., Grieser, F., Beck, C., Rudolf, B., Rubel, F. 2006.Worldmap of the Köppen-Geiger climate classification updated. Meteorol. Z. 15(3), 259–263.

Lesschen, J.P., Cammeraat, L.H., Nieman, T. 2008. Erosion and terrace failure due to agricultural land abandonment in a semi-arid environment. Earth Surf. Process. Landforms, 33, 1574–1584.

Maccherini, S., Marignani, M., Gioria, M., Renzi, M., Rocchini, D., Santi, E., Torri, D., Tundo, J., Honnay, O. 2011. Determinants of plant community composition of remnant biancane Badlands: a hierarchical approach to quantify species-environment relationships. Applied Vegetation Sciences, 14, 378–387.

Maggi, I. 2004. Le precipitazioni nella valutazione dell'erosione del suolo e dell'instabilità dei versanti. Università degli studi di Pavia, Dipartimento di Scienze della Terra e dell'Ambiente. Dottorato di Ricerca in Scienze della Terra XV ciclo. Pavia.

Meisina, C., and Piccio, A. 2003. River dynamics and slope processes along a sector of the Villalvernia-Varzi Line (Northern Italy). Quat. Int., 101-102, 179–190.

Molina, A., Govers, G., Van den Putte, A., Poesen, J., Vanacker, V. 2009. Assessing the reduction of the hydrological connectivity of gully systems through vegetation restoration: field experiments and numerical modeling. Hydrol. Earth Syst. Sci., 13, 1823–1836.

Moretti, S., and Rodolfi, G. 2000. A typical “Calanchi” landscape on the Eastern Apennines margin (Atri, Central Italy): geomorphological features and evolution. Catena, 40, 217–228.

Nearing, M.A., Norton, L.D., Bulgakov, D.A., Larionov, G.A., West, L.T., Dontsova, K.M. 1997. Hydraulics and erosion in eroding rills. Water Resour. Res., 33(4), 865–887.

Panini, F., Fioroni, C., Fregni, P., Bonacci, M. 2002. Le rocce caotiche dell'Oltrepo Pavese: Note illustrative della carta geologica dell'Appennino Vogherese tra Borgo Priolo e Ruino. Atti Ticinensi di Scienze delle Terra 43, 83–109.

Pellegrini, L., Vercesi, P.L. 2017. Landscape and Landforms Driven by Geological Structures in the North-western Apennines. © Springer International Publishing AG 2017 M. Soldati and M. Marchetti (eds.), Landscapes and Landforms of Italy. World Geomorphological Landscapes. 203–213.

Phillips, C.P. 1998. The Badlands of Italy: a vanishing landscape. Appl. Geogr., 18(3), 243–257.

Picarreta, M., Faulkner, H., Bentivenga, M., Capolongo, D. 2006. The influence of physicochemical material properties on soil erosion processes in the Badlands of Basilicata, Southern Italy. Geomorphology, 81, 235–251.

QGIS Development Team, 2018. QGIS Geographic Information System. Open Source Geospatial Foundation Project. http://qgis.osgeo.or.

Richard, D., Mathys, S. 1999. Historique, contexte technique et schientifique des BVRE de Draix Caractéristiques, dennées disponiblkes et princepaux résultats acquisi au cours de dix ans de suivi- In N. Mathys (Ed.) Les bassins versants expérimentaux de Draix, laboratoire d'étude de l'érosion en montagne. Cemagref, Antony, 11–28.

Romero-Díaz, A., Marin Sanleandro, P., Sanchez Soriano, A., Belmonte Serrato, F., Faulkner, H. 2007. The causes of piping in a set of abandoned agricultural terraces in southeast Spain. Catena, 69, 282–293.

Rossetti, R., and Ottone, C. 1979. Esame preliminare delle condizioni pluviometriche dell'Oltrepò Pavese e dei valori critici delle precipitazioni in relazione ai fenomeni di dissesto franoso. Geologia Applicata e Idrogeologia, 14(3), 83–99.

Torri, D., Calzolari, C.M., Rodolfi, G. 2000. Badlands in changing environments: an introduction. Catena 40 (2), 119–125. United States Geological Survey-Earth Explorer. Available online: http://earthexplorer. usgs.gov (accessed on 10 January 2019).

Verachtert, E., Van Den Eeckhaut, M., Martínez-Murillo, J.F., Nadal-Romero, E., Poesan, J., Devoldere, S., Wijnants, N., Deckers, J. 2013. Impact of soil characteristics and land use on pipe erosion in a temperate humid climate: field studies in Belgium. Geomorphology, 192, 1–14.

Vercesi, P.L., Falletti, P., Pasquini, C., Perotti, C., Tucci, G., Papani, L. 2014. Carta Geologica d'Italia alla scala 1:50,000. Foglio 178 'Voghera', note illustrative InfoCartoGrafiche – Picenza. ISPRA (Istituto Superiore per la Protezione e la Ricerca Ambientale).

Vergari, F., Della Seta, M., Del Monte, M., Barbieri, M. 2013. Badlands denudation "hot spots": the role of parental material properties on geomorphic processes in 20 years monitored sites of Southern Tuscany (Italy). Catena, 106, 31–41.

Wang, L., and Liu, H. 2006. An efficient method for identifying and filling surface depressions in digital elevation models for hydrologic analysis and modelling. Int. J. Geogr. Inf. Sci. 20(2), 193–213.

Weier, J., Herring, D. 2000. Measuring Vegetation (NDVI and EVI). NASA Earth Observatory, Washington DC.

Zhang, L., Wang, J., Bai, Z., Lv, Ch. 2015. Effects of vegetation on runoff and soil erosion on reclaimed land in an opencast coal-mine dump in a loess area. Catena, 128, 44–53.

Zizioli, D., Meisina, C., Valentino, R., Montrasio, L. 2013. Comparison between different approaches to modelling shallow landslide susceptibility: a case history in Oltrepò Pavese, Northern Italy. Nat. Hazards Earth Syst. Sci., 13, 559–573.

CHAPTER III: "GEOSTATISTICS"

Bosino Alberto, Paolo Giordani, Geraldine Quénéhervé, Maerker Michael (2020). Assessment of calanchi and rill-interrill erosion susceptibilities using terrain analysis and geostochastics: A case study in the Oltrepo Pavese, Northern Apennines, Italy

Earth Surface Processes and Landforms, 45, 3025-3041

Abstract

Soil erosion is one of the most important environmental problems distributed worldwide. In the last decades, numerous studies have been published on the assessment of soil erosion and the related processes and forms using empirical, conceptual and physically based models. For the prediction of the spatial distribution, more and more sophisticated stochastic modelling approaches have been proposed – especially on smaller spatial scales such as river basins. In this work, we apply a maximum entropy model (MaxEnt) to evaluate Badlands (calanchi) and rill–interrill (sheet erosion) areas in the Oltrepo Pavese (Northern Apennines, Italy). The aim of the work is to assess the important environmental predictors that influence calanchi and rill–interrill erosion at the regional scale. We used 13 topographic parameters derived from a 12 m digital elevation model (TanDEM-X) and data on the lithology and land use. Additional information about the vegetation is introduced through the normalized difference vegetation index based on remotely sensed data (ASTER images). The results are presented in the form of susceptibility maps showing the spatial distribution of the occurrence probability for calanchi and rill–interrill erosion. For the validation of the MaxEnt model results, a support vector machine approach was applied. The models show reliable results and highlight several locations of the study area that are potentially prone to future soil erosion. Thus, coping and mitigation strategies may be developed to prevent or fight the soil erosion phenomenon under consideration.

1. Introduction

Soil erosion is one of the most important environmental issues in Europe causing €1.25 billion/year of economic loss due to reduction of agricultural productivity (Panagos et al., 2018). The Mediterranean regions are in particular prone to water erosion due to the climatic regime and poor vegetation cover (Langbein and Schumm, 1958; Kepner et al., 1997). In Italy, water erosion causes on average 7.4 ton·ha^{-1}·yr^{-1} of soil loss (Bosco et al., 2015; Stolte et al., 2016). In this study, we focus on the assessment and the modelling of soil erosion forms and features in the Oltrepo Pavese, located in Lombardy Region, in the Northern Apennines. The economy of the region is mainly based on agricultural activities. In the study area vineyards and agricultural fields dominate the landscape. The Oltrepo Pavese is characterized by different aquatic erosional forms and features, such as rill-interrill erosion, piping, gullies, and shallow landslides. Additionally, in the study area badlands occur that represent complex composition of the above-mentioned soil erosion- and gravitational processes. However, the soil erosion and sediment dynamics due to surface and subsurface runoff in general, have only scarcely been studied in the Oltrepo Pavese (i.e. Ciancetti et al., 2008; Bosino et al., 2019a). In Italy, Badland formations are called ‘calanchi’, a plural term of ‘calanco’ meaning slowly falling or slumping down (Bucciante, 1922). Calanchi are defined as ‘intensely dissected natural landscapes where vegetation is sparse or absent and which are useless for agriculture’ (Bryan and Yair, 1982). Several studies on calanchi environments were carried on in Italy from the 1920ies onwards (see e.g. Bucciante, 1922; Castiglioni, 1933; Passerini 1937; Vittorini, 1977). During the following decades calanchi erosion have been widely studied from a qualitative and quantitate point of view. In many Italian regions the calanchi are directly associated with the soft unconsolidated, poorly consolidated sedimentary marine clays of Plio-Pleistocene Age (e.g. Phillips, 1998; Gallart et al., 2002; Piccarreta et al., 2006; Vergari et al., 2013; Bosino et al., 2019a). Several authors relate the calanchi formations with the lithological, mineralogical,

geochemical and pedological properties of the clayey deposits (Alexander 1982; Faulkner et al., 2000; Summa et al., 2007; Pulice et al., 2013; Vergari et al., 2013; Grubin et al., 2018). Consequently, calanchi mainly occur in lithologies like claystone, sandstone, interstratified rocks, marls and interstratified marls, melange and unconsolidated deposits. Especially the mineralogy characteristics of the clayey deposits, as well as the superficial crusts which form on the bedrock surface, play a significant role in the behavior of the bedrocks in terms of surface runoff (Grubin, 2013). In the Oltrepo Pavese and other Italian regions clay bedrock is often characterized by shrinking and swelling clays (i.e. smectite group minerals) and hence, are particularly prone to be eroded by running water (Faulkner, 2013; Moreno-de ls Heras and Gallart 2016). Instead, thick regolithes can prevent or limit soil erosion in calanchi areas (Gallart et al., 2002; Cocco et al., 2015). Other specific types of badlands which developed on clay rich deposits are called biancane (Battaglia et al., 2002). Biancane are morphologically characterized as dome-shaped slopes separated from low sloping surfaces (Pulice et al., 2013). Several authors relate the biancane as the end product of calanchi evolution (e.g. Alexander 1982; Pulice et al., 2013). However, in the Oltrepo Pavese area the Biancane are not present. Furthermore, the climatic condition plays a significant role in the formation and the development of calanchi forms and features. As reported by Gallart et al. (2002) the climate is the controlling factor on the balancing between vegetation and soil erosion. Gallart et al. distinguish the calanchi occurring in i) arid conditions (precipitation < 200 mm) on which both, the potential of vegetation colonisation and the erosion rate are low. ii) semiarid conditions (precipitation 200-700 mm) in which the vegetation may control soil erosion and iii) humid conditions (precipitation > 700 mm) with dense vegetation cover contrasting soil erosion dynamics. Finally, the topographic features (e.g. Calzolari and Ungaro 1998; Buccolini et al., 2012; Gallart et al., 2013; Cappadonia et al., 2016) and the human impact (e.g. Buccolini et al., 2007; Capolongo et al., 2008; Castaldi and Chiocchini 2012; Gallart et al., 2013; Torri et al.,

2013) may significantly contribute to the evolution and stabilisation of calanchi areas. During most of the 19th century the landforms were only assessed directly with extensive field surveys and through the identification of aerial photograph. In the last decades GIS systems allowed to detect and model the landforms through remotely sensed data and digital terrain analysis, directly conducted on Digital Elevation Models (Schillaci et al., 2015). Especially multispectral satellite images (i.e. LANDSAT TM/ETM data) can be utilized to estimate erosion forms and processes in badland areas (e.g. Liberi et al., 2009). Calanchi were described in detail by several authors in terms of both: i) field observations (e.g. Farabegoli and Agostini 2000; Battaglia, 2011) and ii) GIS-morphometrical analysis performed on high resolution DEM (e.g. Buccolini and Coco 2010, 2013; Caraballo-Arias et al., 2014, 2015; Cappadonia et al., 2016; Bosino et al., 2019a). Through morphometric indices the connectivity of calanchi landforms was evaluated (Faulkner 2008; Caraballo-arias et al., 2017) using parameters directly related to the drainage density and sediment transport efficiency. In this work, we focus on the assessment of the driving factors of soil erosion processes in the Oltrepo Pavese with special emphasis on calanchi and rill-interrill erosion forms and features. In the last decades several statistical approaches have been developed to evaluate specific erosion processes such as gully erosion (e.g. Conforti et al., 2011; Magliulo 2012; Conoscenti et al., 2013; Conoscenti et al., 2014; Gomez-Gutierrez et al., 2015; Angileri et al., 2016; Rahmati et al., 2017; Al-Abadi and Al-Ali 2018; Zakerinejad at al., 2018; Javidan et al., 2020) or rill-interrill (sheet) erosion (e.g. Conoscenti et al., 2008; Maerker et al., 2011; Magliulo, 2012; Angileri et al., 2016; Pournader et al., 2018). Instead, very few studies have been conducted on the susceptibility modelling of calanchi processes at local and/or basin scale (e.g. Phillips and Dudik, 1998; Vergari, 2015; Bianchini et al., 2016; Maerker et al., 2020). The above-mentioned studies generally focus on small to medium size catchments or slope systems. Susceptibility models based on stochastic approaches normally assess single erosion processes or differentiate between a set of simple

and individual erosion processes. To the knowledge of the authors no stochastic approaches have been applied so far to decipher between complex calanchi erosion or calanchi subtypes and simple erosion processes such as rill-interrill erosion. Moreover, a stochastic approach at regional scale have never been applied so far to decipher between calanchi and rill-interrill erosion processes in the Northern Apennines. Therefore, the aim of this paper is threefold: i) to assess the driving forces of rill-interrill and calanchi erosion processes applying a stochastic modelling approach. ii) to test if the approach can decipher between simple rill-interrill erosion processes and complex soil erosion features like calanchi and finally, iii) to predict the spatial distribution of erosion type susceptibilities on catchment scale based on the model results obtained using the stochastic model.

2. Study area

The study area (Figure 1) is located in the Oltrepo Pavese (Northern Apennines, Italy) and covers an area of roughly 1110 km^2. The Oltrepo Pavese is characterised by a topography of medium to high relief (Figure 2a) ranging between 60 m a.s.l. close the Po River up to 1724 m a.s.l. at the top of Monte Lesima. The climate of the Oltrepo Pavese is defined as temperate (Ardenghi and Polani, 2016), fitting to the temperate oceanic climate (Cfb) following the Köppen climate classification (Kottek et al., 2006). The precipitation ranges between 400 mm/year close to the Po Plain and 1600 mm/year in the southernmost mountainous parts (Rossetti and Ottone, 1979; ARPA Lombardia, 2019). As shown in (Figure 2b) the Oltrepo Pavese region is characterised by a dominant agricultural land use and is one of the most important cereal and vine growing regions of Italy (Regione Lombardia, DUSAF 2015). Agricultural fields and vegetable farming (gardens) are predominant in the northern part of the study area and in the flat valley bottoms on the mountainous parts. The principal agricultural crops are represented by cereals (corn, wheat and grain). Subsequently a large part of the hilly territory is covered by forest with high and low density, meadows and bushes. Moreover,

vineyards and orchards contribute to the rural sustainability of the territory. From a geological point of view the area is covered by soft sedimentary formations belonging to four major geological units namely Subligurian, Ligurian, Tertiary Piedmont Basin (TPB) and Epiligurian. The geological formations are grouped in 11 lithological classes according to the intrinsic lithological characteristics. As described by Bosino et al. (2019b) (Figure 3) the lithologies consist in: i) Alluvial deposits e.g. Voghera Syntem (VOH) (Bellinzona et al., 1971) characterised by gravel, sand, silt and clay deposits of the Po River and its tributaries. ii) River terrace deposits e.g. Codevilla Unit (LLX) (Bellinzona et al., 1971) constituted by pebbles scattered in a fine sandy, silty and clayey matrix. iii) Colluvial deposits e.g. Retorbido Group (RE) (Vercesi and Perotti, 2016) composed of sandy silt, silt and clay silt deposits. iv) Landslides deposits consisting of unlithified deposits generated by landslides and denudation processes. v) Conglomerates e.g. Cassano Spinola Conglomerates (CCS) (Boni and Casnedi, 1970) composed of paraconglomerates and orthoconglomerates, well rounded and usually orientated. vi) Melange Formations e.g. Brecce di Baiso (BAI) (Panini et al., 2002; Vercesi and Perotti, 2016) and Brecce Argillose di Costa Pelata (BPE) (Bellinzona et al., 1971) characterised by centimetric to metric blocks scattered in a fine clay matrix; vii) Sandstone e.g. Monte Vallassa Sandstone (AVL) Formation (Bellinzona et al., 1971) distinguished by massive or stratified sandstone, bioclastic sandstone often rich in fossils (i.e. foraminifers). In addition, the study area is characterised by viii) Claystone e.g. Cassio Varicoloured clays (AVV) Formation (Bellinzona et al., 1971) which are mainly composed by varicoloured claystone with subordinated siltstones and sandstones. ix) Interstratified rocks e.g. Ranzano Formation (RAN) (Bellinzona et al., 1971; Martelli et al, 1998) characterised by alternation of conglomerate, sandstone and pelites in varying portions. x) Interstratified Limestone and Limestone e.g. Flysch di Monte Penice (PEN) Formation (Bellinzona et al., 1968) composed by massive limestone and limestone interbedded with calcareous marls and pelites. xi) Marls and

interstratified marls e.g. Monte Piano Marls (MMP) Formation (Marchesi, 1961; Bellinzona et al., 1971) and the Antognola Formation (ANT) (Bellinzona et al., 1971; Cavanna et al., 1989) characterised by marls and marls interbedded with pelites.

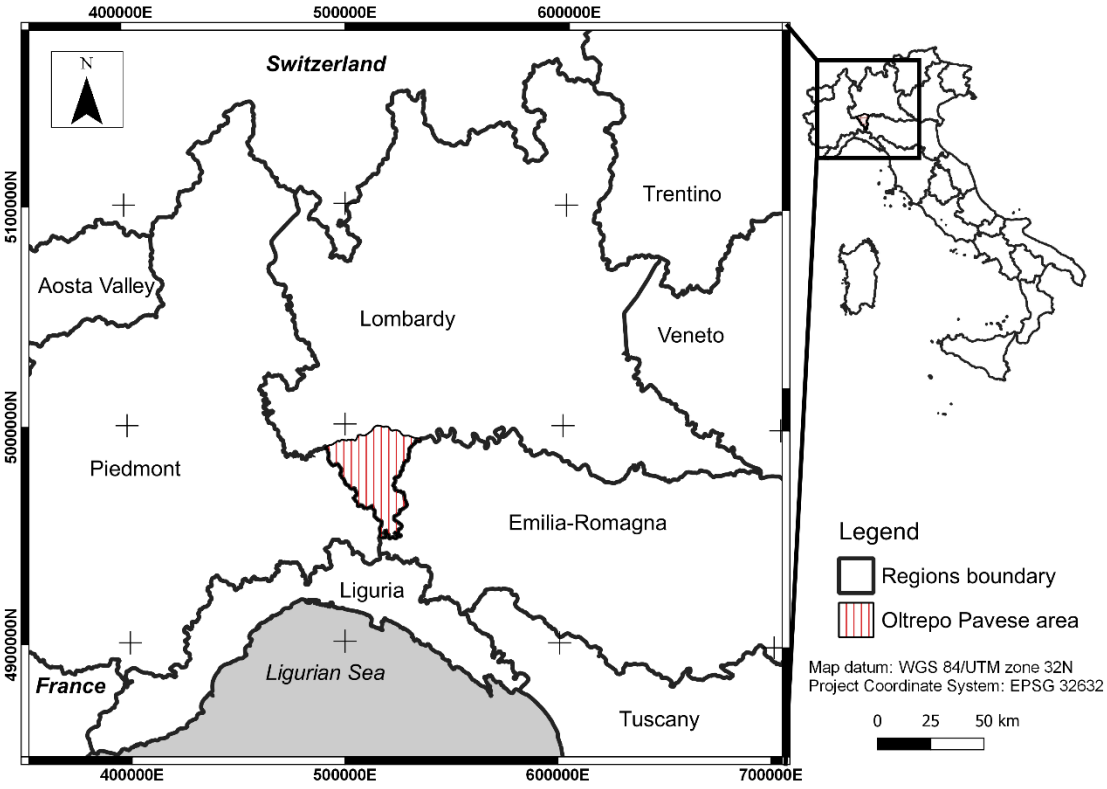

Figure 1: Study area.

The area is strongly controlled by lithological and structural conditions (Pellegrini and Vercesi, 2017) causing a gradual landscape evolution. The main geomorphological processes are related to surface and sub-surface runoff. In the study area, rill-interrill, gully, piping and calanchi erosion, as well as mass movements (Bosino et al., 2019a) are the dominant soil erosion processes.

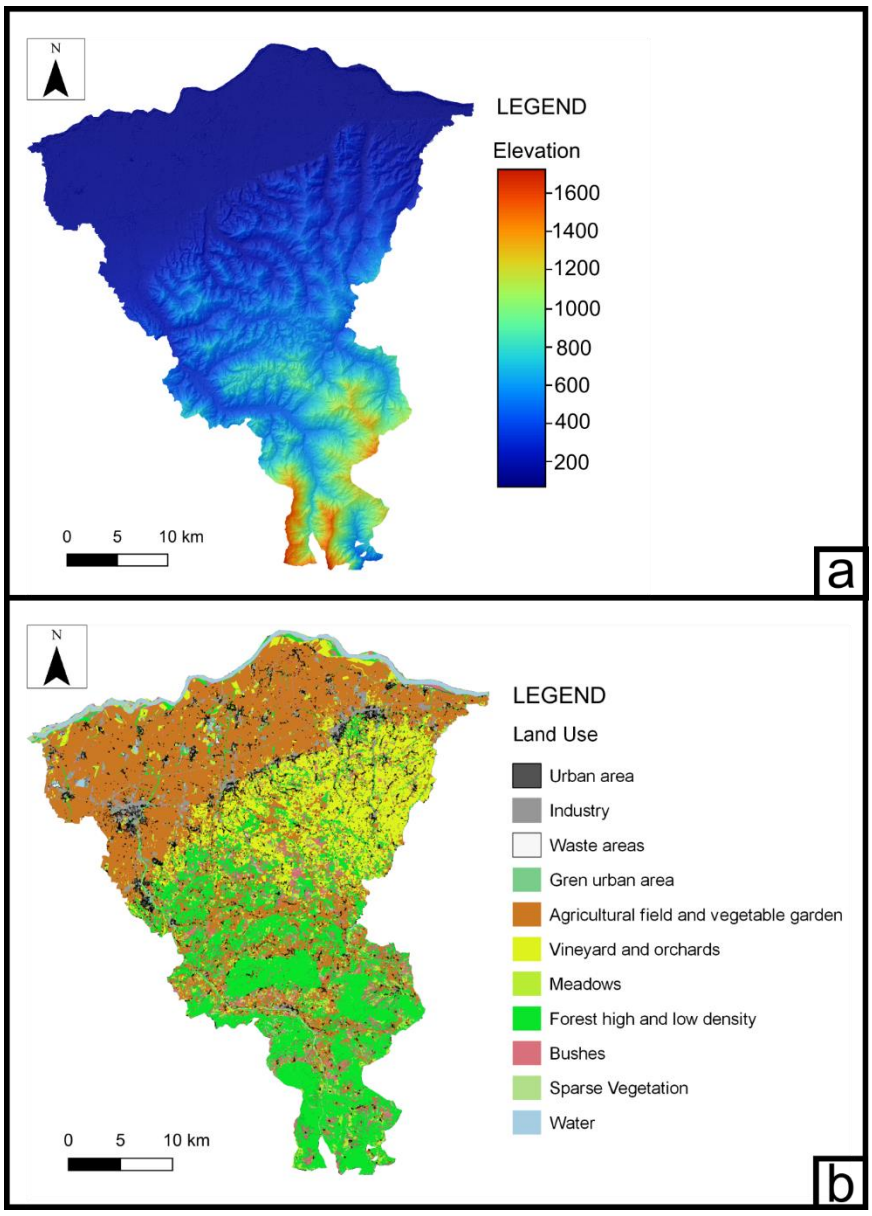

Figure 2: Characteristics of the study area a) Elevation range. b) Land Use classes (from DUSAF 2015).

In this study we focus primarily on water driven soil erosion dynamics such as calanchi and rill-interrill erosion processes as well as on the related forms and features. Even though micro scale gravitational processes might play a role in the evolution of the calanchi (especially Type B) we do not consider deep seated or surficial landslides in this study.

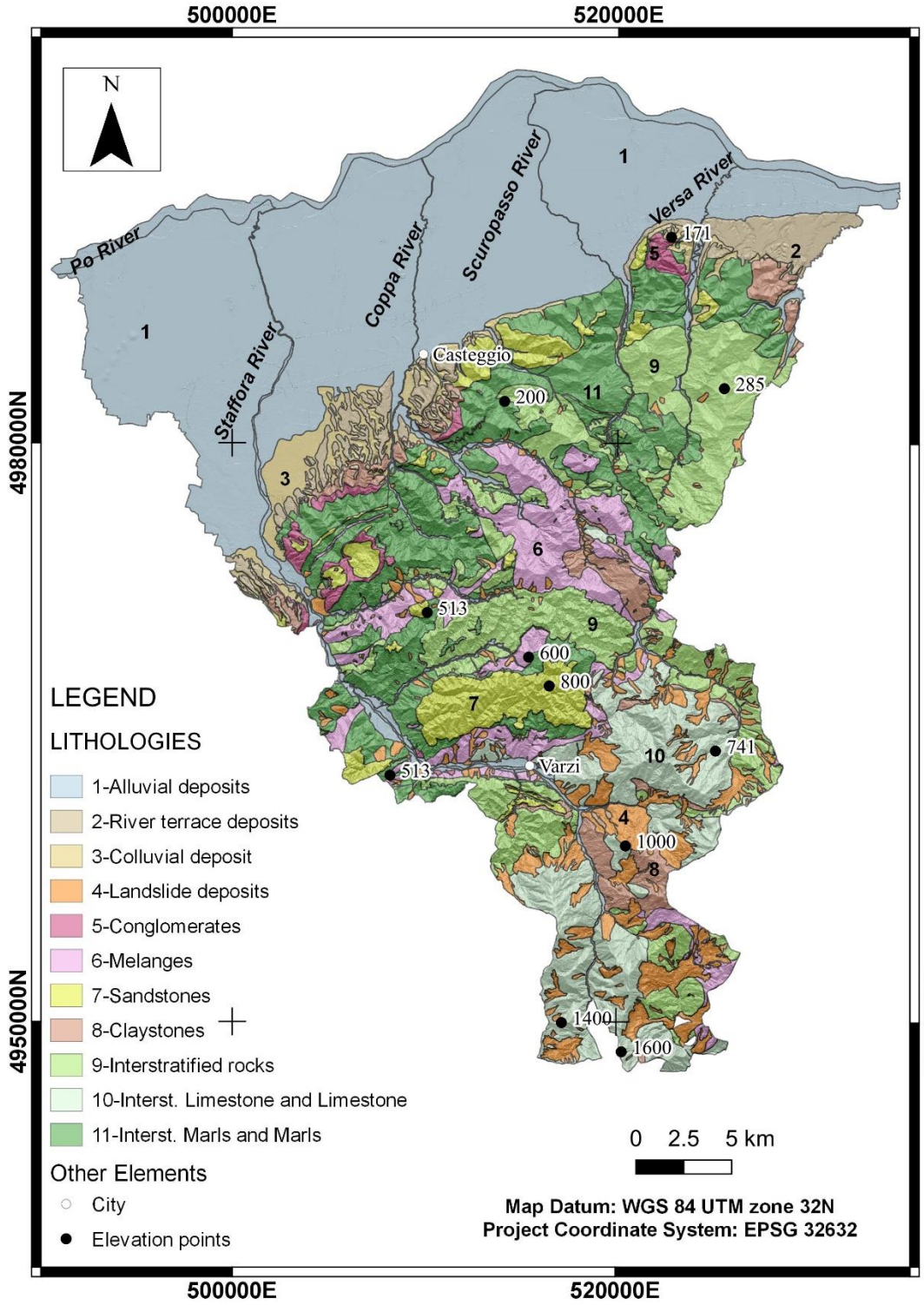

Figure 3: Lithotypes of the study area (Modified from Bosino et al., 2019b).

The calanchi of the Oltrepo Pavese have been described by Bucciante (1922) and Bosino et al. (2019a). In total, 263 calanchi forms were identified and accordingly classified in the field following the classification system developed by Moretti and Rodolfi (2000). Type A calanchi

are represented by knife-shaped slopes with sparse vegetation, a dense drainage pattern and no gravitational process (Figure 4a). Conversely, type B calanchi are characterised by more complex phenomena and occur mainly in soft bedrock/substrates with diffuse vegetation and/or landslide processes (Figure 4b). Instead, rill-interrill erosion is formed by the detachment of soil particles due to laminar (interrill) and turbulent (rill) surface runoff (Figure 4c). The previously mentioned erosional landforms represent important soil erosion features dominant in the Oltrepo area causing onsite and offsite damages. Especially the reduction of soil thickness and the removal of the fertile topsoil have severe implications on the hydrological characteristics of the soil as well as on its fertility and productivity. The eroded material in turn leads to problems in water quality (e.g. eutrophication) and to storage volume losses of reservoirs (Poesen and Hooke, 1997; Gunatilake and Vieth, 2000; Ramos and Martínez-Casasnovas, 2004).

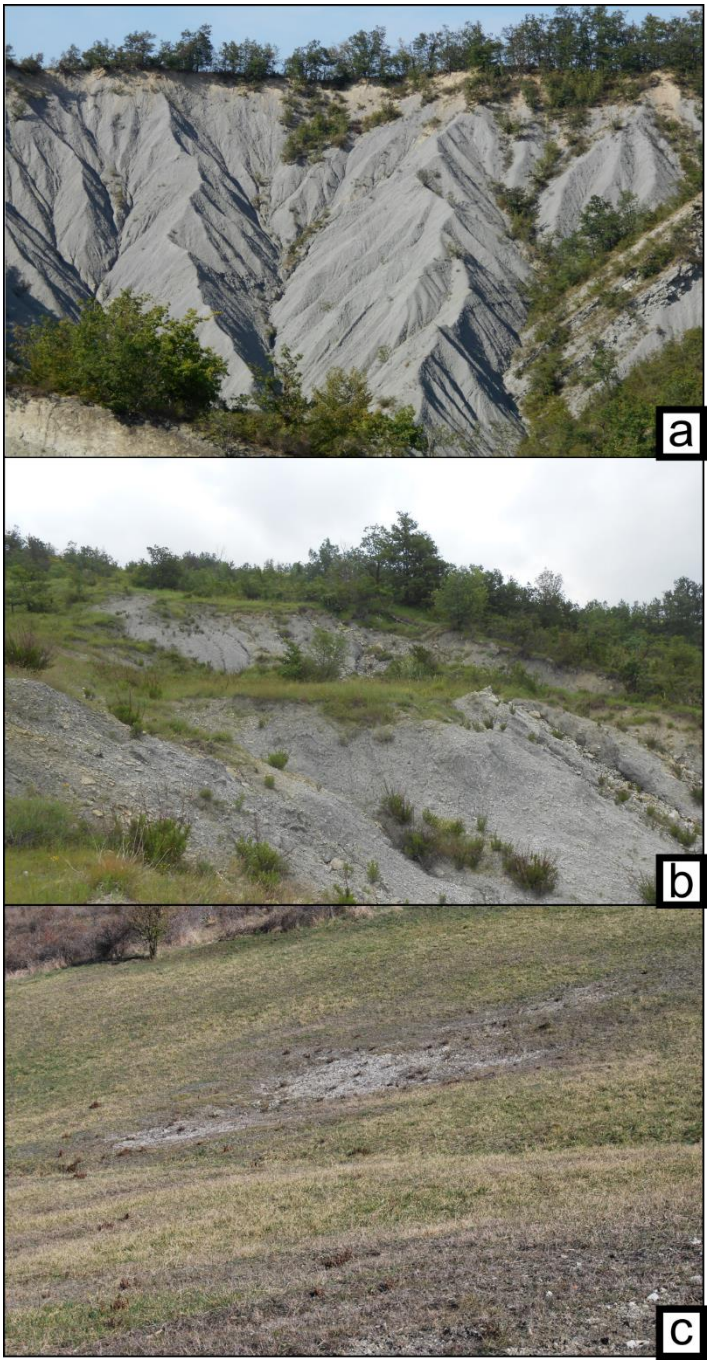

Figure 4: Aquatic erosional landforms in the Oltrepo Pavese. a) Calanchi type A, b) Calanchi type B, c) Rill-interrill erosion.

3. Materials and Methods

The methodology followed in this work consists of four steps that are illustrated in detail in Figure 5:

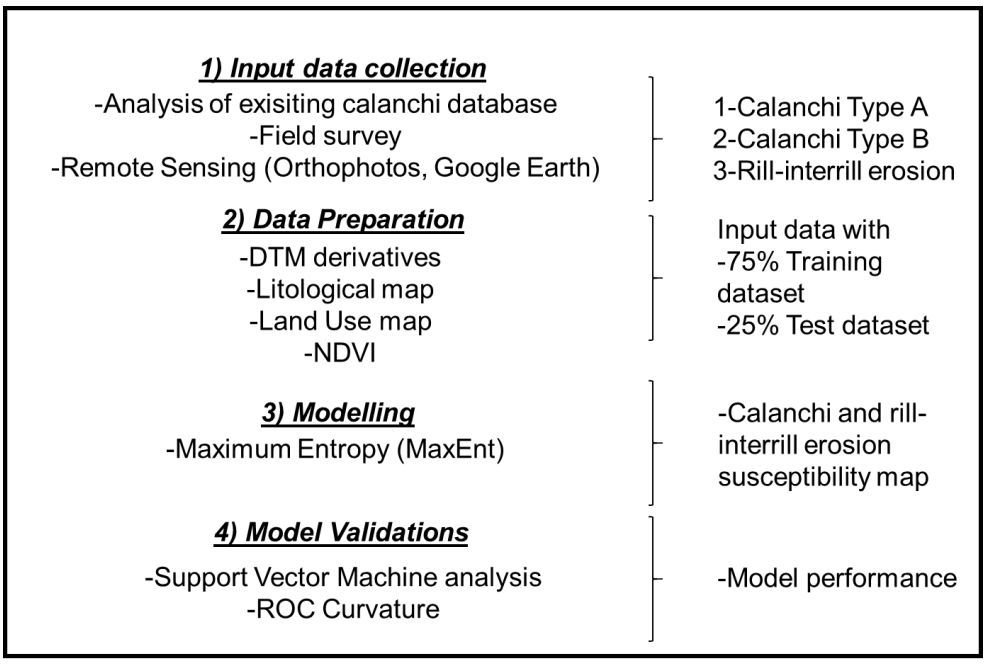

Figure 5: Methodology of the study.

1) Input data collection: The input data utilised for the susceptibility assessment was assembled combining a previously established calanchi database (Bosino et al., 2019a) and an additional mapping of rill-interrill erosion forms and features. The database consists of 263 calanchi, subdivided in 83 type A and 180 type B elements. In total 74 features of rill-interrill erosion were also mapped using remote sensing techniques (Orthophotos of the year 2015 provided by 'Geoportale della Lombardia' at http://www.geoportale.regione.lombardia.it/ as well as Google Earth™ information consisting of the year 2018) and additional field survey. The resulting database containing 337 erosion features was elaborated with SAGA GIS (Conrad et al., 2015). The erosional forms were transformed in a grid with 12 m cell size and the respective centroids were converted in a point dataset. In total we derived 26,388 points representing calanchi type

A; 28,141 points representing calanchi type B as well as 6,549 points that represent rill-interrill erosion.

2) Data Preparation: Using SAGA GIS we applied a detailed digital terrain analysis to quantify and described the terrain through topographic indices extrapolated from a Digital Elevation Model (DEM) (e.g. Maerker et al., 2011; Zakerinejad and Maerker, 2014), environmental parameters and remote sensing data. The extrapolation of the topographic indices was performed using a 12x12m cell size resolution DEM obtained from the TanDEM-X radar imaging satellite platform provided by the Deutsches Zentrum für Luft- und Raumfahrt (DLR). The DEM was pre-processed in order to extract artefacts and to guarantee the hydrological functionality (fill sinks) using the algorithm proposed by Wang and Liu (2006). Subsequently, the following terrain indices have been derived in SAGA GIS from the pre-processed DEM (Table 1): i) three basic terrain derivatives (Slope, Aspect and Catchment Area); ii) Vector Roughness Index (VRM) according to Sappington et al., (2007); iii) Topographic Wetness Index (TWI), based on modified catchment area and slope tangent (Sørensen et al., 2005); iv) Terrain Roughness Index (TRI) following Riley et al. (1999); v) Direct and Diffuse Insolation (Hofierka and Ŝúri, 2002); vi) Valley Depth and Vertical Distance to Channel Network (VDCN) (Conrad et al., 2015).

Table I. Environmental predictors for maximum entropy modelling

Type	Variable range	Reference
Topographic indices		
Elevation	60–1724 m a.s.l.	Wang and Liu (2006)
Slope	0–76.3°	Zevenbergen and Thorne (1987)
Aspect	0–360°	Zevenbergen and Thorne (1987)
VRM	0–0.54	Sappington *et al.* (2007)
TWI	0–9.7	Sørensen *et al.* (2005)
Catchment slope	0–76.3°	Sørensen *et al.* (2005)
Catchment area	144–669403 m^2	Sørensen *et al.* (2005)
Modified catchment area	144–669258 m^2	Sørensen *et al.* (2005)
TRI	0–44.37	Riley *et al.* (1999)
Direct insolation	0–3.7 $kWhm^{-2}$	Hofierka and Šúri (2002)
Diffuse insolation	0.37–0.67 $kWhm^{-2}$	Hofierka and Šúri (2002)
VDCN	0–442 m	Conrad *et al.* (2015)
Valley depth	0–409 m	Conrad *et al.* (2015)
Environmental data		
Lithology	11 classes	Bosino *et al.* (2019b)
Land use	CORINE classes	Regione Lombardia (2015)
Remote sensing data		
NDVI	−1 to +1	USGS Earth Explorer (2019)

The two environmental information layers are represented by the 11 lithotypes described in Bosino et al. (2019b) (Figure 3) and CORINE land use data (Regione Lombardia, 2015). The Normalized Difference Vegetation Index (NDVI) (Rouse, et al., 1973) was derived from remote sensing data. The NDVI is useful to understand the distribution of vegetation and provides information about the relation between the vegetation cover and bare soil. The NDVI data were extrapolated from Advanced Spaceborne Thermal Emission and Reflection Radiometer (ASTER) images. Two images from the 15th May 2015 were downloaded from USGS Earth Explorer (2019). The NDVI was calculated with the SCP Plugin of QGIS (2018) applying the following formula: NDVI = (Band 3N-Band 2) / (Band 3N+Band 2) following Yüksel et al. (2008). The above-mentioned independent variables where subsequently used to predict calanchi and rill-interrill erosion using a machine learning approach. The independent variables (topographic indices, NDVI; lithology and land use) were converted into a raster format. The raster grid centroids were transformed into points and at each point the respective values of the independent variables were added to the attribute table resulting in a dataset of 61,078 points.

3) Modelling: For this study we used a simple Maximum Entropy approach (MaxEnt). The model is a presence only model based on statistical mechanics (Phillips et al. 2006) and

expresses the susceptibility of each location (grid cell) as a function of the environmental variables at that grid cell. MaxEnt is widely used to make predictions of species distribution from incomplete climatic and environmental dataset (Medley, 2010; Javidan, 2020). The MaxEnt model in general performs better than other statistical algorithms in terms of model performance as stated e.g. by Elith et al. (2006), Phillips et al. (2006), Ortega-Huerta and Petersonn (2008) or Medley (2010). Moreover, the presence-only dataset makes the model more robust to spatial error. The MaxEnt model can estimate a target variable probability distribution (π) over a set of incomplete site information of the study area (X). Therefore, every site x (cells of DEM) is characterized by a non-negative value (π), so that the values $\pi(x)$ sum to one (Phillips and Dudik 2008). The probability distribution function of a target variable present in the cell x is indicated as:

$$P(y = 1|x) = \frac{P(x|y = 1)P(y = 1)}{P(x)} = \pi(x)P(y = 1)|X|$$

Where |X| is the number of pixels or locations and P(y=1) is the overall prevalence of the species in the study area. The $\pi(x)$ is estimated by the MaxEnt algorithm and is equal to a Gibbs probability distribution derived from the set of features $f_1, f_2,\ldots,f_n$. The Gibbs distributions are exponential distributions parametrized by a vector of feature weights $\lambda=(\lambda_1,\ldots,\lambda_n)$ (Phillips and Dudik, 2008) and defined as:

$$q_\lambda(x) = \frac{exp\ (\sum_{j=1}^{n} \lambda_j\, f_j(x))}{Z_\lambda}$$

on which Z_λ is a normalization constant. The MaxEnt model q_λ at a specific site x depends on the environmental variables at x. The environmental variables on which the model was trained are represented by continuous predictor variables derived from the DEM analysis and the

NDVI, as well as categorical variables (limited number of discrete values) such as land use and lithology.

High values of the probability function at a particular grid cell indicates that the grid cell is predicted to have suitable conditions for that type of erosion. The computed model is a probability distribution over all the grid cells of the study area.

The model can detect the areas affected by calanchi and rill-interrill erosion assigning a susceptibility value between 0 and 1, respectively for no susceptibility (0) to very high susceptibility (1). In this study the model was set up with 75% of the points for training the model (N_{train}=45,809) and 25% of points used to validate the mode results (N_{test}=15,269). The points were selected randomly from the entire data set. We additionally applied a Support Vector Machine technique (SVM) to verify the results of the MaxEnt classification. Since we have divided our dataset in three different erosion classes (calanchi type A, calanchi type B and rill-interrill) we looked specifically for multi-class analysis algorithms. The SVM approach is implemented in R (R Core Team, 2018), within the e1071 package (Meyer et al., 2019). For further reading of the supervised classification approach based on support vector machines see Vapnik (1995; 1999). For the SVM the same data set divided into an 75% training dataset and a 25% test dataset was used.

4) Model Validation: The final output of the model yields three susceptibility maps representing calanchi type A, calanchi type B and rill-interrill erosion. We analysed the performance of the MaxEnt modelling as well as the relative importance of the thirteen environmental layers for each of the three classes (calanchi A, calanchi B and rill-interrill erosion features). The performance of the MaxEnt models was assessed through the receiver operating characteristic (ROC) curve integral (Goodenough et al., 1974) also known as area under curve (AUC) (Hanley and McNeil, 1982). The ROC curve plots the true positive rate (sensitivity) over a false positive

rate (1-specificity) for all possible cut off points (Swets, 1988). AUC = 1 represents 100% sensitivity *vs* 100% specificity. The closer the AUC value to 1, the higher the predictive performance of the model. Following Hosmer et al. (2013), the prediction skills of the model are acceptable/excellent/outstanding if the AUC values exceed 0.70/0.80/0.90, respectively.

In order to understand more about the differences between the individual classes, we applied a Support Vector Machine (SVM) approach with a classification matrix as output. The confusion matrix provides: i) accuracies for each of the three analysed classes, ii) an overall accuracy as well as iii) Cohen's kappa value for interpretation. The kappa statistic is a score of the consistency in ratings for categorical items (Cohen, 1960). The model has a moderate/substantial/perfect agreement when kappa exceed 0.41/0.61/0.81, respectively (Landis and Koch, 1977). Furthermore, we measure the performance of the SVM model through the ROC curves and the AUC values.

4. Results

For the MaxEnt modelling, the dataset was randomly split into 75% for training and 25% for testing. For each of the three erosional landforms, the variable importance of the single independent variables was assessed (Figure 6). The most important variables that describe the calanchi type A are represented by: i) elevation (39.2%), ii) landuse (33.5%), iii) valley depth (12.4%) and iv) lithology (3.4%). Instead, for the formation of calanchi type B is mainly led by: i) land use (40.5%), ii) elevation (32.6%), iii) valley depth (8%) and iv) lithology (6.4%). Finally, rill-interrill erosion phenomena are dominated by the following independent variables: i) land use (48%), ii) diffuse insolation (30.1%), iii) VRM (11.7%) and iv) TRI (6.3%).

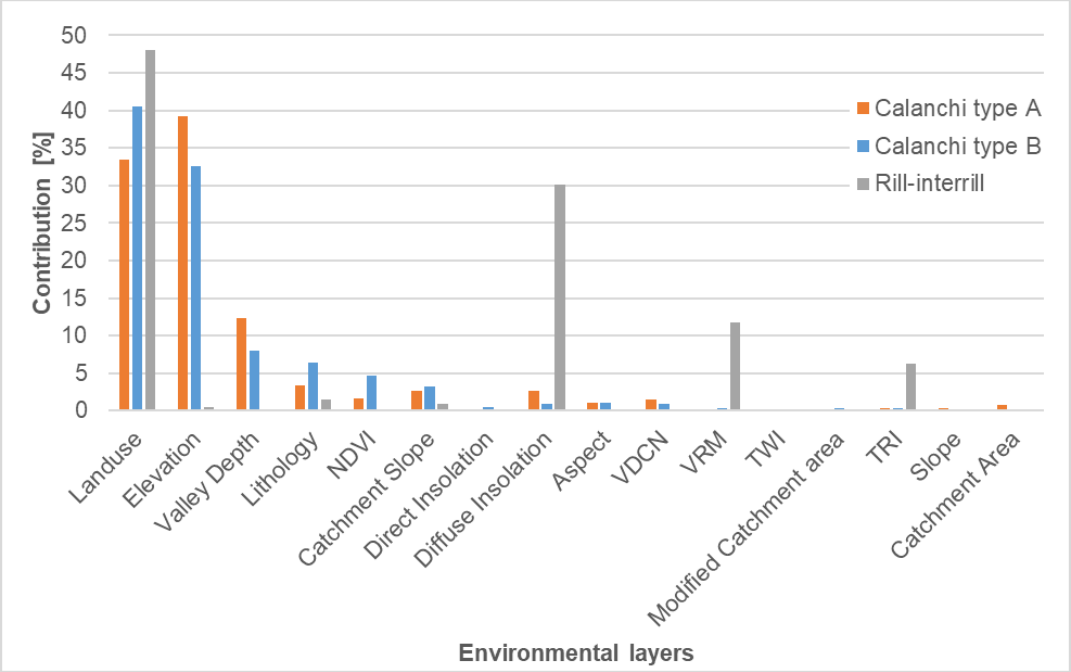

Figure 6: Relative importance of the environmental variables.

As shown in Figure 6, the following environmental layers play a significant role in the formation of the studied erosional landforms: land use, elevation, valley depth, diffuse insolation, TRI and VRM. In order to understand the specific contribution of the variables we derived the individual variable response curves illustrated in Figure 7,8 and 9 for the calanchi type A, B and rill-interrill erosion respectively.

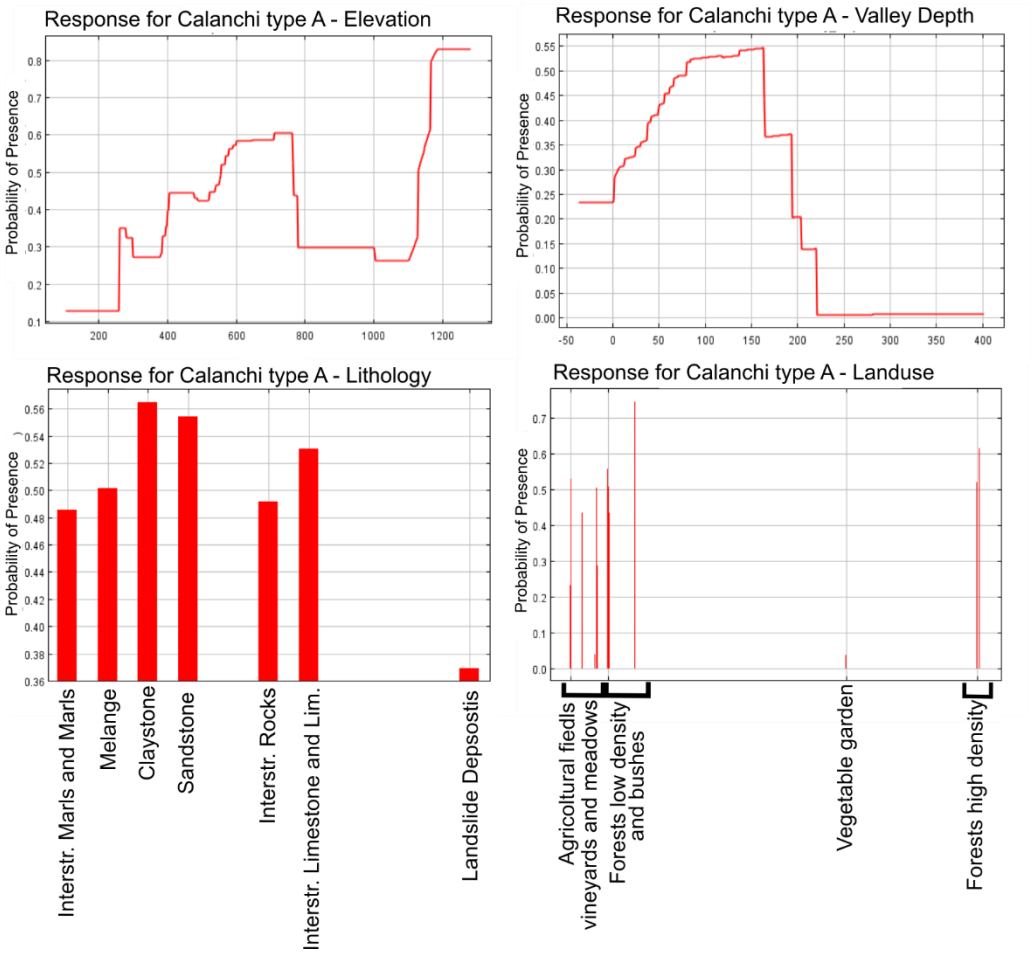

Figure 7: Variable importance for Calanchi type A.

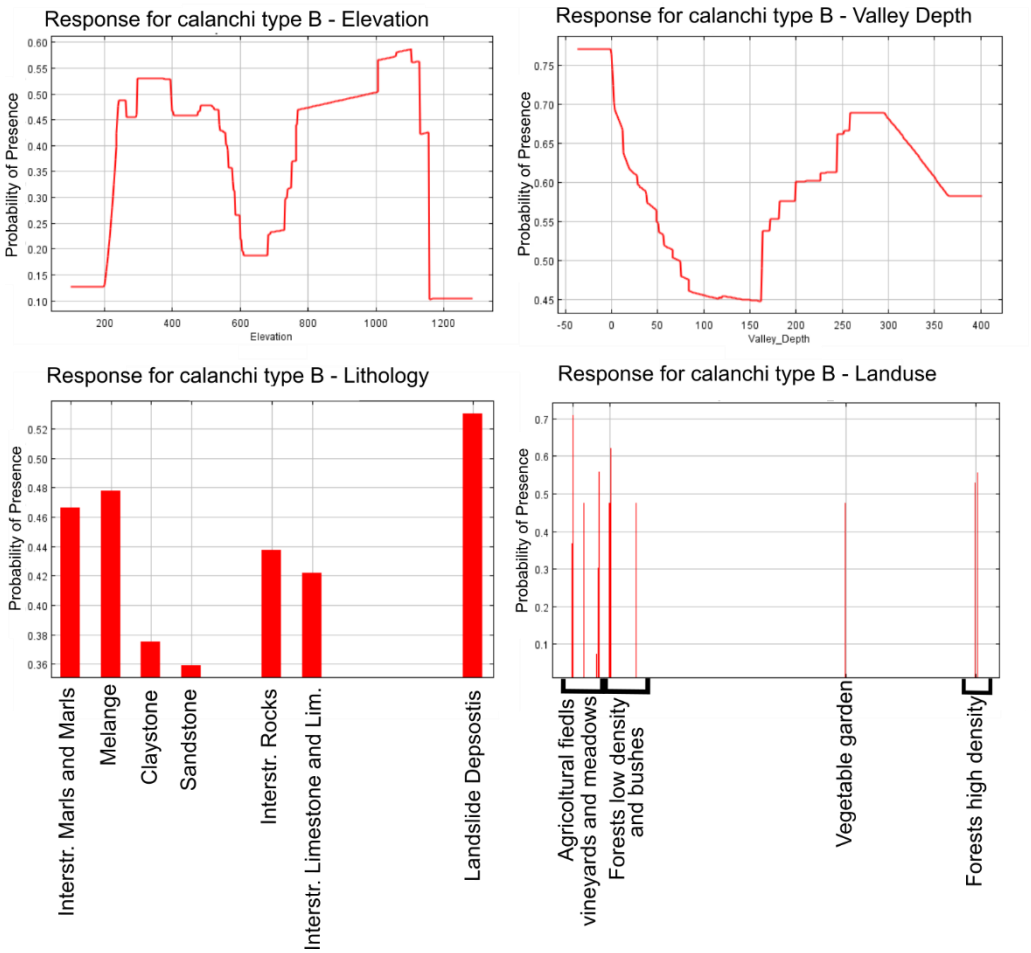

Figure 8: Variable importance for Calanchi type B.

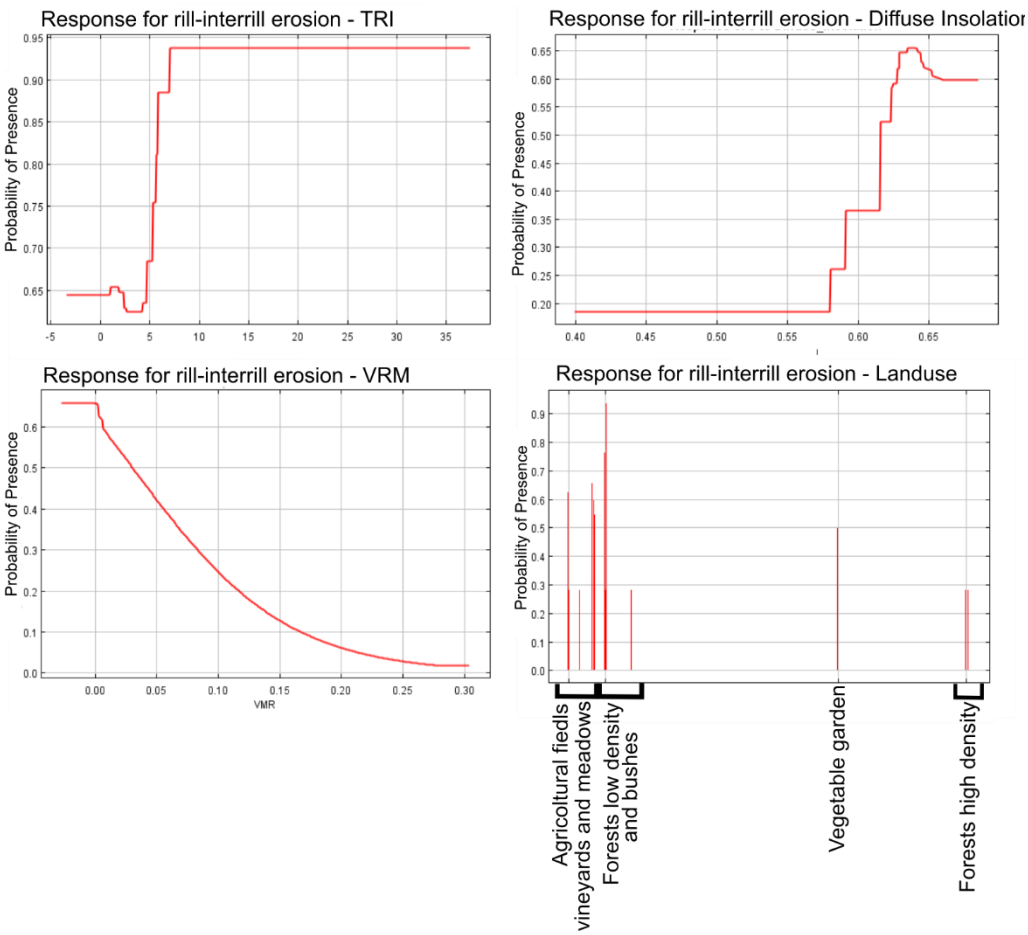

Figure 9: Variable importance for Rill-interrill erosion.

In particular, the calanchi type A are mainly occurring in an elevation range between 580m and 780m as well as higher than 1170m, where valley depth is between 75m and 170m. The most influencing parameter -landuse- is represented by forest with low density of trees and bushes as well as agriculture areas. According to (Figure 7) the lithology plays a minor role in the formation of calanchi types. However, calanchi type A are associated to claystone, sandstone and interstratified rocks. Instead, the calanchi type B are mainly related to elevation ranges between 300m and 400m and between 900m and 1100m with a general valley depth from 20m to 60m as well as higher than 150m. The most influencing land use is represented by agricultural fields, meadows and bushes. The main lithology coming along with the formation of type B calanchi are landslide deposits and the Melange Formation. Type A and B calanchi have inverse

response curve pattern concerning elevation and valley depth. The role of the relief is highlighted by the elevation which is related to the hardness of the bedrock formations and consequently reflected by a respective valley depth. The southern part of the Oltrepo Pavese is characterised by high relief, competent rocks and deep valleys with the prevalent occurrence of type A calanchi. Conversely the northern part of the study area is largely characterised by soft sedimentary formations represented by a hilly landscape and, the respective formation of type B calanchi. On the other hand, the rill-interrill erosion forms and features appear on an elevations lower than 200m. The dominant land use that influence the rill-interrill erosion processes are low density forest, bushes and agricultural fields. Moreover, rill-interrill erosion is characterized by TRI values greater than 5, and VRM values less than 0.05. Finally, the MaxEnt Model was applied to regionalize the susceptibilities of the three erosion types. The resulting maps are illustrated in Figure 10 a, b and c, in addition details of susceptibility maps are reported in Figure 10 g and h. The susceptibility values were classified in four susceptibility classes. In particular, we attributed ‘Not susceptible’ to all pixels with susceptibility values of less than 0.50, ‘low susceptibility’ from 0.50 to 0.60, ‘medium susceptibility’ from 0.60 to 0.80 and ‘high susceptibility’ from 0.8 to 1.

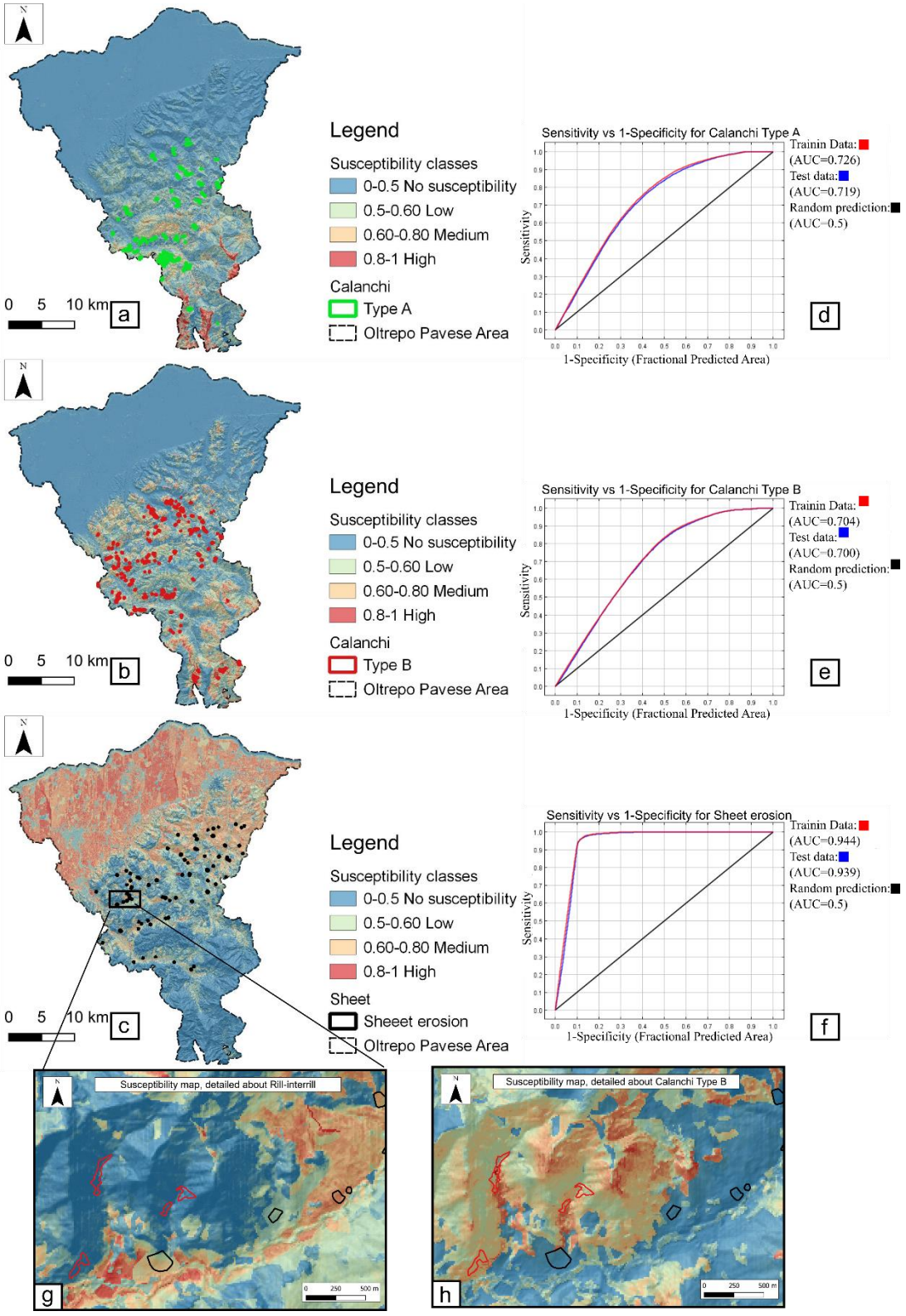

Figure 10: MaxEnt model susceptibilities for the three erosion types. Left side: Susceptibility maps. a) Calanchi type A; b) Calanchi type B; c) Rill-interrill erosion. Right side: ROC curvature and AUC values for d) Calanchi type A; e) Calanchi type B; and f) Rill-interrill erosion. Details of the susceptibility map for g) Rill-interrill erosion. h) Calanchi type B.

Following Bianchini et al. (2016), we summarised the number of pixels for each susceptibility class for the three erosional forms (see Table 2). The ROC curves were drawn for both test and training datasets in order to verify the possible overfitting effects. The model performances were assessed using the ROC curves. Following Hosmer et al. (2013), the AUC values show acceptable values for the calanchi forms and outstanding values for the rill-interrill erosion detection. The training data for the calanchi shows an AUC of 0.72/0.72 and for the testing dataset of 0.70/0.70, respectively for calanchi types A and B (Figure 10 d, e). In addition, the AUC values for the rill-interrill erosion susceptibility provides AUC values of 0.94 and 0.94 for training and test datasets, respectively (Figure 10 f).

Table 2: Number of Pixel for each susceptibility class for each erosion type.

Susceptibility classes	Number of Pixel Calanchi Type A	Type A [%]	Number of Pixel Calanchi Type B	Type B [%]	Number of Pixel Rill-interrill erosion	Rill-interrill erosion [%]
No susceptibility	3567814	94.61	3252262	86.2	2092066	55.47
Low	108781	2.88	326707	8.66	413315	10.95
Medium	79859	2.11	190051	5.03	1258101	33.36
High	15280	0.4	2714	0.11	8255	0.22

In order to validate the MaxEnt approach we used the same dataset as for the MaxEnt model (training and testing) to perform a multi-class machine learning approach. The results of the SVM is represented by the confusion matrix shown in Table 3.

Table 3. Confusion matrix for SVM, n=15,269.

	Inventory				
	Calanchi Type A	Calanchi Type B	Rill-interrill erosion	**Sum**	**User's accuracy**
Predicted					
Calanchi A	4513	2079	5	6597	68.41%
Calanchi B	1541	5455	39	7035	77.54%
Rill-interrill erosion	8	67	1562	1637	95.42%
Sum	6062	7601	1606		
Producer's accuracy	74.45%	71.77%	97.26%		
Overall accuracy	*80.46%*				
Cohen's kappa	*58.34%*				

The SVM classifier provides an overall accuracy of 80%. Table 3 shows the differences between the calanchi classes and the rill-interrill erosion class. User's accuracy values are 68,41%, 77,54% and 95,42% for calanchi type A, B and rill-interrill erosion respectively. Both calanchi classes can be distinguished, even if their accuracy is lower than the one observed for rill-interril erosion. The Cohen's kappa value represents a moderate performance with a value of 58,34%. Subsequently, we extracted the ROC curve to test the performance of the SVM model (Figure 11). Model performance is expressed by the AUC values yielding 0,96, 0,95 and 0,99 for calanchi type A, calanchi type B and rill-interrill erosion respectively.

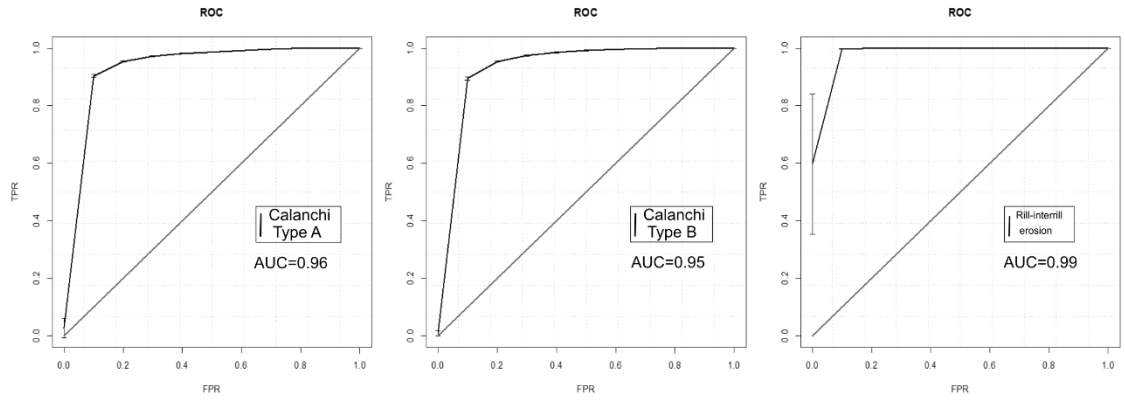

Figure 11. ROC Curve and AUC values of the SVM model.

5. Discussion

Calanchi and rill-interrill erosion represent the most important forms of soil erosion in the Oltrepo Pavese area. Since calanchi are complex phenomena characterised by a set of various erosive processes (i.e. rill, gully, piping and landslides), it is difficult to implement a performant susceptibility modelling and decipher between complex calanchi erosion and single erosion processes such as rill-interrill erosion. Especially at regional scale no studies have been carried out so far. However, we show, that the MaxEnt approach can differentiate with acceptable precision the independent variables that may drive the formation of calanchi and rill-interrill erosion forms. In fact, the ROC curves obtained for both erosional forms show AUC values for training and testing data above the acceptable threshold value of 0,7. The model evaluation based on the SVM classification matrix shows a good accuracy of 80,46%. With a kappa value of 58,34% the overall model evaluation achieves a moderate performance. In general, SVM differentiate with a very high accuracy between calanchi and rill-interrill erosion, whereas it performs with lower values when distinguishing between the two calanchi types. In order to get information on the driving factors explaining the spatial distribution of the three erosional landforms we evaluated the variable importance. The results show that land use, elevation, valley depth, lithology, TRI, VMR and diffuse insolation have a significant impact in the

calanchi and rill-interrill formation. In general, the mountainous part of the Oltrepo Pavese is more susceptible to calanchi erosion as shown in (Figure 4b and c). Rill-interrill erosion mainly occur in the low sloping areas and the Po Plain. This trend is confirmed by the individual response curves (elevation, valley depth; see Figure 7, 8 and 9). Furthermore, the land use plays a key role in the development of the three erosional landforms. The Oltrepo Pavese is a rural area dominated by agricultural activities. According to Bosino et al. (2019a) the calanchi areas are generally shrinking in size in the Oltrepo Pavese in the last decades. This is mainly due to the abandonment of the agricultural activities and of scarce maintenance of the territory especially in the upper part of the Oltrepo Pavese. The revegetation processes can reduce soil erosion phenomena contributing to the stabilisation of the calanchi areas. On the other hand, intense agricultural activities such as tillage conducted in the vineyards promote rill-interrill erosion phenomena. The response curves highlight a correlation between calanchi type A with forest and bushes and calanchi type B and agricultural areas and meadows. Moreover, rill-interrill erosion occur mainly related to agricultural fields and bushes. Regarding the lithology as shown in Figure 7 and as specified by Bosino et al. (2019a) the calanchi type A mainly occur in soft sedimentary formations which crop out in Oltrepo Pavese i.e. claystone, sandstone and interstratified rocks. Instead the type B calanchi mainly develop in the Melanges Formations and are often characterised by landslides deposits and processes (see Bosino et al. 2019a). As shown in Figure 6 the other environmental layers seem to play a minor role in the model application, however, their specific response curves may be useful for the interpretation of the spatial distribution of the complex calanchi landforms (type A and B). Figure 12 illustrates the response curves for Catchment area and Vertical Distance to Channel Network (VDCN) for calanchi type A and B. Low values of catchment area indicate that calanchi type A developed in small basins or close to the watershed divides. Additionally, type A calanchi forms are characterised by high values of Vertical Distance to Channel Network. The VDCN expresses

the vertical distance of the calanchi landform to the valley bottom and hence, is a proxy for the erosional energy of surface runoff. Instead, the calanchi type B are characterised by larger drainage areas and lower values of VDCN. Thus, the knife shaped calanchi of type A, have steep slopes and high erosional potential due to higher local relief energy. On the other hand, the calanchi type B seems to be associated to a final evolutive stage of calanchi formation where the catchment area is larger, and the potential energy of erosion is lower (low VDCN). This hypothesis may be sustained by the findings of Ciccacci et al., 2008 who report the evolution of calanchi from type A to type B in the Radicofani area (Tuscany). However, in the Oltrepo Pavese study area there might be also an additional influence related to the lithology considering the nature of the Melange Formations (centimetric and metric blocks scattered in a clayey matrix). In general, this formation is related to calanchi type B and characterised by gravitative processes leading to a slightly smoother morphology. Concerning rill-interrill erosion the MaxEnt model indicate land use, diffuse insolation, TRI and VRM as the most important variables. The response curve of the Terrain Roughness Index shows very high values demonstrating a certain heterogeneity of the territory affected by sheet erosion. However, the rill-interrill erosion areas show low values of VRM. The latter indicates that slopes are homogeneous in terms of gradient and aspect favouring laminar to slightly turbulent surface runoff typical for rill-interrill erosion phenomena.

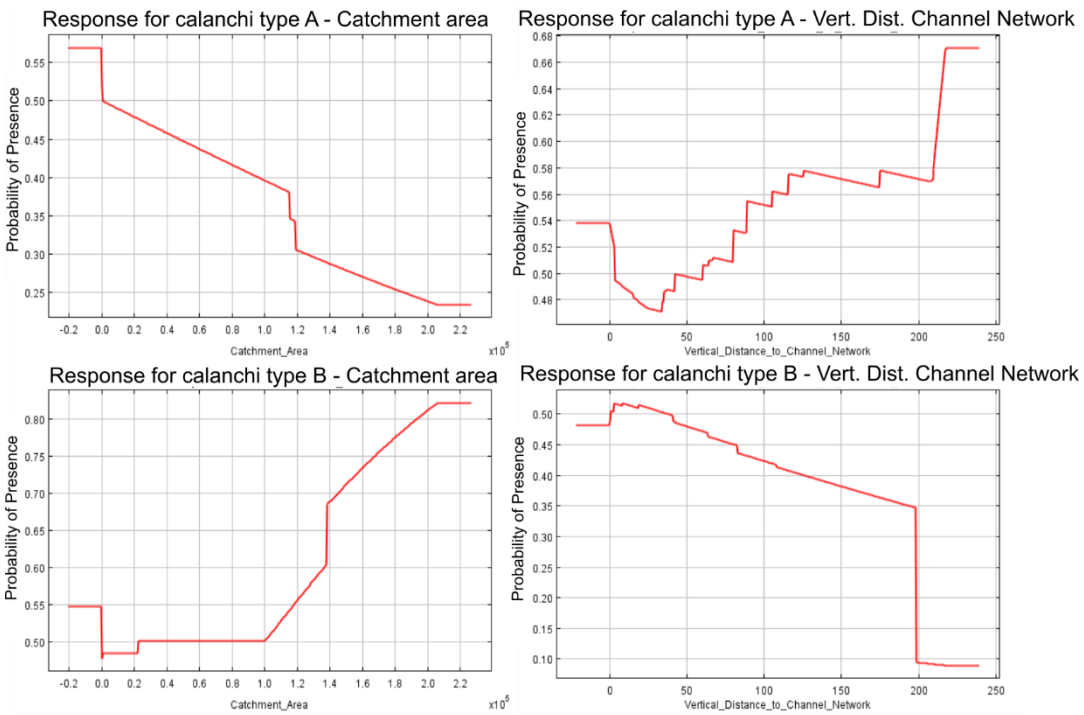

Figure 12: Variable importance calanchi type A and B.

As reported by other authors also soil type plays a role to explain the spatial distribution of the three erosional landforms (see e.g. Pournader et al., 2018). Unfortunately, there is no detailed soil information available in the Oltrepo Pavese study area and thus, the soil type was not considered in this study. Regarding the calanchi forms and features the susceptibility maps show that 8% of the territory is affected by medium/high susceptibilities. Concerning rill-interrill erosion 34% of the study area is characterised by medium/high values of susceptibility. Consequently, there is more than 40% of the study area susceptible to the described erosion processes. Moreover, our analysis is sustained and externally validated by recent field observations during a precipitation event on the 21/10/2019 with 117 mm in 14 hours. The precipitation was measured by a pluviometric station close to Voghera (Arpa Lombardia https://www.arpalombardia.it/siti/arpalombardia/meteo/richiesta-dati__misurati/Pagine/RichiestaDatiMisurati.aspx). This event caused severe damage in the agricultural area close to Retorbido city (Figure 13a) showing sediment loaded flows due to rill-interrill erosion. Figure 13b illustrates this area (pink boundary) that is characterised by a high susceptibility to rill-interrill erosion as identified by

the MaxEnt model application (Figure 13c). We demonstrate that the MaxEnt probabilistic model yield valuable results for the spatial distribution of calanchi and rill-interrill erosion susceptibilities in the Oltrepo Pavese study area. The large variety of different environmental characteristics covered within our study area underpin the general applicability of the approach. In our area elevation and land use play a major role due to the fact that agricultural activity is widespread on the one hand promoting erosional features and where agriculture is abandoned erosional processes seem to be reduced due to more dense vegetation. An increase in elevation reflects in general higher potential energy and increasing valley depth, thus, higher erosional potential. The latter characteristics are given also in other parts of the Apennines. Consequently, the model can be employed to predict soil erosion phenomena in other areas of the Northern Apennines, especially, where similar lithological, pedological and land use conditions can be found (e.g. Maerker et al., 2020). Furthermore, the approach can also be extended to detect susceptibilities of other landforms that have been mapped accurately and where appropriate predictor variables are available e.g. susceptibilities to gully erosion in different environmental conditions (e.g. Zakerinejad and Maerker, 2014, Zakerinejad et al., 2018).

Finally, to manage and maintain the landscape the knowledge of the spatial distribution of the erosional forms and their driving factors yield valuable information for local and regional administration as well as for agricultural and landscape planning purposes.

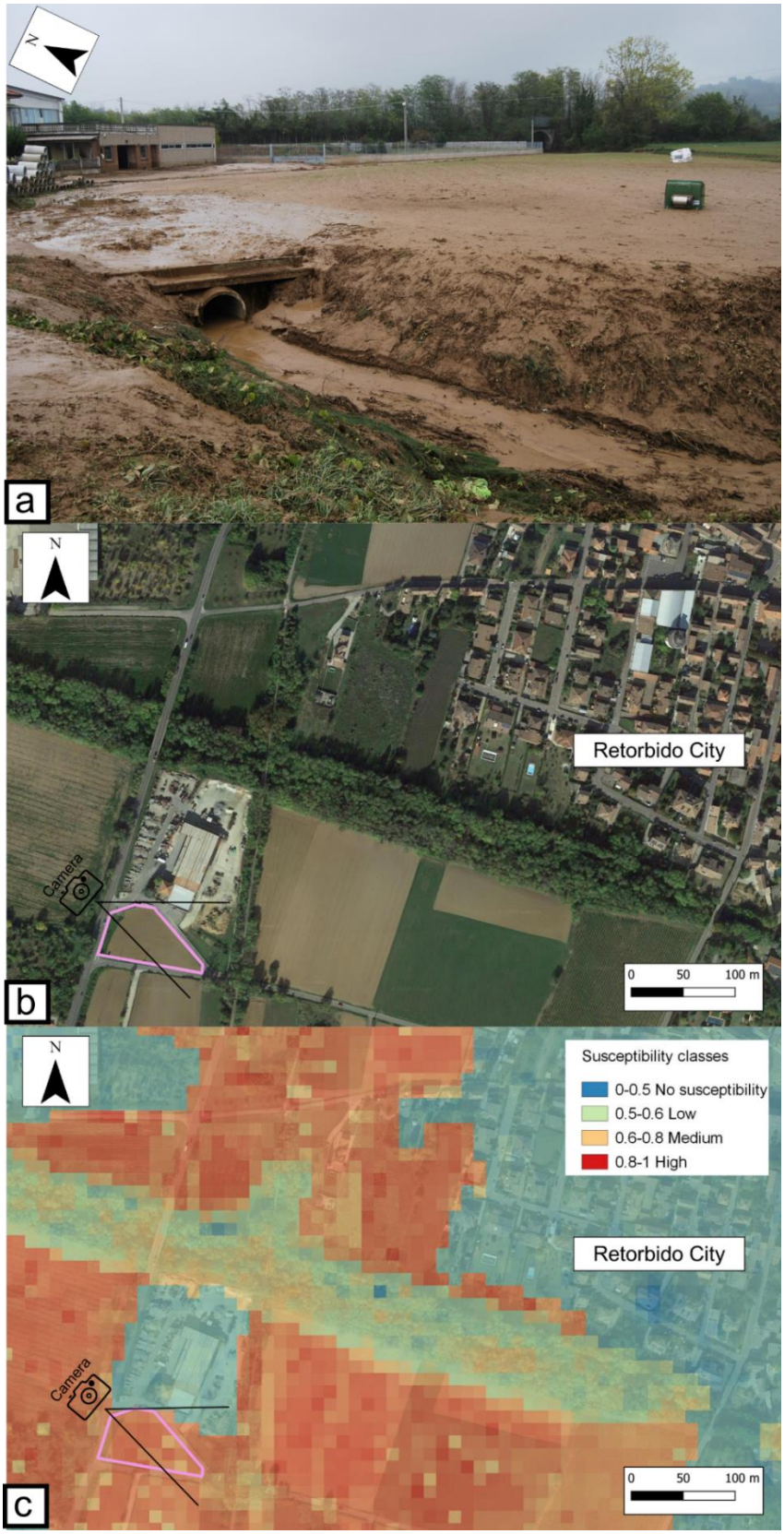

Figure 13: a) Effect of the intense precipitation (21/10/2019 event). b) Agricultural field closed to the city of Retorbido. c) Rill-interrill susceptibility map.

6. Conclusion

Soil erosion represents one of the most important problems in Europe and especially Italy is one of the main countries affected by aquatic erosion processes (Panagos et al., 2018). In this paper we assessed the calanchi and rill-interrill erosion susceptibility in the rural area of the Oltrepo Pavese, Northern Apennines. The calanchi and rill-interrill erosion susceptibility was evaluated using detailed terrain analysis and stochastic modelling (MaxEnt; SVM). Generally, both model approaches yield acceptable to outstanding performance values (ROC integral, confusion matrix) indicating that a differentiation between the three soil erosion landforms is achievable with a quite good accuracy. Especially the classification of calanchi type A and B was conducted with acceptable (MaxEnt) to excellent (SVM) results. However, as shown by the ROC integrals MaxEnt yield even outstanding results concerning rill-interrill susceptibilities. Instead, we yield much lower but still suitable model performance parameters for calanchi type A and B (72%-70%). The low ROC integral values for calanchi A and B might be explained with the much larger variety of environmental conditions that are considered in the model runs in comparison to the rill-interrill conditions. Generally, calanchi landforms are very complex due to their multi-process nature. Furthermore, we show that the formation of the two calanchi types (A and B) depends mainly on the following dependent variables: elevation, landuse, valley depth and lithology. The most important variables for rill-interrill erosion are TRI, VRM, diffuse insolation and land use.

The area most susceptible to calanchi erosion is located in the mountainous part of the Oltrepo Pavese, particularly where the soft sedimentary formations crop out. Additionally, agricultural fields and scarce vegetation like bushland and degraded areas favour the development of calanchi landforms. Our study highlights that an important part of the territory (34%) shows high susceptibilities to rill-interrill erosion. We further show that especially the lower Oltrepo Pavese and the low sloping foot slope areas are potentially prone to rill-interrill erosion. Even

though only 8% of the study area is affected by calanchi landforms the latter have strong implications for the drainage system since they are often directly connected. Thus, sediments are effectively washed into the drainage system leading to problems with water quality and quantity. As shown in the past there are several applications dealing with a stochastic assessment of rill-interrill and calanchi erosion forms and features (e.g. Phillips and Dudik 1998; Vergari, 2015; Bianchini et al., 2016; Maerker at al., 2020). However, to the knowledge of the authors this study is the first assessing calanchi and rill-interrill erosion susceptibilities on a regional scale. We demonstrated that a stochastic model based on a detailed terrain analysis performed on a high-resolution DEM is a powerful approach for spatial prediction at regional scale. In general, we have to state that the model was trained and applied for the specific conditions of the study area. Thus, the relevant environmental predictors identified are reflecting the specific environmental settings of the study area. However, we suppose that model predictions with independent variables like lithology, landuse, elevation, etc. that show a significant model contribution in the Oltrepo Pavese, might also yield acceptable results in areas of the Northern Apennines with similar environmental settings.

Thus, our work contributes to identify erosion process susceptibilities and provides a methodology to compare rill-interrill and calanchi landforms on regional scale. This knowledge may be used in local and regional planning procedures, agricultural investment, and rural support strategies.

Acknowledgment

Alberto Bosino and Paolo Giordani wrote the paper doing respectively the MaxEnt and machine learning classification analysis. Geraldine Quénéhervé contributed partly to the SVM modelling. Michael Maerker provided guidance and support throughout the research process to develop the methodology and did the final editing. We would like to thank University of Pavia for financial and logistic support as well as for providing computing infrastructure.

References

Al-Abadi, A. and Al-Alii, A. 2018. Susceptibility mapping of gully erosion using a GIS-based statistical bivariate models: a case study from Ali Al-Gharbi District, Maysan Gvernorate, Southern Iraq. Environmental Earth Sciences, 77(249): 1-20.

Angileri, S.E., Conoscenti, C., Hochshild, V., Maerker, M., Rotigliano, E., Agnesi, V. 2016. Water erosion susceptibility mapping by applying Stochastic Gradient Treeboost to the Imera Meridionale River Basin (Sicily, Italy). Geomorphology, 262, 61-76.

Ardenghi, N. M. G., and Polani, F. 2016. La flora della provincia di Pavia (Lombardia, Italia settentrionale). 1. L'Oltrepò Pavese. Natural History Sciences, 3(2), 51–79.

ARPA Lombardia, 2019. Agenzia Regionale per la Protezione dell'Ambiente. Retrieved from http://www.arpalombardia.it/siti/arpalombardia/meteo/richiesta-dati misurati/Pagine/RichiestaDatiMisurati.aspx

Bachofer, F., Quénéhervé, G., Märker, M., and Hochschild, V. 2015. Comparison of SVM and Boosted Regression Trees for the Delineation of Lacustrine Sediments using Multispectral ASTER Data and Topographic Indices in the Lake Manyara Basin. Photogrammetrie, Fernerkundung, Geoinformation (PFG). (1), 81–94.

Battaglia, S., Leoni, L., Sartori, F., 2002. Mineralogical and grain size composition of clays developing Calanchi and biancane erosional landforms. Geomorphology, 49, 153–170.

Battaglia, S., Leoni, L., Rapetti, F., Spagnolo M. 2011. Dynamic evolution of badlands in the Roglio basin (Tuscany, Italy). Catena, 86, 14-23.

Bellinzona, G., Boni, A., Braga, G., Casnedi, R., and Marchetti, G. 1968.Carta Geologica della Finestra di Bobbio. Atti Ist. Geol. Univ. Pavia, 19, Pavia.

Bellinzona, G., Boni, A., Braga, G., and Marchetti, G. 1971. Note Illustrative della Carta Geologica D'Italia in scala 1:100,000 – Foglio 71 Voghera. Roma.

Bianchini, S., Del Soldato, M., Solari, L., Nolesini, T., Pratesi, F., and Moretti, S. 2016. Badland susceptibility assessment in Volterra municipality (Tuscany, Italy) by means of GIS and statistical analysis. Environmental Earth Sciences, 75(10), 1–14.

Boni A. and Casnedi R. 1970. Note illustrative della Carta Geologica d'Italia alla scala 1:100.000. Fogli 69-70, Asti-Alessandria. Serv. Geol. d'It.: pp. 63, Roma.

Bosco, C., De Rigo, D., Dewitte, O., Poesen, J. J., and Panagos, P. P. 2015. Modelling soil erosion at European scale: towards harmonization and reproducibility. Natural Hazards and Earth System Sciences, 15(2), 225–245.

Bosino, A., Omran, A., and Maerker, M. 2019a. Identification, characterisation and analysis of the Oltrepo Pavese calanchi in the Northern Apennines (Italy). Geomorphology, 340, 53–66.

Bosino, A., Pellegrini, L., Omran, A., Bordoni, M., Meisina, C., and Maerker, M. 2019b. Litho-structure of the Oltrepo Pavese, Northern Apennines (Italy). Journal of Maps, 15(2), 382–392.

Bryan, R., and Yair, A. (Eds.). 1982. Badland geomorphology and piping. Norwich: Geo Books.

Bucciante, M. 1922. Sulla distribuzione geografica dei calanchi in Italia. L'Universo, 38, 585–605.

Buccolini, M., Gentili, B., Materazzi, M., Aringoli, D., Pambianchi, G., Piacentini, T. 2007. Human impact and slope dynamics evolutionary trends in the monoclinal relief of Adriatic area of central Italy. Catena, 71, 96–109.

Buccolini, M., and Coco, L. 2010. The role of the hillside in determining the morphometric characteristics of "Calanchi": The example of Adriatic central Italy. Geomorphology, 123, 200-210.

Buccolini, M., and Coco, L., 2013. MSI (morphometric slope index) for analysing activation and evolution of Calanchi in Italy. Geomorphology, 191, 142-149

Calzolari, C., and Ungaro, F. 1998. Geomorphic features of a badland (biancane) area (Central Italy): characterisation, distribution and qualitative spatial analysis. Catena, 31, 237-256.

Capolongo, D., Pennetta, L., Picarreta, M., Fallacara, G., Boenzi, F. 2008. Spatial and temporal variations in soil erosion and deposition due to land-levelling in a semi-arid area of Basilicata (Southern Italy). Earth Surfurface Processes and Landforms, 233, 364-379.

Cappadonia, C., Coco, L., Buccolini, M., Rotigliano, E. 2016. From slope morphometry to morphogenetic processes: an integrated approach of field survey, geographic information system morphometric analysisis and statistics in italian Calanchi. Land Degrad. Develop., 27, 851-862.

Caraballo-Arias, N.A., Conoscenti, C., Di Stefano, C., Ferro, V. 2014. Testing GIS-morphometric analysis of some Sicilian Calanchi. Catena, 113, 370-376.

Caraballo-Arias, N.A., Conoscenti, C., Di Stefano, C., Ferro, V. 2015. A new empirical model for the estimating calacnhi Erosion in Sicily, Italy. Geomorphology, 231, 292-300.

Caraballo-Arias, N. A., Di Stefano, C., Ferro, V. 2017. Morphological characterisation of calanchi (badland) hillsope connectivity. Land Deg. Dev., 29, 1190-1197.

Castaldi, F., and Chiocchini, U. 2012. Effect of land use changes on Badlands erosion in clayey drainage basin, Radicofani, Central Italy. Geomorphology, 169, 98-108.

Cavanna, F., Di Giulio, A., Galbiati, B., Monsa, S., Perotti, C. R., and Pieri, M. 1989. Carta geologica dell'estremità orientale del Bacino Terziario Ligure Piemontese. Atti Ticinensi di Scienze della Terra. (32).

Ciancetti, G., Dolza, G., and Pilla, G. 2008. Il trasporto solido nei corsi d'acqua minori dell'Oltrepo Pavese: alcuni caratteri peculiari nel contenuto delle torbide del T. Versa. Italian Journal of Quaternary Sciences, 21(1B), 161–168.

Ciccacci, S., Galiano, M., Roma, M.A., Salvatore M. C. 2008. Morphological analysis and erosion rate evaluation in badlands of Radicofani area (Soutern Tuscany - Italy). Catena, 74, 89-97.

Cocco, S., Brecciaroli, G., Agnelli, A., Weindorf, D., Corti, G., 2015. Soil genesis and evolution on Calanchi (badland-like landform) of central Italy. Geomorphology, 248, 33 46.

Cohen, J. 1960. A Coefficient of Agreement for Nominal Scales. Educational and Psychological Measurement, 20(1), 37–46.

Conforti, M., Aucelli, P.P.C., Robustelli, G., Scarciglia, F. 2011. Geomorphology and GIS analysis for mapping gully erosion susceptibility in the Turbolo stream catchment (Northern Calabria, Italy). Nat Hazard, 56:881-898.

Congedo, L. 2016. Semi-Automatic Classification Plugin Documentation. DOI: http://dx.doi.org/10.13140/RG.2.2.29474.02242/1

Conoscenti, C., Di Maggio, C., and Rotigliano, E. 2008. Soil erosion susceptibility assessment and validation using a geostatistical multivariate approach: a test in Southern Sicily. Nat Hazards, 46(3), 287–305.

Conoscenti, C., Agnesi, V., Angileri, S., Cappadonia, C., Rotigliano, E., Maerker, M. 2013. A GIS-based approach for gully erosion susceptibility modelling: a test in Sicily, Italy. Environm Earth Sci., 70, 1179-1195.

Conoscenti, C., Angileri, S., Cappadonia, C., Rotigliano, E., Agnesi, V., Maerker, M. 2014. Gully erosion susceptibility assessment by means of GIS-based logistic regression: A case of Sicily (Italy). Geomorphology, 204, 399-411.

Conrad, O., Bechtel, B., Bock, M., Dietrich, H., Fischer, E., Gerlitz, L., Böhner, J. 2015. System for Automated Geoscientific Analyses (SAGA) v. 2.1.4. Geoscientific Model Development Discussions, 8(2), 2271–2312.

Elith, J., Graham, C.H., Anderson, R.P., Dudík, M., Ferrier, S., Guisan, A., Hijmans, R.J., Huettmann, F., Leathwick, J.R., Lehmann, A., Li, J., Lohmann, L.G., Loiselle, B.A., Manion, G.,Moritz, C., Nakamura, M., Nakazawa, Y., Overton, J. McC. M.,Peterson, A.T., Phillips, S.J., Richardson, K., Scachetti-Pereria, R., Schapire, R.E., Soberón, J., Williams, S., Wisz, M.S. and Zimmerman, N.E. 2006. Novel methods improve prediction of species' distributions from occurrence data. Ecography, 29,129–151.

Fauklner, H. 2008. Connectivity as a crucial determinant of badland morphology and evolution. Geomorphology, 100, 91-103.

Faulkner, H., Spivey, D., Alexander, R. 2000. The role of some site geochemical processes in the development and stabilisation of three Badlands sites in Almeria, Southern Spain. Geomorphology, 35, 87-99.

Faulken, H. 2013. Badlands in marl lithologies: A field guide to soil dispersion, subsurface erosion and piping-origin gullies. Catena, 106, 42-53.

Gallart, F., Solè, A., Puigdefàbregas, J., Lázaro, R. 2002. Calanchi System in the Mediterranean. -In: BULL, L.J. and M.J. Kirkby (eds): Dryland Rivers: hydrology and geomorphology of semi-arid channels. -Chichester: John Wiley and Sons Ltd., 299-326.

Gallart, F., Marignani, M., Perez-Gallego N., Santi, E., Maccherini S. 2013. Thirty years of studies on badlands, from phisical to vegetational approaches. A succinct review. Catena, 106 4-11.

Gomez-Gutierrez, A., Conoscenti, C., Angileri, SE., Rotigliano E., Schnebel S. 2015. Using topographical attributes to evaluate gully erosion proneness (susceptibility) in the Mediterranean basin: advantages and limitations. Nat Hazard, 79:291-314.

Goodenough, D. J., Rossmann, K., and Lusted, L. B. 1974. Radiographic applications of receiver operating characteristic (ROC) curves. Radiology, 110(1), 89–95.

Grubin, K. M. 2013. Clay mineralogy as a crucial factor in badland hillslope processes. Catena, 106, 54-67.

Grubin, K. M. Vergari, F., Troiani, F., Della Seta, M. 2018. The role of Lithology: Parent Material Control on badland Develompment. In Badland Dynamics in the Context of global Change, 61-109.

Gunatilake, H. M., and Vieth, G. R. 2000. Estimation of on-site cost of soil erosion: A comparison of replacement and productivity change methods. Journal of Soil and Water Conservation, 55(2), 197–204.

Hanley, J. A., and McNeil, B. J. 1982. The meaning and use of the area under a receiver operating characteristic (ROC) curve. Radiology, 143(1), 29–36.

Hofierka, J., and Ŝúri, M. 2002. The solar radiation model for Open source GIS: implementation and applications: Proceedings of the Open Source GIS - GRASS user conference 2002, Trento, Italy, 11-13 September 2002, 1–19.

Hosmer, D. W., Lemeshow, S., and Sturdivant, R. X. 2013. Applied logistic regression (3rd ed.). Wiley series in probability and statistics. Hoboken, N.J.: Wiley.

Javidan, N., Kavian, A., Pourghasemi, H.R. Conoscenti, C., Jafarian, Z. 2020. Data Mining Technique (Maximum Entrophy Model) for Mapping Gully Erosion Susceptibility in the Gorganrood Watershed, Iran. In: Gully Erosion Studies from India and Surrounding Regions. Pravat Kumar Shit, hamid Reza Pourghasemi, Gouri Sankar Bhunuia Editors. Springer 427-448.

Kepner, W. G., Rubio, J. L., Mouat, D. A., and Pedrazzini, F. 2006. Desertification in the Mediterranean Region. A Security Issue. NATO Security Through Science Series: Vol. 3. Dordrecht: Springer.

Kosmas, C., Danalatos, N., Cammeraat, L. H., Chabart, M., Diamantopoulos, J., Farand, R., Vacca, A. 1997. The effect of land use on runoff and soil erosion rates under Mediterranean conditions. Catena, 29(1), 45–59.

Kottek, M., Grieser, J., Beck, C., Rudolf, B., and Rubel, F. 2006. World Map of the Köppen-Geiger climate classification updated. Meteorologische Zeitschrift, 15(3), 259–263.

Landis, J. R., and Koch, G. G. 1977. The Measurement of Observer Agreement for Categorical Data. Biometrics, 33(1), 159.

Langbein, W. B., and Schumm, S. A. 1958. Yield of sediment in relation to mean annual precipitation. Transactions, American Geophysical Union, 39(6), 1076.

Liberti, M., Simoniello, T., Carone, M.T., Coppola, R., D'Emilio, M., Macchiato, M. 2009. Mapping badland areas using LANDSAT TM/ETM satellite imagery and morphological data. Geomorphology, 106, 333-343.

Maerker, M., Pelacani S., Scröder, B. 2011. A functional entity approach to predict soil erosion processes in a small Plio-Pleistocene Mediterranean catchment in Northern Chianti, Italy. Geomorphology, 125, 530-540.

Maerker, M., Bosino, A., Scopesi C., Giordani, P., Firpo, M., Rellini, I. 2020. Assessment of calanchi and rill-interrill erosion susceptibility in northern Liguria, Italy: A case study using a probabilistic modelling framework. Geoderma, 371, 114367.

Magliulo, P. 2012. Assessing the susceptibility to water-induced soil erosion using a geomorphological, bivariate statistics-based approach. Environmental Earth Sciences, 67(6), 1801-1820.

Marchesi, R. 1961. Serie stratigrafica di M. Piano. Bollettino della Società Geologica Italiana, 80, 71–77.

Martelli, L., Cibin, U., Di Giulio, A., and Catanzariti, R. 1998. Litostratigrafia della formazione di Ranzano (Priaboniano-Rupeliano, Appennino settentrionale e Bacino Terziario Piemontese). Italian Journal of Geosciences, 117(1), 151–185.

Medley, K.A. 2010. Niche shifts during the global invasion of the Asian tiger mosquito, Aedes albopictus Skuse (Culicidae), revealed by reciprocal distribution models. Global Ecol. Biogeogr., 19, 122-133.

Meyer, D., Dimitriadou, E., Hornik, K., Weingessel, A., and Leisch, F. 2019. e1071: Misc Functions of the Department of Statistics, Probability Theory Group. v1.7-2. TU Wien. Retrieved from https://CRAN.R-project.org/package=e1071

Moreno-de las Heras, M., Gallart, F. 2016. Lithology controls the regional distribution and morphological diversity of montane Mediterranean Badlands in the upper Llobregat basin (eastern Pyrenees). Geomorphology, 273, 107-115

Moretti, S. and Rodolfi, G. 2000. A typical “calanchi” landscape on the Eastern Apennine margin (Atri, Central Italy): Geomorphological features and evolution. Catena, 40(2), 217–228.

Ortega-Huerta, M.A. and Peterson, A.T. 2008. Modeling ecologi-cal niches and predicting geographic distributions: a test of six presence-only methods. Revista Mexicana de Biodiversidad, 79, 205–216.

Panagos, P. P, Standardi, G., Borrelli, P., Lugato, E., Montanarella, L., and Bosello, F. 2018. Cost of agricultural productivity loss due to soil erosion in the European Union: From direct cost evaluation approaches to the use of macroeconomic models. Land Degradation and Development, 29(3), 471–484.

Panini, F., Fioroni, C., Fregni, P., and Bonacci, M. 2002. Le rocce caotiche dell’Oltrepo pavese: note illustrative della carta geologica dell’Appennino vogherese tra Borgo Priolo e Ruino. Atti Ticinensi di Scienze della Terra, 43, 83–109.

Passerini, G. 1937. “Influenza dell’immersione degli strati ed influenza dell’orientamento dei versanti sulla degradazione delle argille plioceniche”. Boll. Soc. Geol., 56, 45-62.

Pellegrini, L., and Vercesi, P. L. 2017. Landscapes and Landforms Driven by Geological Structures in the Northwestern Apennines. In M. Soldati and M. Marchetti (Eds.), Landscapes and Landforms of Italy (pp. 203–213). Cham: Springer International Publishing.

Phillips, C. P. 1998. The badlands of Italy: a vanishing landscape? Applied Geography, 18(3), 243–257.

Phillips, S. J., Anderson, R. P., and Schapire, R. E. 2006. Maximum entropy modeling of species geographic distributions. Ecological Modelling, 190(3–4), 231–259.

Phillips, S.J., and Dudik, M. 2008. Modeling of species distributions with Maxent: new extensions and a comprehensive evaluation. Ecography, 31, 161-175.

Piccarreta, M., Faulkner, H., Bentivenga, M., Capolongo, D. 2006. The influence of physico-chemical material properties on soil erosion processes in the Badlands of Basilicata, Southern Italy. Geomorphology, 81, 235-251.

Poesen, J.W.A., and Hooke, J. M. 1997. Erosion, flooding and channel management in Mediterranean environments of southern Europe. Progress in Physical Geography: Earth and Environment, 21(2), 157–199.

Pournader, M., Ahmadi, H., Feiznia, S., Karimi, H., and Peirovan, H. R. 2018. Spatial prediction of soil erosion susceptibility: an evaluation of the maximum entropy model. Earth Science Informatics, 11(3), 389–401.

Pulice, I., Di Leo., P, Robustelli, G., Scarciglia, F., Cavalcante, F., Belviso, C. 2013. Control of climate and local topography on dynamics evolution of Badlands from southern Italy (Calabria). Catena, 109, 83-95.

QGIS Development Team 2018. QGIS Geographic Information System. Retrieved from http://qgis.org

R Core Team 2018. R: A language and environment for statistical computing. Vienna, Austria. Retrieved from R Foundation for Statistical Computing website: https://www.R-project.org/

Rahmati, O., Tahmasebipour, N., Haghizadeh, A., Pourghasemi H. R., Feizizadeh, B. 2017. Evaluation of different machine learning models for predicting and mapping the susceptibility of gully erosion. Geomorphology, 298, 118-137.

Ramos, M. C., and Martínez-Casasnovas, J. A. 2004. Nutrient losses from a vineyard soil in Northeastern Spain caused by an extraordinary rainfall event. Catena, 55(1), 79–90.

Regione Lombardia, 2015. http://www.geoportale.regione.lombardia.it/

Riley, S. J., De Gloria, S. D., and Elliot, R. 1999. A Terrain Ruggedness that Quantifies Topographic Heterogeneity. Intermountain Journal of Sciences. (5), 23–27.

Rossetti, R., and Ottone, C. 1979. Esame preliminare delle condizioni pluviometriche dell'Oltrepò Pavese e dei valori critici delle precipitazioni in relazione ai fenomeni di dissesto franoso. Geologia Applicata e Idrogeologia, 14(3), 83–99.

Rouse, J. W., Hass, R. H., Schell, J. A., and Deering, D. W. 1973. Monitoring vegetation systems in the Great Plains with ERTS. Proceedings of the 3rd ERTS symposium, Goddard Space Flight Center, December 1973. Washington, DC: NASA, 309–317.

Sappington, J. M., Longshore, K. M., and Thompson, D. B. 2007. Quantifying Landscape Ruggedness for Animal Habitat Analysis: A Case Study Using Bighorn Sheep in the Mojave Desert. The Journal of Wildlife Management, 71(5), 1419–1426.

Schillaci, C., Braun, A., and Kropáček, J. 2015. Terrain analysis and landform recognition. British Society of Geomorphology, 2, 4.2 1-18.

Sørensen, R., Zinko, U., and Seibert, J. 2005. On the calculation of the topographic wetness index: Evaluation of different methods based on field observations. Hydrology and Earth System Sciences Discussions. (2), 1807–1834.

Stolte, J., Tesfai, M., Øygarden, L., Kværnø, S., Keizer, J., Verheijen, F., Hessel, R. 2016. Soil threats in Europe: status, methods, drivers and effects on ecosystem services: A review report, deliverable 2.1 of the RECARE project (JRC Technical Reports).

Summa, V., Tateo, F., Medici, L., and Gianossi, M.L. 2007. The role of mineralogy, geochemistry and grain size in badland development in Pisticci (Basilicata, Southern Italy). Earth Surface Processes and Landforms, 32, 980-997.

Swets, J. A. 1988. Measuring the accuracy of diagnostic systems. Science, 240 (4857), 1285–1293.

Torri D, Santi E, Marignani M, Rossi M, Borselli L, Maccherini S. 2013. The recurring cycles of biancana badlands: erosion, vegetation and human impact. Catena, 106, 22–30.

USGS Earth Explorer, 2019. Retrieved from http://earthexplorer.usgs.gov

Vapnik, V. N. 1995. The nature of statistical learning theory. New York, NY, USA: Springer.

Vapnik, V. N. 1999. An overview of statistical learning theory. Neural Networks, IEEE Transactions, 10(5), 988–999.

Vercesi, P. L., and Perotti, C. 2016. Carta geologica d'Italia alla scala 1:50.000 Foglio 178. Voghera: ISPRA Serv. Geologico d'Italia.

Vergari, F., Della Seta, M., Del Monte, M., Barbieri, M. 2013. Badlands denudation "hot spots": The role of parental material properties on geomorphic processes in 20-years monitored sites of Southern Tuscany (Italy). Catena, 106, 31-41.

Vergari, F. 2015. Assessing soil erosion hazard in a key badland area of Central Italy. Nat Hazards, 79(S1), 71–95.

Vittorini S., 1977. Osservazioni sulle origini e sul ruolo di due forme di erodione nelle argille; calanchi e biancane. Bollettino Società Geografica Italiana, Serie 10, 6.

Wang, L., and Liu, H. 2006. An efficient method for identifying and filling surface depressions in digital elevation models for hydrologic analysis and modelling. International Journal of Geographical Information Science, 20(2), 193–213.

Yüksel, A., Akay, A. E., Gundogan, E. 2008. Using ASTER Imagery in Land Use/cover Classification of Eastern Mediterranean Landscapes According to CORINE Land Cover Project. Sensor, 8, 1237-1251.

Zakerinejad, R., and Maerker, M. 2014. Prediction of gully erosion susceptibilities using detailed terrain analysis and maximum entropy modeling: A case study in the Mazayejan plain, southwest Iran. Geografia Fisica E Dinamica Quaternaria, 37(1), 67–76.

Zakerinejad, R., Omran, A., Hochscild, V., and Maerker, M. 2018. Assessment of gully erosion in relation to lithology in the southwestern Zagros Mountains, Iran using ASTER data, GIS, and stochastic modelling. Geogr. Fis. Dinam. Quat., 41, 95-104.

CHAPTER IV: "SEDIMENT DYNAMICS"

Bosino Alberto, Szatten Dawid Aleksander, Omran Adel, Becker Rike, Bettoni Manuele, Schillaci Calogero, Maerker Michael (submitted). Assessment of sediment dynamics in a small Northern Apennines catchment (Italy).

Abstract

The quantification of the suspended sediments leaving a basin is often unknown in terms of their quantity and dynamics. Hence, the objective of this study is to assess in a quantitative way the sediment dynamics of a small watershed in the Northern Apennines dominated by suspended sediment transport. Therefore, we analysed and correlated the sediment volume concentration and grain size distribution of the suspended sediments with the precipitation pattern. The study area is sited in the Northern Apennines, Italy and is represented by a small watershed (0.15 km^2) that is dominated by intensive soil erosion processes and related forms and features. The basin is East-West oriented with South-facing slopes characterised by badlands processes. The North-facing slopes are cultivated and dominated by laminar surface runoff and related rill-interrill phenomena. Initially, a morphometrical characterisation of the basin was performed using a high-resolution Digital Elevation Model with a 15 cm resolution. Subsequently, the physical characteristics of the topsoil and of the vegetation were investigated based on grain size analysis and a detailed NDVI analysis performed on Sentinel-2A images. Finally, we assessed the suspended sediments at the outlet of the basin using a laser diffraction technique. The Suspended Sediment volume Concentration (SSC) and the Sauter Mean Diameter (SMD) of the eroded sediments, allow insights into the morphogenetic processes and the sediment dynamics of the basin. The measurements were conducted in Autumn 2018 after an intense precipitation period and in Spring 2019. The results show a direct correlation between precipitation and SSC with a concentration delay of about 2 hours after the most intense precipitation events. Moreover, we reveal that the SMD values are inversely related to the precipitation due to turbidity effects. The SSC and SMD measurements conducted in an intensively eroding catchment reveal for the first time the

dynamics between precipitation, discharge, and suspended sediments load in badlands areas in Northern Italy.

1. Introduction

Soil erosion is a widespread phenomenon in the Mediterranean region including a set of landforms such as rill-interrills, gullies, tunnelling, and badlands (e.g. Komas et al., 1997; García-Ruiz et al., 2013; Martínez-Murillo et al., 2013). The quantification of the suspended sediments leaving a basin is directly related to: i) the precipitation input, ii) the vegetation cover, iii) the initial soil moisture, iv) the intensity of soil erosion processes as well as v) the morphometry of the basin (see e.g. Ziadat and Taimeh, 2013). In addition, human activities cause soil degradation increasing the erosion through the alteration of land cover and modifying the soil structure (Yang et al., 2003). Furthermore, it should be mentioned that in Plio-Pleistocene deposits of the Mediterranean regions the sediment budget is mainly dominated by suspended sediments (e.g. Webb et al., 1995; Nadal-Romero et al., 2008). In particular, in Italy, water erosion causes on average 7.4 $t \cdot ha^{-1} \cdot yr^{-1}$ of soil loss (Bosco et al., 2015; Stolte et al., 2016). The Northern Apennines are mainly characterised by soft sedimentary bedrock formations i.e. claystone, marl, melanges etc., which are particularly prone to be eroded by surface runoff (Bosino et al., 2019a). Especially badlands are defined as 'intensely dissected natural landscapes where vegetation is sparse or absent and which are "useless" for agriculture' (Bryan and Yair, 1982). In the Italian context, badlands are called "calanchi" (Bucciante, 1922), a word derived from the Latin verb "*chalare*", meaning slowly falling or slumping down.

Concerning the quantitative assessment of erosion processes in several Mediterranean countries different techniques were applied: e.g. i) pin measurements (e.g. Sirvent et al., 1997; Clarke and Rendell, 2006; Ciccacci et al., 2008; Cappadonia et al., 2011), ii) root analysis (e.g. Saez et al., 2011; Corona et al., 2011), iii) measurements of suspended sediment concentration

(Licciardello et al., 2019), iv) turbidimeter analysis and runoff sampler (Nadal-Romero et al., 2008; Vergari et al., 2015), v) back-scattering infrared techniques (Regüés and Nadal-Romero, 2013), vi) H-flume gauging approaches (Brakensiek et al., 1979; Cantón et al., 2001), vii) profilometer measurements (Benito et al., 1992; Sirvent et al., 1997), viii) remotely sensed volumetric measurements and morphometric derivations (De Poley and Gabriels, 1980; Sirvent et al., 1997; Buccolini et al., 2012; Kropáček et al., 2016) or ix) hight resolution topographic survey methods (Tarolli, 2014; Krenz and Kuhn, 2018; Llena, 2020).

However, these measurements have several limits because the direct measurements of the sediments leaving the entire catchment are often not available. Thus, the calibration and validation of erosion models remains very difficult. The aim of this paper is to assess the concentration as well as the diameter of the suspended sediments eroded in the catchment area and transported further down into the drainage network. Hence, we apply a method that directly measures the suspended load of small creeks or river tributaries. The Suspended Sediment Volume Concentration (SSC) as well as the Sauter Mean Diameter (SMD) of the suspended sediments were assessed in situ through a laser diffraction method utilising a LISST-25X sensor (Sequoia Scientific, Inc. Bellevue, WA, USA). The LISST instruments are widely utilised to perform in situ as well as laboratory measurements (e.g. Thonon et al., 2005; Pedocchi and Garcia, 2006; Williams et al., 2007; Meral, 2008; Filippa et al., 2011; Filippa et al., 2012; Felix et al., 2013; Schwarz et al., 2017; Szymczak and Burska, 2018; Szatten et al., 2018). In this work we assessed soil erosion through the measurement of suspended sediments drained off the study basin. Moreover, we compared the SSC as well as the SMD of the eroded sediments with the precipitation measured during two rainfall events in Autumn 2018 and in Spring 2019. To estimate the soil loss of the study area as well as to better understand qualitatively the sediment dynamics a physiographic characterisation of the basin was performed. Therefore, we derived seven significant topographic indices from a 15 cm cell size DEM following Bianchini et al.

(2016). Additionally, we derived information relevant to assess soil erosion processes i.e. vegetation status and type as well as the soil texture.

To characterize the vegetation, we delineated the Normalized Difference Vegetation Index (NDVI) that was calculated based on high-resolution Sentinel-2A images. For each land use type the green cover (NDVI) was estimated and the grain size of the topsoils was also associated accordingly.

2. Materials and methods

2.1. Study area

The study area is sited in the Varzi Municipality, Lombardy Region, Northern Apennines Italy, and is represented by a small catchment strongly affected by calanchi and rill-interrill erosion phenomena (Figure 1). The basin orientation is East-West and the basin shows a typical asymmetry between the South-facing slope, characterized by a knife-shape slope calanco (calanco type A after Moretti and Rodolfi, 2000; see also Bosino et al., 2019b), and the North-facing slope which is cultivated and characterised by widespread rill-interrill erosion.

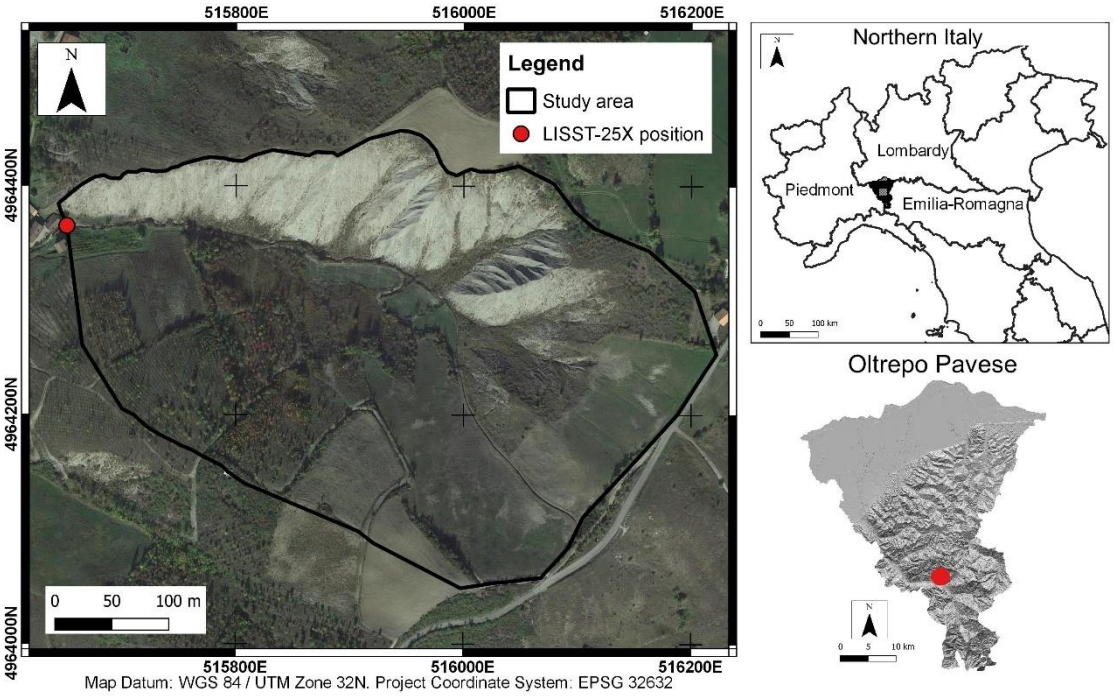

Figure 1: Study area.

The catchment covers about 0.15 km^2 and ranges in altitude from 436 to 564 m a.s.l. The climate of the Oltrepo Pavese is defined as temperate (Ardenghi and Polani, 2016) belonging to a temperate oceanic climate (Cfb) following the Köppen climate classification (Kottek et al., 2006). The mean annual precipitation of the area in the last 40 years is about 650 $mm \cdot yr^{-1}$ (ARPA Lombardia; Rossetti and Ottone, 1979).

As a result of soft sedimentary bedrock, the Oltrepo Pavese is characterised by several soil erosion forms and features i.e. rill-interrill, piping, gully, landslide, and calanchi (Bosino et al., 2019b). Particularly calanchi forms and features represent the complex interaction between different soil erosion processes directly exposing the underlying highly erodible bedrock (Bosino et al., 2020).

The study area is geologically homogeneous and composed by the 'Brecce Argillose di Baiso' Units (BAI) (SERVIZIO GEOLOGICO D'ITALIA, 2014). This Formation belongs to the Epiligurian Units and represent Eocene submarine landslides which mobilised the sediments belonging to the External Ligurian Units (Vercesi et al., 2014). These rocks are lithological composed by centimetric to metric blocks scattered in a fine silty-clayey matrix. The mineral composition of the fine matrix was measured through a proximal sensing techniques utilising a field spectrometer (Spectral Evolution RS-3500 instrument) (Viscarra Rossel et al., 2016) and yielding a mineralogical composition of sediments dominated by illite-montmorillonite clay minerals.

The soils developing in the area are very thin, with maximum depth of about 30 cm on the North-facing slope. These soils can be classified as Entisols following the USDA soil classification (Soil Survey Staff, 2010) or as Regosols/Cambisols according to the World Reference Base for Soil Resources (IUSS Working Group WRB, 2015) as reported in the pedological map of Lombardy 1:250.000 available at (http://www.geoportale.regione.lombardia.it/).

The watershed is consisting in two slopes with opposite exposition, and different morphological and vegetational characteristics (Figure 2).

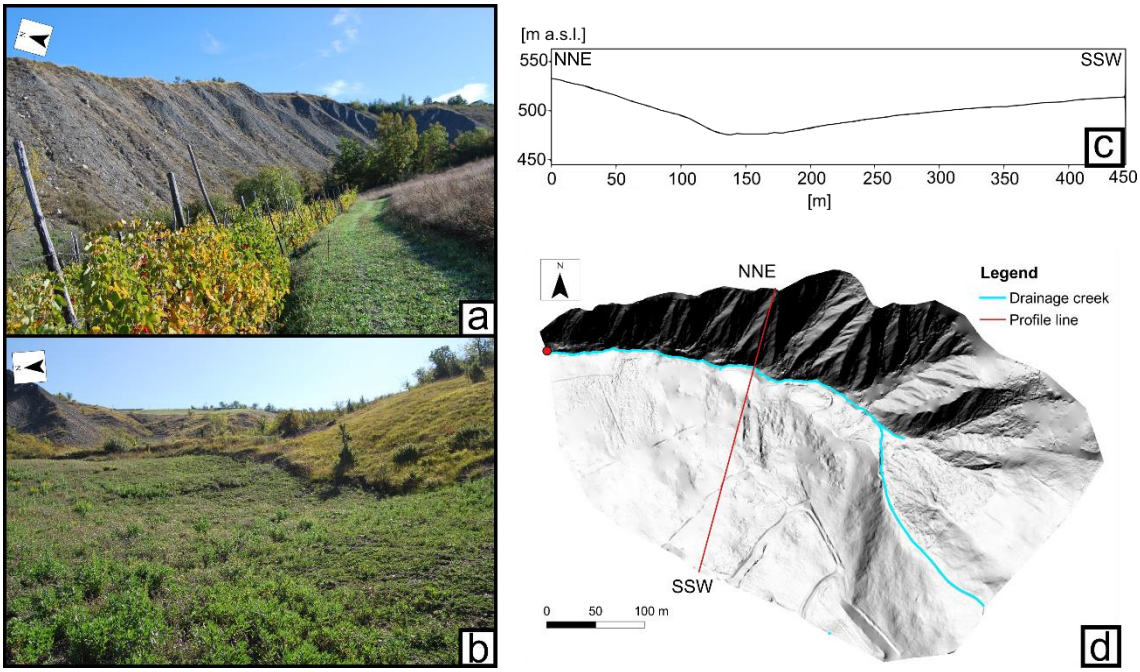

Figure 2: a) Calanco landforms on North-facing slope with the exposed bedrock. b) Vegetated South-facing slope. c) Transversal profile of the catchment. d) Principal stream network of the basin.

The South-facing slope is characterized by exposed bedrock as well as sparse bushes such as *Spartium junceum L.* and pioneer plant associations. Consequently, runoff processes can act directly on the soft clays, developing the typical calanco landforms (Figure 2a). Conversely the North-facing slope is characterised by an arboreal (i.e. *Fraxinus* and *Quercus*) and shrubby (i.e. *Spartium junceum L.*) vegetation which partially protect the bedrock preventing or hindering concentrated runoff phenomena (Figure 2b). Generally, the asymmetry and the slope of the basin (Figure 2c) indicate a high runoff potential on the South-facing slope. The basin is drained by a small creek which is up to 1.5 m wide and shows a torrential regime (Figure 2d). The creek is draining towards the West and is active only during precipitation events. Since a permanent monitoring of the creek was not feasible we simulated the discharge dynamics of the creek using the Soil Water Assessment Tool (SWAT) (Arnold et al., 1998) that in turn was calibrated

and validated using the measured terrain parameters as well as climatic data of a nearby rainfall station (Varzi-Nivione https://www.arpalombardia.it/Pages/Meteorologia/Richiesta-dati-misurati.aspx). In order to assess the suspended sediments directly eroded in the study area, we installed a LISST-25X device on the outlet of the basin (Figure 1).

2.2. Morphometrical and physical characterisation of the basin

In order to characterise morphometrically the study area, we performed a detailed Terrain Analysis on a 15 cm cell size Digital Elevation Model (DEM). The DEM was generated using a Structure from Motion (SfM) algorithm starting from a point cloud derived from aerial photographs (e.g. Micheletti et al., 2015; Kropáček et al., 2016) acquired during a drone survey in November 2018.

We utilised SAGA GIS (Conrad et al., 2015) to delineate seven representative morphometric indices following Bianchini et al. (2016). Initially, the DEM was hydrologically corrected to eliminate sinks using the algorithm proposed by Wang and Liu (2006). Subsequently four basic terrain indices were derived: i) Elevation, which yield general information on the morphology of the area. ii) Slope, which gives information on terrain steepness. iii) Aspect, that represent the direction of maximum gradient and iv) Profile Curvature, which represent the curvature in the direction of the maximum slope. Subsequently, we generated the v) Stream Power Index (SPI), that yield information on the erosive power of concentrated surface runoff, vi) LS-Factor, as one of the components of the USLE model (Wischmeier and Smith, 1978) describing the transport capacity of surface runoff and hence, of the erosional potential and vii) Topographic Wetness Index (TWI), a factors that indicates the potential of soil saturation and runoff generation. The environmental parameters and the topographic indices are presented in Table 1. Land use was mapped through a detailed field survey in November 2018. The results were stored in a vector format. Information of vitality of vegetation and green cover are derived using

freely available Sentinel-2A images that were downloaded from the ESA's (European Space Agency) Copernicus hub project website. The Google Earth Engine (GEE) is a cloud-based geospatial processing platform which provides online access to its archived datasets. In this study, the JavaScript application programming interface (API) was used for calling, pre-processing, mosaicking, and processing. We obtained, corrected, and filtered the images in order to acquire cloud-free products. The Normalized Difference Vegetation Index values were calculated based on eight Sentinel-2A images acquired from 28/11/2018 to 23/3/2019. The Sentinel-2 satellites with 5-day revisit time over land and coastal areas is equipped with a multispectral imager (MSI) with 13 bands (Drusch et al., 2012). The Sentinel-2A images were resampled to 10 m resolution for all bands. The first Sentinel image is from November 2018, coeval to the LISST measurements, the last available image is from the end of March 2019. Subsequently, in order to correlate the green cover with the physical characteristics of the eroded sediments, we investigated the Normalized Difference Vegetation Index (NDVI) based on Sentinel-2A images. The NDVI provides information on the spatial distribution of green biomass and its vitality. Thus, the NDVI gives also valuable hints on the effects of the green cover on soil erosion and the evolution of the calanchi landforms in terms of ground cover and protection as well as in decelerating surface runoff. Finally, soil grain size distribution was analysed for the entire catchment following the ASTM Standard (American Society for Testing Materials, 1988). As mentioned above the sediment load especially in the Plio-Pleistocene deposits of the Mediterranean area is often dominated by suspended sediments (e.g. Webb et al., 1995; Nadal-Romero et al., 2008). Consequently, we analysed the fine fractions such as clay, silt and sand excluding the particles larger than 2 mm (skeleton). The average grain size values for any land use type was plotted in a triangular grain size diagram following the USDA-based soil texture classes.

Table 1. Environmental parameters

Type	*Variable Range Value*	*Mean*	*SD*	*Reference*
Topographic indices				
Elevation	436/564 m a.s.l.	504.7	31.06	Wang and Liu, 2006
Slope	0/56°	21.7	8.45	Zevenbergen and Thorne, 1987
Aspect	0/360°	251	101.98	Zevenbergen and Thorne, 1987
Profile Curvature	-2/+2	0.0011	0.17	Zevenbergen and Thorne, 1987
SPI	0/735	206.6	91.56	Moore et al., 1991
LS-Factor	0/47	3.43	1.68	Moore et al., 1991
TWI	-4/6.4	-0.08	0.97	Baven and Kirkby, 1979
Environmental data				
Land Use	6 classes			Field survey
Remote Sensing data				
NDVI	-1 to +1			ESA

2.3. SMD and SSC measurements, rainfall analysis and comparison

The Sauter Mean Diameter (SMD) and Suspended Sediment Volume Concentration (SSC) were measured with a LISST-25X device that is using a Lorenz-Mie scattering (Tyndall effect) of a low angle laser light (Sequoia, 2008). The Mie-theory of light scattering suggests that collimated laser light illuminating particles will scatter most of its energy at particular angles. Small particles scatter their energy at larger angles and large particles at smaller angles. By recording the scattering at different angles, the LISST-25X can mathematically invert the scattering to determine the size distribution and concentration of particles in the water (Filippa et al., 2011). The sample grain size is calculated as the Sauter Mean Diameter that represents an average of particle size. It is defined as the diameter of a sphere that has the same volume/surface area ratio as a particle of interest. SMD is typically defined in terms of the surface diameter, d_s:

$d_s = (A_p/\pi)^{0.5}$

and volume diameter, d_v:

$d_v = (6V_p/\pi)^{1/3}$

where A_p and V_p are the surface area and volume of the particle, respectively. If d_s and d_v are measured directly by other means without knowledge of A_p or V_p, the Sauter diameter for a given particle is:

$SD = d_{32} = d_v^3/d_s^2$

If the actual surface area, A_p and volume, V_p of the particle are known the equation simplifies further to:

$SD = d_{32} = 6(V_p/A_p)$

This is usually taken as the mean of several measurements, to obtain the Sauter Mean Diameter. The instrument can detect a particle size range between 2.5 and 500 µm with a resolution of 1 µm. The SSC range between 0.1 and 1000 $mg \cdot L^{-1}$ with a resolution of 0.025%, for an optical length of 2.5 cm. Both the SMD and SSC vary linearly and inversely according to the optical path length of the instrument.

The instrument was set up to measure the Sauter Mean Diameter (SMD) in two classes: i) silt and sand particles (2.5-500 µm; Full-range) and ii) fine and medium sand (63-500 µm; Sub-range) as well as the respective Suspended Sediment Volume Concentration (SSC) every 10 minutes. The collected results were correlated with the precipitation data measured by ARPA LOMBARDIA at the Varzi-Nivione climate station in the period October 2018 to April 2019 (https://www.arpalombardia.it/Pages/Meteorologia/Richiesta-dati-misurati.aspx). The LISST-25X measurements were conducted from the 31/10/2018 to the 12/11/2018 after a three days rainfall (Figure 3a), and from 02/4/2019 to 08/4/2018 after a longer dry period. (Figure 3c). The total amount of precipitation measured during the first measuring period totals 52.8 mm, while in the second period 25.6 mm of rain were measured. The rainfall intensity recorded during the

observation periods are reported in Figure 3b and 3d reaching respectively 3.4 $mm \cdot h^{-1}$ and 4.6 $mm \cdot h^{-1}$. Finally, the SSC and SMD data were compared with the precipitation and the physical characteristics of the basin.

Due to missing discharge data for the LISST measuring period the hydrological model SWAT (Soil and Water Assessment Toll, Arnold et al., 1998) was utilised to estimate the rainfall-runoff dynamics in the study area. The model was set up with local climate data provided by ARPA Lombardia, Vazi-Nivione meteorological station (precipitation, solar radiation, temperature and relative humidity) as well as detailed data of soil physical characteristics which were collected through field measurements and assessed with laboratory analyses (e.g. grain size distribution, bulk density, hydraulic conductivity).

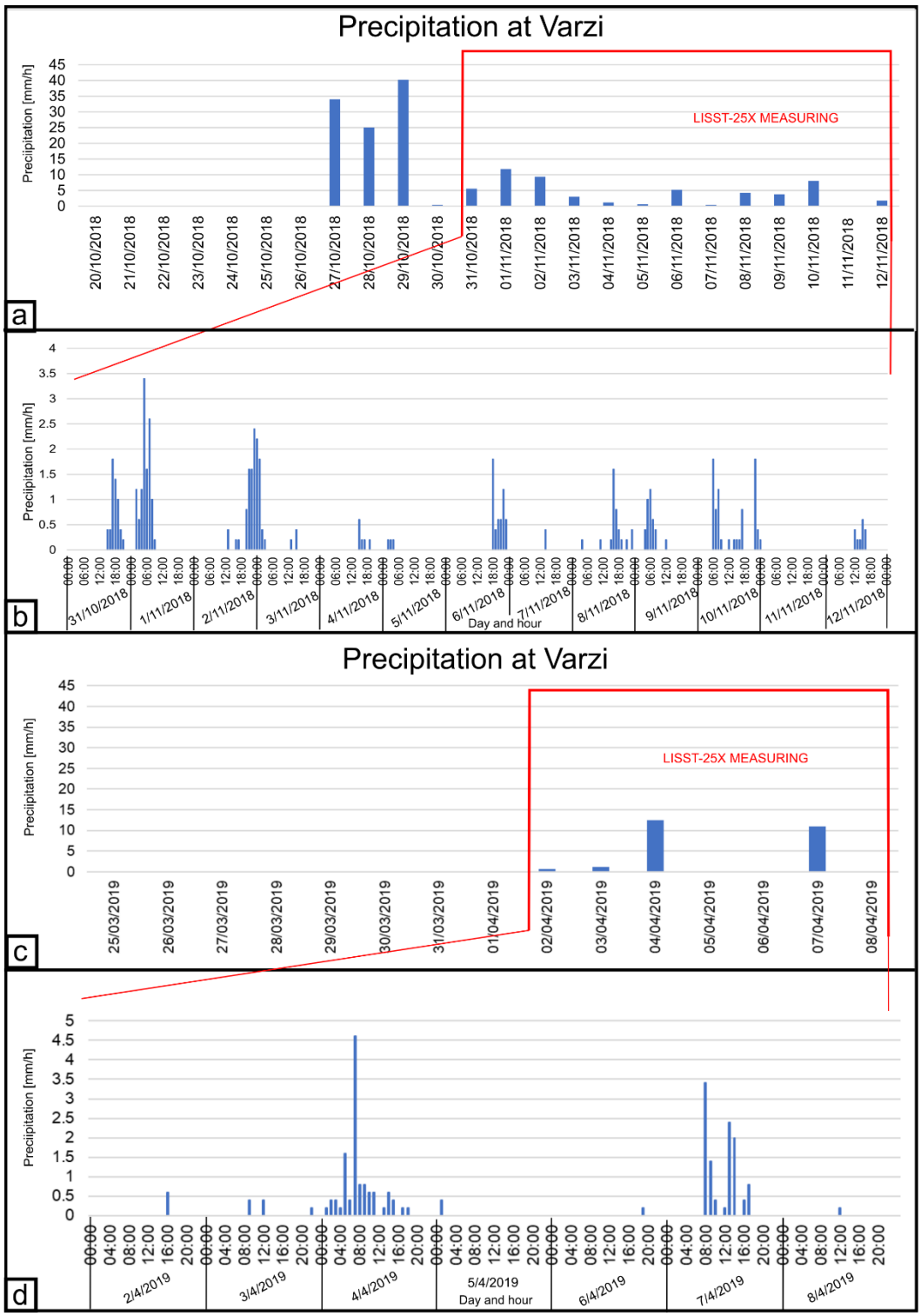

Figure 3: Rainfall characteristics for Varzi Station. a) Daily precipitation values for the period 31/10/2018 to 12/11/2018. b) Hourly precipitation for the same interval. c) Daily precipitation values for the period 02/4/2019 to 08/4/2019. d) Hourly precipitation for the same interval.

3. Results

The morphometrical and physiographic characteristics of the study area yields detailed insights into morphological processes and their dynamics. Therefore, we derived seven topographic indices from a 15 cm DEM (Figure 4). The basin ranges between 436 and 563 m a.s.l. with a mean slope of 17° on the North-facing slope, to 38° on the South-facing slope. Regarding the Exposition and Profile Curvature, the area can be generally separated in a North and a South-facing slope system. We observe a general straight slope profile curvature on the North-facing slopes, whereas the South-facing slopes show a convex profile curvature in the upper slope sections and a prevailing concave profile curvature in the lower slope sections.

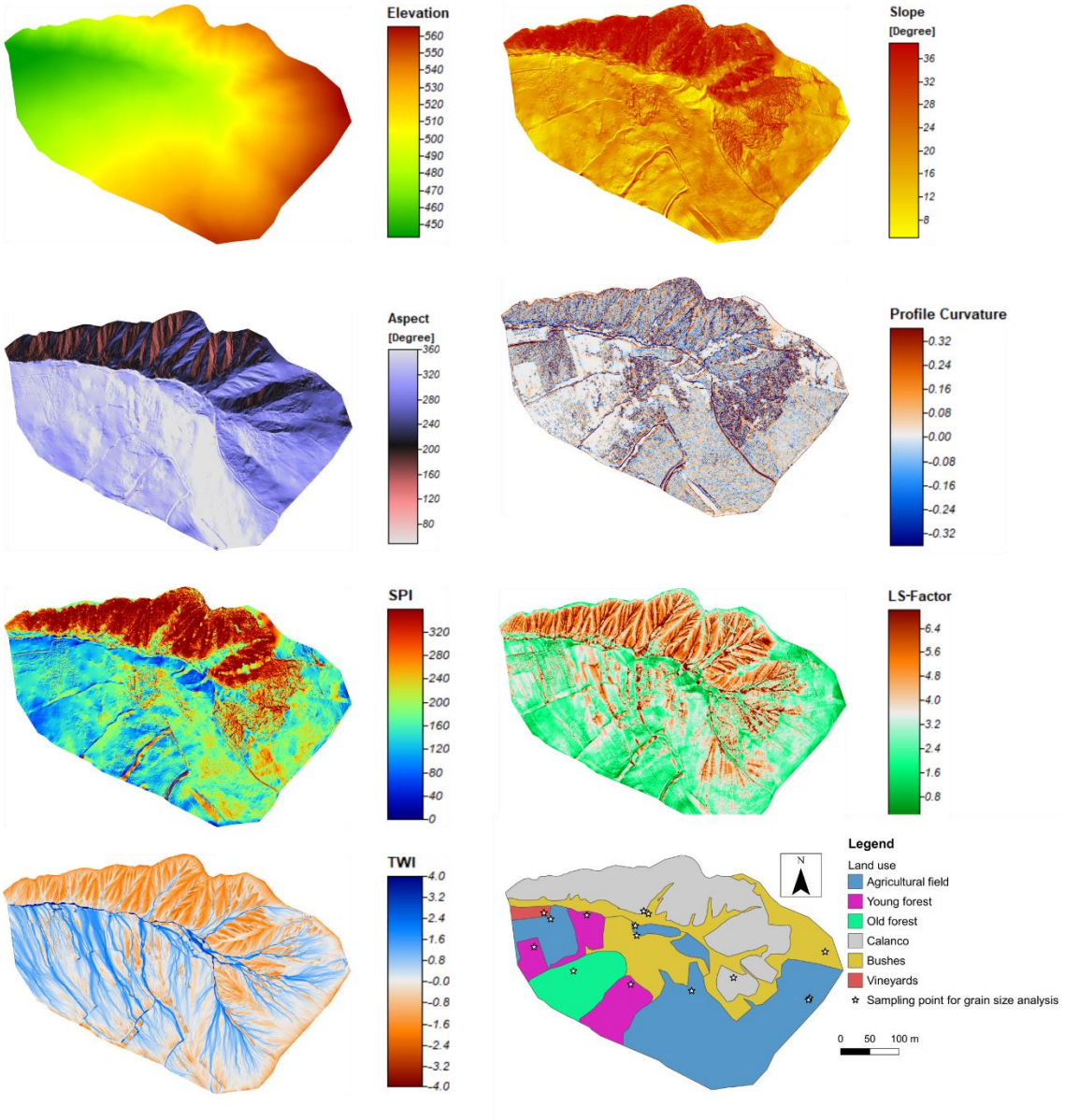

Figure 4: Morphometrical and physical parameters of the study area.

Furthermore, the TWI values show high saturation excess runoff generation potential on the lower North-facing slopes with values up to 4. The South-facing slopes instead show low TWI values indicating a fast drainage and general dryer conditions. The SPI is a measure of the erosive power of concentrated linear runoff showing very high values of up to 320 in the central calanco area. The LS-Factor that describes the transport capacity shows high values, up to 5, in the incisions of the South-facing slopes. Generally, the South-facing slopes show a higher potential to be eroded by surface runoff than the North-facing slope. This is also supported by the spatial distribution of the NDVI values (Figure 5). Figures 5a and 5b show that the green

cover on the North-facing slope and in the central parts of the study area decreased from November 2018 to March 2019 (Figure 5c and 5d). Conversely, the South-facing slope shows in general low values of NDVI which correspond to the exposed bedrock or very sparse or absent vegetation, unable to protect the substrate from erosion.

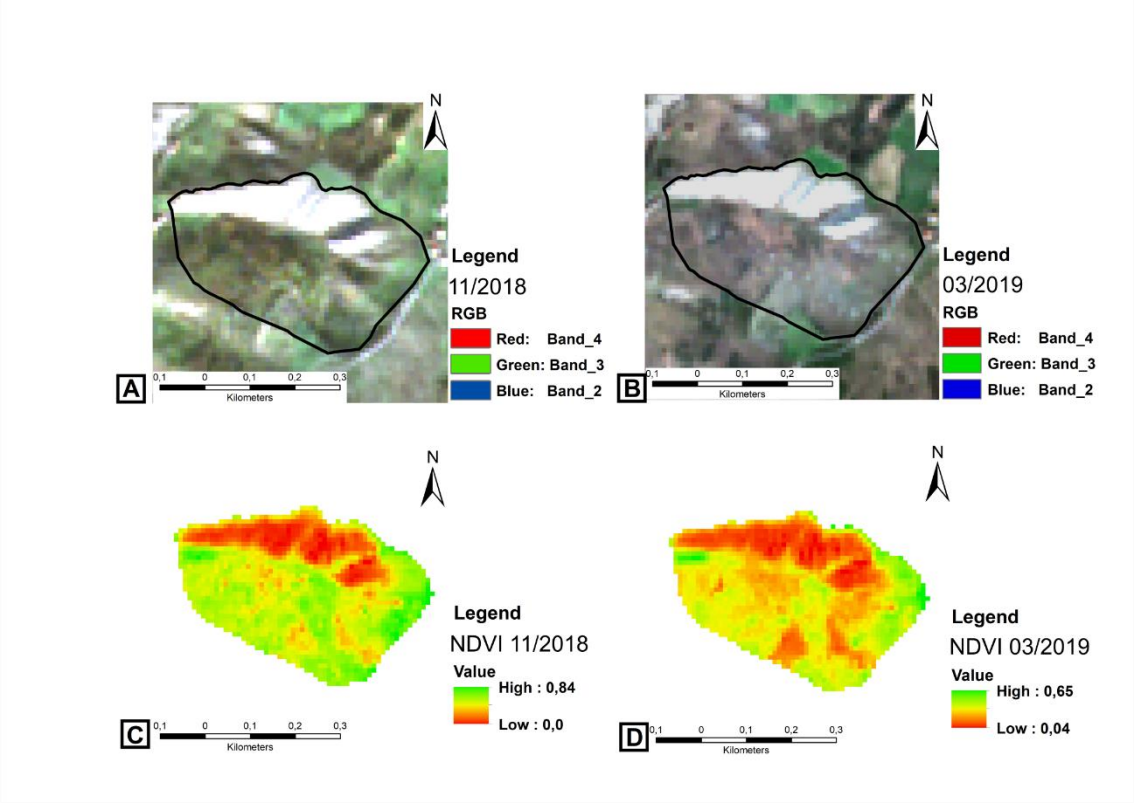

Figure 5: NDVI characteristics of the study area. *a) Sentinel-2A image for November 2018. b) Sentinal-2A image for March 2019. c) NDVI for November 2018. d) NDVI for March 2019.*

We compared the NDVI values of November 2018 and March 2019 for each land use type (Figure 6). In particular, we observed changes in NDVI values of bushes and in the agriculturally used areas in the South-Eastern part of the study area, when compared with the more stable vineyard areas in the North-Western part of the study area. Analysing a complete time series of the available Sentinel-2A images we observed a general decrease of the NDVI values in all different land use types from November 2018 to April 2019 (Figure 6).

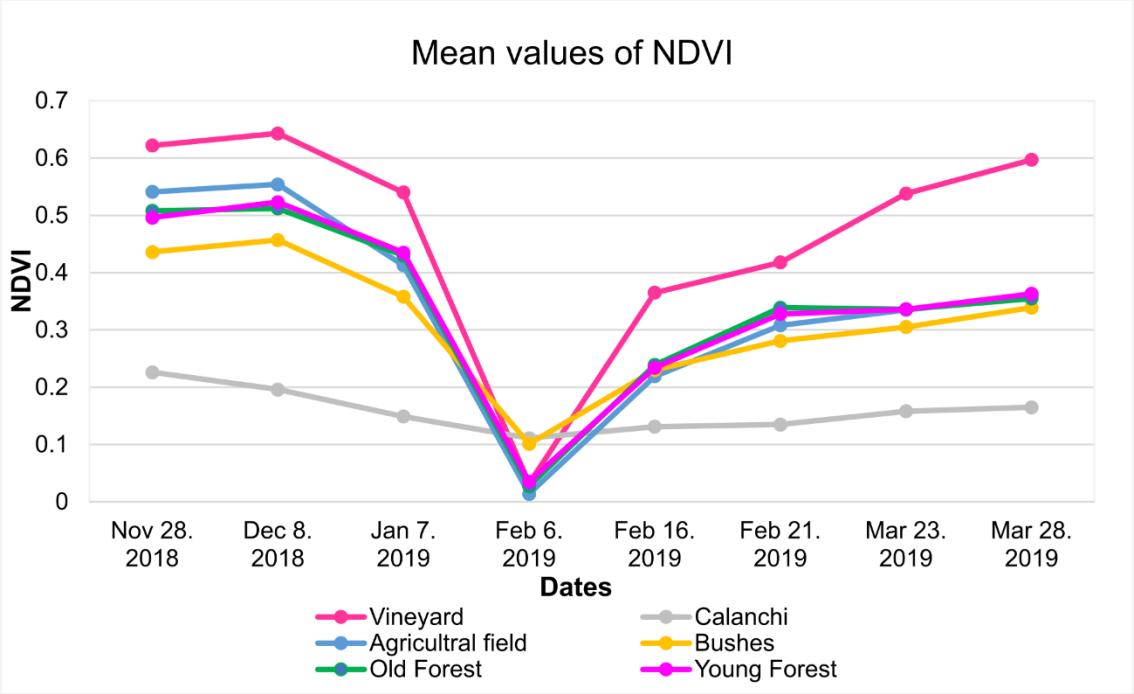

Figure 6: NDVI time series calculated on Sentinel-2A images.

Subsequently, for each land use type several grain size analyses were performed on topsoil following the ASTM Standard, and the average values were plotted in a triangular grain size graph (Figure 7).

Land use	C	Si	Sa
Agricoltural field	56	36	8
Young Forest	57	37	6
Old forest	63	30	7
Calanco	48	47	5
Bushes	56	41	3
Vineyard	60	33	7

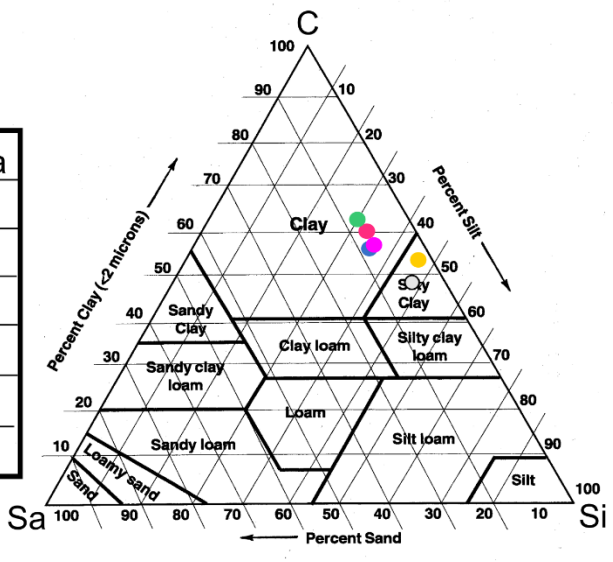

Figure 7: Average grain size (topsoil) distribution for each land use class according to ASTM Standard plotted on a ternary diagram.

The clay fraction ranges between 48 and 60%, the silt fraction between 30 and 47% and the sand fraction between 3 and 8% highlighting a high lithological homogeneity of both North and South-facing slopes. However, the grain size analyses highlight for the Calanco and Bush land use classes fall in the silty clay domain, conversely the other samples belong to the clay fractions (Figure 7).

In order to assess the eroded sediment characteristics and dynamics, we plotted the rainfall intensity (10 minute intervals) versus the Full-range (silt and sand fractions) and the Sub-range (fine-medium sand fraction) of Suspended Sediment volume Concentration (SSC) (Figure 8a, b and 9a, b) as well as the Full and Sub-range of the Sauter Mean Diameter (SMD) (Figure 8c, d and 9c, d). As illustrated in Figs. 8a, b and 9a, b, the SSC trend is time lapsed but generally following the precipitation curve. The peaks of the Full-range SSC are around 2000-4500 $\mu L \cdot L^{-1}$ and the maximum concentration is observed about 2 hours after each precipitation event. Subsequently, the sediment concentration remains constant or constantly decreases over time to values below 1000 $\mu L \cdot L^{-1}$. The same trend can be observed also for the fine-medium sand fraction (Sub-range) SSC. However, the fine-medium sand Sub-range SSC do not show the initial peaks in concentration.

Conversely, both the Full-range and Sub-range SMDs are inversely related to the intensity of precipitation events. During precipitation peaks very small particles are transported in the creek. The particle diameter rises to 40 μm (Full range SMD) and to 140 μm (Sub range SMD) (Figure 8c, d). Regarding the measurements conducted in April the Full-range fraction particle diameter rises to 15-30 μm and to 140-250 μm for the fine-medium sand fraction Sub-range SMD (Figure 9c, d).

Finally, the intensity of the SSC as well as the SMD was correlated to the initial humidity conditions. The measurements conducted in October and November 2018 were performed after intense storm events that saturated the topsoil. On the other hand, the measurements performed

under drier spring conditions were conducted in April 2019. The maximum SSC values reach 4500 $\mu L \cdot L^{-1}$ during humid autumn period in 2018 and up to 5100 $\mu L \cdot L^{-1}$ after the drier spring period. Regarding the SMD the maximum size measured is 140 µm in autumn 2018 and 250 µm in spring 2019. The modelled discharge is represented in Figure 8e and 9e and shows the immediate and impulsive regime of the basin. Generally, the discharge peaks follow the precipitation pattern.

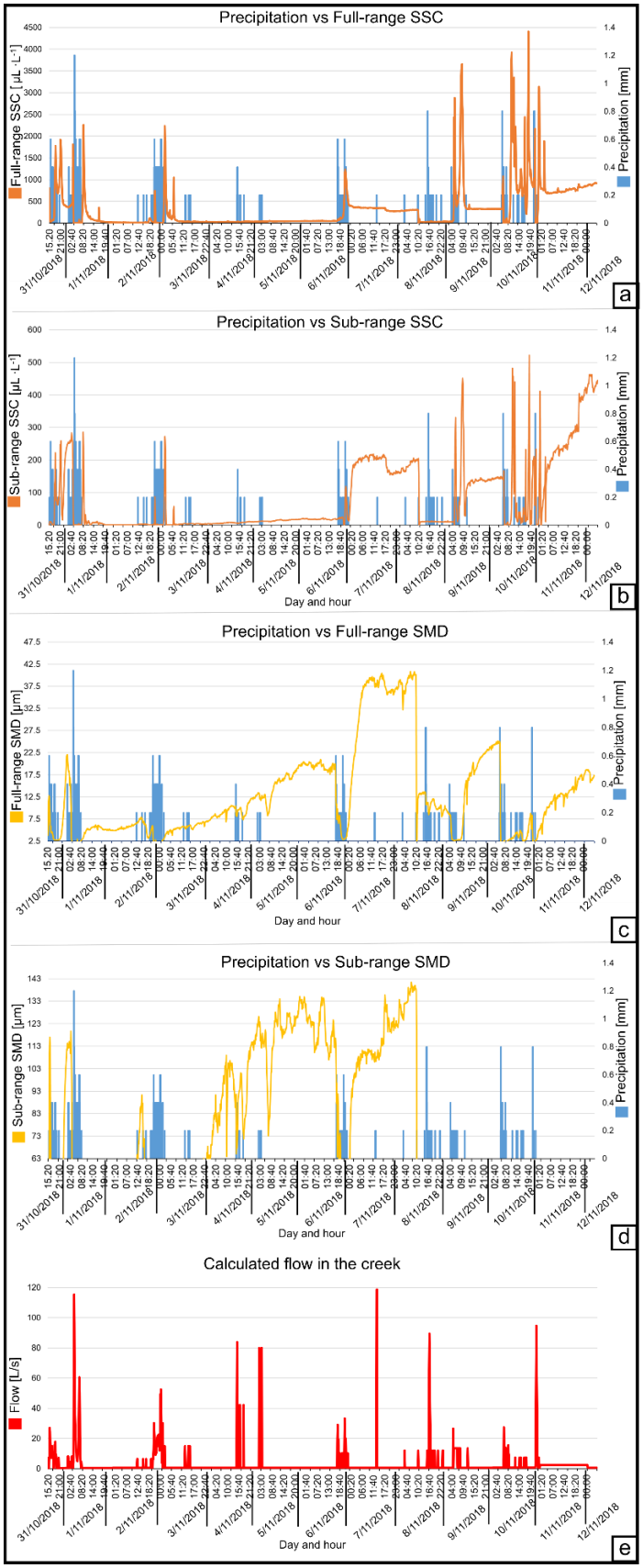

Figure 8: Suspended sediment measurements in November 2018. a) Precipitation vs silt and sand fraction Full-range SCC. b) Precipitation vs fine-medium sand Sub-range fraction *SCC c) Precipitation vs silt-sand Full-range fraction SMD. d) Precipitation vs* fine-medium sand *Sub-range fraction SMD. e) Calculated discharge flow in the creek.*

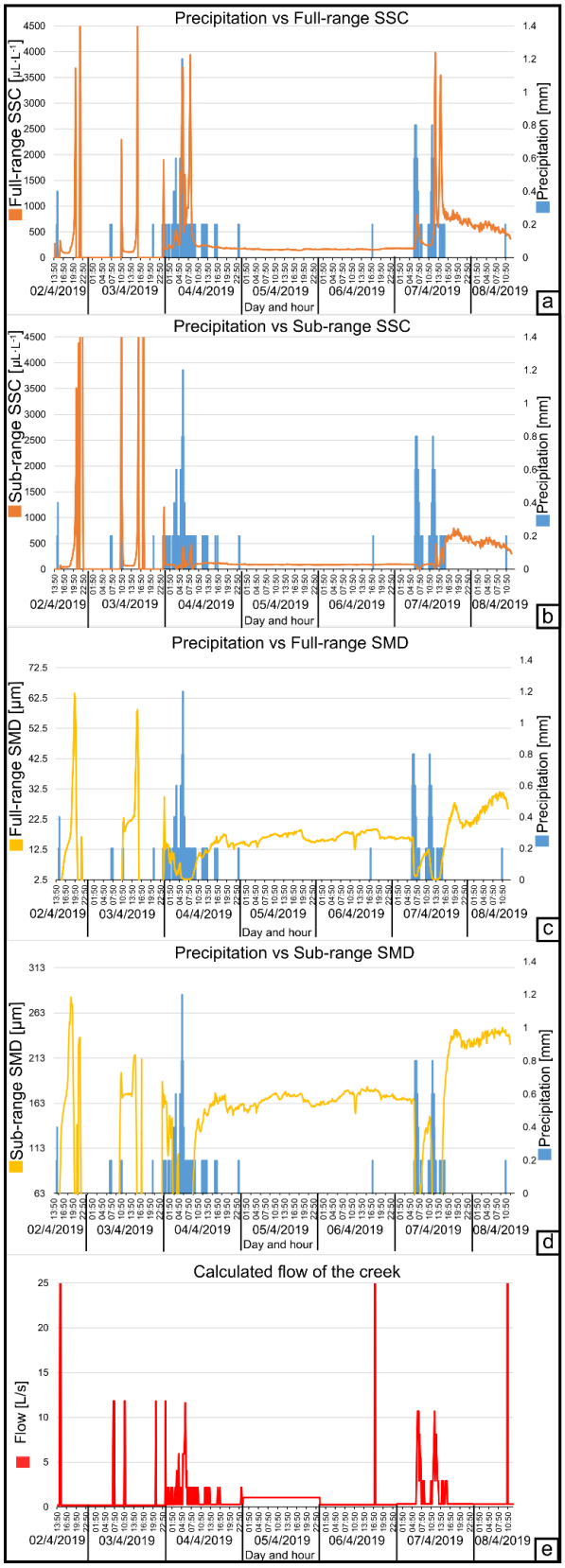

Figure 9: Suspended sediment measurements in April 2019. a) Precipitation vs silt and sand fraction Full-range SCC. b) Precipitation vs fine-medium sand Sub-range fraction *SCC c) Precipitation vs silt-sand Full-range fraction SMD. d) Precipitation vs* fine-medium sand S*ub-range fraction SMD. e) Calculated discharge flow in the creek.*

4. Discussion

The quantification of soil erosion in calanchi areas was historically studied through different techniques as mentioned in section 1 (e.g. Brakensiek et al., 1979; Benito et al., 1992; Komas et al., 1997; Nadal-Romero et al., 2008; Cappadonia et al., 2011; Corona et al., 2011; Licciardello et al., 2019). In this paper we present an approach based on the direct measurement of SSC and SMD data using a LISST-25X laser diffraction device in a small Apennine watershed deeply affected by rill-interrill and calanchi erosion. Figure 8 and 9 reports the SSC and the SMD measurements conducted from the 31/10/2018 to 12/11/2018 for a humid autumn period and from the 02/4/2019 to 08/4/2019 for a drier spring period. Thin Entisols which characterise the North-facing slopes, as well as the fine textured exposed bedrock that characterise the South-facing slopes are affected by fractures such as mudcracks, induced by wetting and drying cycles in active montmorillonite and illite clays (Villagra-Mendoza and Horn, 2019). After long dry periods these cracks allow water infiltration into the first decimetres of the soil. The initial delay between precipitation and sediment concentration can be directly connected to the secondary macropore infiltration phenomena (cracks) which take place in the topsoil after dry periods. Subsequent, to initial infiltration the discharge and the SCC increases reaching finally stable values.

Figure 8 reports the field measurements after the humid autumn period (31/10/2018-12/11/2018). At the beginning of the measurement period (03-05/11/2018) very low concentrations are registered that increase only immediately after the rainfall events for both the fine-sand Sub-range and silt-sand Full-range concentrations. After the precipitation event of the 06/11/2018 the concentrations rise and remain stable over the following days with 400 $\mu L \cdot L^{-1}$ for the Full-range SSC and 200 $\mu L \cdot L^{-1}$ for the Sub-range SSC. Thereafter, SSC is increasing again after the precipitation event of the 10/11/2018 with 700 $\mu L \cdot L^{-1}$ for the silt-sand Full-range SSC and 400 $\mu L \cdot L^{-1}$ for the fine-medium sand Sub-range SSC. The SMD values

show a distinct behaviour in comparison to the SSC. Generally, the SMD is increasing over the time period with highest values on the 07-08/11/2018. In the following period we observe mainly silty components documented by low values of Full and Sub-range SMD.

Figure 9 reports the field measurements after the spring period with antecedent dry conditions (see Figure 3b). The precipitation of the 2nd and 3rd April are not high enough to maintain a constant flow in the drainage systems and the SSC measurements show only a short pulse (two hours maximum). Instead, after the more intense precipitations of the 4th April (12.2 mm) the water flux is high enough to measure the sediment concentration in the stream determining an average value of SSC of about 200 $\mu L \cdot L^{-1}$ for the next two days.

Regarding the SMD the intense precipitation causes the initial mobilization of particularly fine silt particles triggering high turbidity. The initial high peaks in SMD (02-04/4/2019) are followed by stable values of SMD (04-07/4/2019). After the fluctuations in the first days prevalently medium silt and fine sand fractions were transported into the creek (04-07/4/2019). After the precipitation of the 7th of April SMD increases slightly to medium silt and medium sand for the respective grainsize fraction ranges. Figure 9c and d show the differences between Full-range (silt and sand) and the Sub-range (fine-medium sand) SMDs after the first precipitation event (04/4/2019) and the second rainfall event (07/4/2019) with smaller differences for the Full-range fraction SMD than form the fine-medium sand fraction. Hence, the material of the second event is generally larger in SMD due to a higher runoff energy.

Generally, the SSC and SMD values are slightly higher for the spring 2019 period than for the autumn period 2018 nonetheless higher precipitation and antecedent moisture conditions in autumn. We hypothesize due to field observations that there is a much larger infiltration component in the autumn period due to secondary macropore fluxes provoked by deep soil cracks in the montmorillonite rich clay substrates. As observed in the field these cracks close

after the first precipitation events only at the surface up to a few centimetres of depth and reopen even though with smaller cracks when evaporation restarts after the precipitation event.

In the spring period the evaporation is generally reduced due to lower temperatures and the wetting of the subsoil closing the cracks in the subsoil during the late autumn and winter period. This explains among other factors the higher runoff and sediment concentration in the spring period. In moist conditions the clay rich substrates favour rapid runoff processes due to low infiltration rates as well as due to generally shallow soil profiles with minimum storage capacities. The limited soil water storage capacities can also be seen in the low average runoff conditions between storm events of only 0.5 $L \cdot s^{-1}$.

Finally, we compared the SSC and SMD peaks (Figure 8 and 9) with the soil characteristics. The peak value increases from November 2018 to April 2019 which is among other factors related to the initial soil cover as well as the soil moisture conditions. Observing the NDVI time series (Figure 5b) the values decrease from November 2018 to March 2019 especially on the North-facing slope. This variation is caused by seasonality and additional triggers such as precipitation intensity and related soil erosion, or due to human intervention such as agriculture activities (ploughing on the North-facing slopes). The abrupt NDVI decrease in February 2019 is due to snow cover in the study area as detected on the Sentinel-2A image collected for the 6th February 2019 (Figure 6b). Therefore, the green cover index is reduced in this period in all land use areas. After this period, the change of NDVI is gradually increasing up to March 2019 even if they remain lower than in November 2018. The changing in green cover is mainly related to the seasonal cycle of vegetation as well as to the interruption of agricultural activity. The vegetation cover shows a significant reduction in March 2019 on the North-facing slope (Figure 5) and consequently the peaks of SSC increase. Comparing the peaks, it is evident that the initial soil conditions as well as the vegetation play a significant role in determining the concentration of eroded sediments as well as their diameter. Particularly, the initial moisture condition must

be taken in consideration as a factor that influences soil erosion as reported by e.g. Martínez-Murillo et al., 2013 or Ziadat and Taimeh (2013). Moreover, as shown above, the hydrophobic behaviour of soils induces surface runoff generation causing also soil erosion (Martínez-Murillo and Ruiz-Sinoga, 2007). The LISST-25X SMD and SSC data recorded in April 2019 after a dry period results higher with respect to November 2018 after a humid period. As mentioned above we observed in the field soil desiccation cracks up to 1 m depth. On the other hand, the soils may show hydrophobicity favouring runoff processes and sediment transport. Moreover, the rainfall intensity is higher in April 2019 leading to a higher erosive power. Furthermore, it must be considered that the dry clays present less cohesion in the topsoil horizon in respect to the wet clay. However, saturated clay bedrock is characterized by poor mechanical properties favouring soil erosion.

In addition, to understand the sediment dynamics in relation to topographic characteristics of the study area a detailed morphometrical assessment was conducted on a high-resolution DEM with 15 cm cell size resolution. The terrain analysis highlighted the asymmetry of the watershed, as well as a distinct contribution of the two slopes to the sediment production. Especially the Aspect, TWI, LS-Factor and SPI provides information about the potential soil moisture content, the potential of saturation excess runoff generation as well as the potential erosive power of the surface runoff (i.e. Bianchini et al., 2016). The East-West orientation of the basin shows a South-facing slope that is exposed to higher irradiation and thus are exposed to more pronounced dry-wet cycles. Instead, the North-facing slope is generally moister. High values of TWI on the North-facing slopes highlight a high potential of saturation excess surface runoff. Conversely, even if the TWI values are lower on the South-facing slopes the SPI confirms a high concentration of surface runoff and hence, a high erosion potential on the soft clayey bedrock. Regarding the slope sediment dynamics, also the LS-Factor that describes the transport capacity must be taken in consideration. Generally, in areas with higher LS-Factor

values more sediments can be transported (Maerker et al., 2020). In the study area the highest values are given in the incised valleys and mainly on the South-facing slopes. Conversely, lower LS-Factor values can be observed in the accumulation sector between the calanchi sides and the interfluves. Finally, the slope gradient must be considered because sediment loss is directly related to slope steepness. As shown in Figure 2c the study area shows a clear asymmetry of the basin. The steeper slopes on the South-facing slopes drain faster and therefore tend to be more eroded by the surface runoff.

A detailed grain size analysis was conducted based on soil samples from all different land use types of the basin showing a prevalent clay to silty clay texture. However, the grain size analysis performed in the calanco land use as well as in the vegetated area show very similar silty clay textures. In the first case the bedrock is directly exposed to runoff processes that erode the fine clays, as a consequence the grain size distribution results a bit coarser. Furthermore, the initial wetness condition of the clay must be considered. In fact, the superficial strata of dry clays are less cohesive than the wet one, thus, dry clays show a higher erodibility. However, under saturated conditions the mechanical properties of clays are quite weak leading to mirco slumps and micro earth flows observed in the field (e.g. Al-Sayea , 2001).The vegetated areas in the accumulation zone and in the head zones of the calanco show coarser grain sizes distributions mainly due to redeposition processes leading to a certain deposition sequence with larger particles deposited first and smaller particles that may leave completely the slope system.

5. Conclusion

The study reveals for the first time the dynamics between precipitation and suspended sediments transport in a Northern Apennine watershed strongly affected by soil erosion processes generating in rill-interrill and calanco landforms.

We installed a LISST-25X device at the outlet of the watershed basin and collected every 10 minutes the SSC and the SMD of the fine sediment transported by the creek. Moreover, we simulated the discharge dynamics of the creek using a SWAT simulation approach.

The principal outcome of the paper can be generally summarised as follows:

a) The fine 'Brecce Argillose di Baiso' Formation, a typical Apennine melange formation, is prone to be eroded by surface runoff. The grain size analysis confirms dominant clay and silty clay bedrock substrates and topsoil-texture with a prevalence of montmorillonite and illitie clays.
b) The water flux is drained from the basin through a small ephemeral creek that has a torrential regime (Figure 8e and 9e).
c) The SSC is directly related to the precipitation, even if a delay of about 2 hours was observed by the data analysis. Especially after 'dry conditions' the delay with respect to the precipitation is higher. This might be due to the initial infiltration behaviour of the soils characterized by desiccation cracks. Particularly, these soil cracks permit the initial infiltration of the surface runoff resulting in a delay of runoff and sediment transport documented by the SSC and SMD value dynamics.
d) The SMD is inversely related to the precipitation. The initial water flux comes along with small, suspended particles replaced later by stable values in the particle diameter.
e) Every consecutive precipitation event generally increases SSC and SMD of particles.
f) The poor cohesive saturated clays can be easily eroded by water. As shown in Figure 8c after the precipitation of the 4th April the SMD values reach up to 19 μm increasing up to 31 μm after the precipitation of 7th April. The same trend is reported in Figure 9c, the increasing of SMD of particles and SSC can be related to saturated surface substrates-soils decreasing the mechanical properties and favouring particle detachment and transport.

g) The morphometrical analysis highlight the asymmetry of the basin and the related high potential of saturation excess overland flow on the slopes exposed to the North as well as quick drainage and mainly infiltration excess overland flow on the slopes exposed to the South leading to a distinct spatial distribution of soil erosion phenomena and calanchi evolution.

h) The NDVI time series illustrate a general decrease in the vegetation cover related to the seasonal dynamics.

i) The vegetation cover reduction combined with the initial soil moisture as well as the higher precipitation intensity increase runoff and is hence, related to higher values of SMD and SCC in April 2019.

j) The study reveals the importance of the vegetation cover protecting the soils in the area.

k) The LISST-25X can be utilised to conduct a long-term monitoring of suspended sediment transport in a small basin and allows to assess the effect of the land use changes on the sediment dynamics.

Acknowledgements

This research was conducted with financial support of the University of Pavia.

References

Al-Shayea, N.A. 2001. The combined effect of clay and moisture content on the behaviour of remolded unsaturated soils. Engineering Geology, 62(4), 319-342.

American Society for Testing Materials, 1988. Annual Book of ASTM Standards. American Society for Testing and Materials, Philadelphia.

Ardenghi, N.M.G. and Polani, F. 2016. La flora della provincia di Pavia (Lombardia, Italia settentrionale). 1. L'Oltrepò Pavese. Natural History Sciences. Atti Soc. it. Sci. nat. Museo civ. Stor. nat. Milano, 3(2), 51-79.

Arnold, J.G., Srinivasan, R., Muttiah, R.S., Williams, J.R. 1998. Large area hydrologic modeling and assessment. Part I: Model development. J. Am. Water Resour. Assoc. 34, 73–89.

Benito, G., Gutiérrez, M. and Sancho, C. 1992. Erosion rates in badlands areas of the Central Ebro Basin (NE-Spain). Catena, 19, 269-286.

Beven, K.J., Kirkby, M.J. 1979. A physically-based variable contributing area model of basin hydrology' Hydrology Science Bulletin, 24(1), 43-69.

Bianchini, S., Del Soldato, M., Solari, L., Nolesini, T., Pratesi, F., and Moretti, S. 2016. Badland susceptibility assessment in Volterra municipality (Tuscany, Italy) by means of GIS and statistical analysis. Environmental Earth Sciences, 75(10), 1–14.

Bosco, C., De Rigo, D., Dewitte, O., Poesen, J. J., Panagos, P. P. 2015. Modelling soil erosion at European scale: towards harmonization and reproducibility. Natural Hazards and Earth System Sciences, 15(2), 225–245.

Bosino, A., Giordani, P., Quénéhervé, G., and Maerker, M. 2020. Assessment of calanchi and rill-interrill erosion susceptibilities using terrain analysis and geostochastics: A case study in the Oltrepo Pavese, Northern Apennines, Italy. Earth Surf. Process. Landforms, https://doi.org/10.1002/esp.4949.

Bosino, A., Pellegrini, L., Omran, A., Bordoni, M., Meisina, C., Maerker, M. 2019a. Litho-structure of the Oltrepo Pavese, Northern Apennines (Italy). Journal of Maps, 15(2), 382–392.

Bosino, A., Omran, A., and Maerker, M. 2019b. Identification, characterisation and analysis of the Oltrepo Pavese calanchi in the Northern Apennines (Italy). Geomorphology, 340, 53–66.

Brakensiek, D.L., Osborn, H.B., and Rawls, W.J. 1979. Field manual for research in agricultural hydrology. Agricultural Handbook No. 224, U.S. Department of Agriculture: Washington, DC.

Bryan, R., and Yair, A. (Eds.). 1982. Badland geomorphology and piping. Norwich: Geo Books.

Bucciante, M. 1922. Sulla distribuzione geografica dei Calanchi in Italia. L'universo. 38, 585-605.

Buccolini, M., Coco, L., Cappadonia, C., Rotigliano, E. 2012. Relationships between a new slope morphometric index and calanchi erosion in northern Sicily, Italy, Geomorphology, 149–150, 41-48.

Cantón, Y., Domingo, F., Solé-Benet, A., Puigdefábregas, J. 2001. Hydrological and erosion response of a badlands system in semiarid SE Spain. Journal of Hydrology, 252, 65-84.

Cappadonia, C., Conoscenti, C., Rotigliano, E. 2011. Monitoring of erosion on two calanchi fronts – Northern Sicily (Italy). Landforms Analysis, 17, 21-25.

Ciccacci, S., Galiano, M., Roma, M.A., Salvatore M. C. 2008. Morphological analysis and erosion rate evaluation in badlands of Radicofani area (Soutern Touscany - Italy). Catena, (74), 89-97.

Corona, C, Lopez Saez, J, Rovéra, G, Stoffel, M, Astrade, L, Berger, F. 2011. High resolution, quantitative reconstruction of erosion rates based on anatomical changes in exposed

roots at Draix, Alpes de Haute-Provence—critical review of existing approaches and independent quality control of results. Geomorphology, 125, 433–444.

Clarke, M. L. and Rendell, H. M. 2006. Process-form relationship in Southern Italian Badlands: erosion rates and implications for landforms evolution. Earth Surface Processes and Landforms, 31, 15-29.

Conrad, O., Bechtel, B., Bock, M., Dietrich, H., Fischer, E., Gerlitz, L., Wehberg, J., Wichmann, V., Böhner, J. 2015. System for Automated Geoscientific Analyses (SAGA) v. 2.1.4, Geosci. Model Dev., 8, 1991-2007.

De Ploey, J., Gabriels, D. 1980. Measuring soil loss and experimental studies. In Soil Erosion, Kirkby MJ, Morgan RPC (eds). Wiley: New York; 63–108.

Drusch, M., Del Bello, U., Carlier, S., Colin, O., Fernandez, V., Gascon, F., Hoersch, B., Isola, C., Laberinti, P., Martimort, P. 2012. Sentinel-2: ESA's optical high-resolution mission for GMES operational services Remote Sens. Environ., 120, 25-36.

Felix, D., Alabayrak, I., Boes, R.M. 2013. Laboratory investigation on measuring suspended sediments by portable laser diffractometer (LISST) focusing on particle shape. Geo-Mar Lett., 33, 485-489.

Filippa, L., Trento, A., Álvarez, A. M. 2012. Sauter mean diameter determination for fine fraction of suspended sediments using a LISST-25X diffractometer. Measurements, 45, 2346-368.

Filippa, L., Freire, L., Trento, A., Álvarez, A. M., Gallo, M., Vinzó S. 2011. Laboratory evaluation of two LISST-25X using river sediments. Sedimentary Geology, 238, 268-276.

García-Ruiz, J. M., Nadal-Romero, E., Lana-Renault, N., Beguerí, S. 2013. Erosion in Mediterranean landscapes: Changes and future challenges. Geomorphology, 198, 20-36.

IUSS Working Group WRB, 2015. World Reference Base for Soil Resources 2014, update 2015 International soil classification system for naming soils and creating legends for soil maps. World Soil Resources Reports No. 106. FAO, Rome.

Kosmas, C., Danalatos, N., Cammeraat, L.H., Chabart, M., Diamantopoulos, J., Farand, R., Gutierrez, L., Jacob, A., Marques, H., Martinez-Fernandez, J., Mizara, A., Moustakas, N., Nicolau, J.M., Oliveros, C., Pinna, G., Puddu, R., Puigdefabregas, J., Roxo, M., Simao, A., Stamou, G., Tomasi, N., Usai, D., Vacca, A. 1997. The effect of land use on runoff and soil erosion rates under Mediterranean conditions. CATENA, 29(1), 45-59.

Kottek, M., Grieser, F., Beck, C., Rudolf, B., and Rubel, F. 2006. World Map of the Köppen-Geiger climate classification updated. Meteorologische Zeitschrift, 15(3), 259-263.

Krenz, J., Kuhn, NJ. 2018. Assessing badland sediment sources using unmanned aerial vehicles. In Badland Dynamics in the Context of Global Change, Nadal-Romero E, Martínez-Murillo JF, Kuhn NJ (eds). Elsevier: Amsterdam

Kropáček, J., Schillaci, C., Salvini, R. and Märker, M. 2016. Assessment of gully erosion in the Upper Awash, Central Ethiopian Highlands based on a comparison of archived aerial photographs and very high resolution satellite images. Geografia Fisica e Dinamica Quaternaria, 39(2), 161-170.

Licciardello, F., Barbagallo, S., Gallart F. 2019. Hydrological and erosional response of a small catchment in Sicily. J. Hydrol. Hydromech., 67(3), 201–212.

Llena, M., Smith, M.W., Wheaton, J.M., Vericat, D. 2020. Geomorphic process signatures reshaping sub-humid Mediterranean Badlands: 2. Application to 5-year dataset. Earth Surface Processes and Landforms, 45(5), 0197-9337.

Maerker, M., Bosino, A., Scopesi, C., Giordani, P., Firpo, M., Rellini, I. 2020. Assessment of calanchi and rill-interrill erosion susceptibility in northern Liguria, Italy: A case study using a stochastic modelling framework. GEODERMA, 114367.

Martínez-Murillo, J.F., Nadal-Romero, E., Regüés, D., Cerdà, A., Poesen, J. 2013. Soil erosion and hydrology of the western Mediterranean badlands throughout rainfall simulation experiments: A review. CATENA, 106, 101-112.

Martínez-Murillo, J.F., Ruiz-Sinoga J.D. 2007. Seasonal changes in the hydrological and erosional response of a hillslope under dry-Mediterranean climatic conditions (Montes de Málaga, South of Spain). Geomorphology, 88 (1-2), 69-83.

Meral, R., 2008. Laboratory Evaluation of Acoustic Backscatter and LISST methods for Measurements of Souspended Sediments. Sensor, 8, 979-993.

Micheletti, N., Jim H Chandler, J.H., Lane, S. 2015. Structure from Motion (SfM) Photogrammetry. British Society for Geomorphology, Geomorphological Techniques, 2, Sec. 2.2 (2015)

Moore, I.D., Grayson, R.B., Ladson, A.R. 1991. 'Digital terrain modelling: a review of hydrological, geomorphological, and biological applications' Hydrological Processes, 5, 1.

Moretti, S., Rodolfi, G. 2000. A typical "Calanchi" landscape on the Eastern Apennines margin (Atri, Central Italy): geomorphological features and evolution. Catena, 40, 217-228.

Nadal-Romero, E., Latron, J., Marti-Bono, C., Regüés, D. 2008. Temporal distribution of suspended sediment transport in a humid Mediterranean Badlands area: The Araguás catchment, Central Pyrenees. Geomorphology, 97 (3-4), 601-616.

Pedocchi, F., Garcia M. H. 2006. Evaluation of the LISST-ST instrument for suspended particle size distribution and settling velocity measurements. Cont. Shelf Res., 26, 943-958.

Regüés, D. and Nadal-Romero, E. 2013. Uncertainty in the evaluation of sediment yield from badland areas: Suspended sediment transport estimated in the Araguás catchment (central Spanish Pyrenees). CATENA, 106, 96-100.

Rossetti, R., and Ottone, C. 1979. Esame preliminare delle condizioni pluviometriche dell'Oltrepò Pavese e dei valori critici delle precipitazioni in relazione ai fenomeni di dissesto franoso. Geologia Applicata e Idrogeologia, 14(3), 83-99.

Saez, J.L., Corona, C., Stoffel, M., Rovéra G., Astrade, L., Berger, F. 2011. Mapping of erosion rates in marly badlands based on a coupling of anatomical changes in exposed roots with slope maps derived from LiDAR data. Earth Surface Processes and Landforms 36, 1162–1171.

Schwarz, C., Cox, Y., van Engeland, T., van Oevelen, D., van Belzen, J., van de Koppel, J., Soetaert, K., Bouma, T.J., Meire, P., Temmerman, S. 2017. Field estimates of floc dynamics and settling velocities in a tidal creek with significant along-channel gradients in velocity and SPM. Estuarine, Coastal and Shelf Science, 197, 221-235.

Sequoia, 2008. Operating principles of LISST-25 constant calibration sediment sensor. http://www.sequoiasci.com/product/lisst-25x/

SERVIZIO GEOLOGICO D'ITALIA. 2014. Carta Geologica d'Italia alla scala 1:50.000, Foglio 178 Voghera. Roma.

Sirvet, J. Desir, G. Gutierrez, m. Sancho, C. Benito, G. 1997. Erosion rate in badlands areas recorded by collectors, erosion pins and profilometer techniques (Ebro Basin, NE-Spain). Geomorphology, 18, 61-75.

Soil Survey Staff. 2010. Key to Soil Taxonomy, Eleventh edition. United Stated Department of Agriculture, National Resources Conservation Services.

Stolte, J., Tesfai, M., Øygarden, L., Kværnø, S., Keizer, J., Verheijen, F., Hessel, R. 2016. Soil threats in Europe: status, methods, drivers and effects on ecosystem services: A review report, deliverable 2.1 of the RECARE project (JRC Technical Reports).

Szatten, D.A., Babinski, Z., Habel, M. 2018. Reducing of water tourbidity by Hydrotechnical Structures on the Example of the Wloclawek Reservoire. Journal of Ecological Engineering, 19(3), 197-205.

Szymczak, E. and Burska, D. 2018. Distribution of souspended Sediments in the Gulf of Gdansk off the Vistula River Mounth (Baltic Sea, Poland). World Multidisciplinary Earth Sciences Symposium (WMESS 2018). Doi:10.1088/1755-1315/221/1/01/2053.

Tarolli, P. 2014. High-resolution topography for understanding earth surface processes: opportunities and challenges. Geomorphology, 216, 295–312.

Thonon, I., Roberti, J. R., Middelhoop, H., Van der perk, M., Burrough, A. 2005. In situ measurements of sediments settling characteristics in floodplains using a LISST-ST. Earth Surface Processes and Landforms, 30, 1327-1343.

Vercesi, P.L., Falletti, P., Pasquini, C., Perotti, C., Tucci, G., Papani, L. 2014. Carta Geologica d'Italia alla scala 1:50,000. Foglio 178 'Voghera', note illustrative. InfoCartoGrafiche – Piacenza. ISPRA, Istituto Superiore per la Protezione e la Ricerca Ambientale.

Vergari, F., Della Seta, M., Del Monte, M., Pieri, l., Ventura, F. 2015. Integrated Approach to the Evolution of Denudation Rates in an Experimental Catchment of the Northern Italian Apennines. G. Lollino et al. (eds), Engeneering Geology for Society and Territory – Volume 1, Springer International Publishing Switzerland 2015.

Villagra-Mendoza, K. and Horn, R. 2019. Changes in Water Infiltration after Simulated Wetting and Drying Periods in two Biochar Amendments. Soil Syst. 3, 63.

Viscarra Rossel, R. A., Behrens, T., Ben-Dor, E., Brown, D. J., Demattê, J. A. M., Shepherd, K. D., Shi, Z., Stenberg, B., Stevens, A., Adamchuk, V., Aïchi, H., Barthès, B.G., Bartholomeus, H.M., Bayer, A.D., Bernoux, M., Böttcher, K., Brodský, L., Du, C.W., Chappell, A., Fouad, Y., Genot, V., Gomez, C., Grunwald, S., Gubler, A., Guerrero, C., Hedley, C.B., Knadel, M., Morrás, H.J.M., Nocita, M., Ramirez-Lopez, L., Roudier, P.,

Rufasto Campos, E.M., Sanborn, P., Sellitto, V.M., Sudduth, K.A., Rawlins, B.G., Walter, C., Winowiecki L.A., S.Y. Hong, Ji, W. 2016. A global spectral library to characterize the world's soil. Earth-Science Reviews, 155, 198-230.

Wang, L., and Liu, H. 2006. An efficient method for identifying and filling surface depressions in digital elevation models for hydrologic analysis and modelling. International Journal of Geographical Information Science, Vol. 20(2), 193-213.

Webb, B. W., Foster, I.D.L., Gurnell, A.M. 1995. Hydrology, water quality and sediment behaviour. In: Foster, I., Gurnell, A., Webb, B. (Eds.), Sediment and Water Quality in River Catchments. John Wiley & Sons ltd., Chichester, pp 1-30.

Williams, N.D., Walling, D.E., Leeks, G.J.L. 2007. High temporal resolution in situ measurement of the effective particle size characteristics of fluvial suspended sediment. WATER RESEARCH, 41, 1081–1093.

Wischmeier, W. H., and Smith, D. D. 1978. Predicting rainfall-erosion losses e A guide to conservation farming. In: U.S. Dept. Of Agric., Agr. Handbook no. 537.

Yang, D., Kanae S., Oki, T., Koike., T., Musiake, K. 2003. Global potential soil erosion with reference to land use and climate changes. Hydrol. Process., 17, 2913-2928

Zevenbergen, L. W. and Thorne, C. R. 1987. Quantitative analysis of land surface topography. Earth Surface Processes and Landforms 12, 47-56.

Ziadat, F.M., Taimeh, A.Y. 2013. Effect of rainfall intensity, slope, land use and antecedent soil moisture on soil erosion in an arid environment. Land Degradat. Developm., 24, 582-590.

SUMMARY OF RESULTS AND DISCUSSION

This thesis focuses on the identification, classification, description, and modelling of calanchi forms and features in the Oltrepo Pavese study area. The work contributes to fill existing research gaps in the larger context of the Northern Apennines. Moreover, innovative techniques to assess sediment dynamics through in situ measurements were applied.

Initially the study area was assessed from a geological and structural point of view. The results highlight the complex landscape of the Oltrepo Pavese study area that is mainly characterised by sedimentary bedrock. The lithotypes were grouped in 11 lithotypes based on pre-existing maps (Official Italian cartography CARG 1:50.000; old geological maps 1:100.000) as well as on own field surveys. The lithology triggers the morphology and the elevation range of the study area. The territory is widely covered by alluvial and fluvial deposits in the Northern part, soft sedimentary bedrock such as melange, clays and marls in the central part, and finally interstratified rocks and limestones in the Southern mountainous part. In addition, shallow landslides cause the detachments of the shallow soil cover favouring the bedrock exposition and facilitating soil erosion processes. From the 5m DTM analysis major tectonic lineaments were extrapolated. The final lithological map represents a prerequisite that allows to classify the calanchi from a lithological point of view. Therefore, the map is provided as raster-based inventory. The study of the lithology and tectonic processes was summarised in the first paper highlighting that the study area is particularly characterised by soft sedimentary bedrock material which is highly erodible by surface and sub-surface runoff.

Subsequently, the calanchi which crop out in the Oltrepo Pavese were assessed based on detailed field surveys, Google Earth image interpretation and GIS analysis carried out with orthophotos of 2015. In total 263 calanchi were mapped and described from a geomorphological, geological, morphometrical and vegetational point of view. 68% of the

calanchi fall in the type B class described by Moretti and Rodolfi (2000) and are represented by smooth morphology with diffuse vegetation and/or landslide processes. The lithology of the bedrock seems to play an important role in the development of type A or B calanchi. The study highlights that type B calanchi principally developed in melange, marls and interstratified marls, interstratified rocks, and landslides deposits. Instead, type A calanchi mainly developed in interstratified rocks, melanges, marls and claystones. The results are in accordance with a wide range of detailed studies reported in the previous chapters. Moreover, based on a comprehensive terrain analysis performed on a 5 m DTM, the Oltrepo Pavese calanchi show specific characteristics such as convex slopes with 10° to 40°, mainly exposed to South and subject to thermoclastic weathering. Subsequently, a second dataset of calanchi was obtained derived from the analysis of orthophotos of the year 1975. The areal shape variation was assessed through the comparison of the 1975 with the 2015 inventory. 73% of calanchi are shrinking due to the triggering factors change and decrease. The lithology of the bedrock, the morphometry of the slopes, land use change and land use management, climate change as well as morphogenetic activities can significantly contribute to the evolution of the calanchi. In the Oltrepo Pavese the reduction in areal shape is essentially due to a reduction of precipitation and land use change. The precipitation is decreasing over the last 40 years passing from 800 to 700mm/year. The decrease in precipitation leads to generally drier conditions with less erosion. However, if the precipitation will significantly decrease under 700 mm due to climate change, other processes will have to be considered (e.g. soil cracking). Regarding land use change we observed that vineyards, and agricultural fields are decreasing in the last decades (1980-2015) respectively from 14.5 to 27%. Instead, forests and bushes are increasing respectively from 41 to 113%, indicating a certain succession of the vegetation. The land use change was also highlighted by the NDVI analysis conducted on LANDSAT images that show an increase in green cover and dense vegetation. Moreover, plating operations with Pinus Nigra and Fraxinus

excelsior have contributed to the stabilisation of the calanchi areas. Instead Castaldi and Chiocchini, (2012) reported the opposite. The stabilization and shrinking of the calanchi in our study area is also observed in other areas in Italy as reported by Moretti and Rodolfi (2000), Buccolini et al. (2007) and Castaldi and Chiocchini (2012) highlighting the importance of land use change for the development of badlands. However, other researchers like Capolongo et al. (2008), Vergari et al. (2013) or D'Intino et al. (2020) indicate an increase of calanchi area and erosive processes. The various trends reported in bibliography should be studied in depth taking into account the difference of the study site conditions and the factors that guide the genesis and the evolution of the calanchi. In particular, the bedrock lithotypes, morphometrical parameters, morphogenetic activities i.e. mass movements and neotectonics activity, changes in land use as well as the changes in precipitations intensity and amount may influence the increase or decrease of calanchi areas in the Italian context (see also the discussion in paper III).

The third module of the work was dedicated to the application of a stochastic modelling approach (Maximum Entropy model/ MaxEnt) to evaluate calanchi and rill-interrill erosion in the Oltrepo Pavese. Initially a detailed terrain analysis was conducted starting from a 12m DEM. 13 topographic indices (e.g. slope, aspect etc. see chapter III), two environmental layers (lithology and land use) as well as the NDVI index were used as independent layers whereas the dependent variable was represented by the calanchi inventory and mapped rill interrill erosion processes. Subsequently, the dependent and independent variables were assessed with the MaxEnt model using 75% of the dataset for training. The results are illustrated in form of three susceptibility maps respectively for calanchi type A, type B and rill-interrill erosion. The model performance was evaluated through the ROC curve and the AUC values that shows values of 0.726, 0.704, and 0.944 respectively for calanchi type A, type B and rill-interrill erosion for the train dataset. The other 25% of the entire dataset was used for testing the model

yielding 0.719, 0.700, 0.939 respectively. Hosmer et al., 2013 indicates 0.70 as the threshold of acceptable results. The AUC values indicate a robust model able to decipher between the two calanchi types and rill interrill erosion, nonetheless the fact that calanchi are represented by a very complex nature. Thus, finally we were able to apply the MaxEnt model for the entire study area at a regional scale.

Furthermore, MaxEnt estimates the contribution of the single variables through the predictor variable analysis giving information about the variable importance. Land use, elevation, valley depth and lithology represent the most important predictors in the development of both calanchi type A and B. The predictor response curves show for land use, for example, that the agricultural activities such as tillage promote rill-interrill erosion. Conversely the erosion phenomena decrease in the forest and bush lands. Instead, Calanchi are correlated with bushland and degraded areas as well as forest. The results indicate that calanchi develop prevalently in already degraded areas. Moreover, it can be deducted that re-vegetation processes are also playing a fundamental role on soil erosion control as highlighted by the time series analysis of the land use. If the major predictors (i.e. land use, lithology, elevation etc.) are commonly described by other authors, the minor predictors are often not considered. In the study we highlight that less important predictors like Vertical Distance to Channel Network should be considered since they are contributing additional information. For example, type-A calanchi are associated with low values of VDCN that indicate less runoff energy as occurs often, for example, in small watersheds and close to the watershed divide. All these evidence lead to the conclusion that type-B calanchi may be an evolution of the type-A calanchi. This was highlighted also by Ciccacci et al., 2008 who emphasized that type B calanchi are the natural evolution of type A calanchi. Moreover, he stated that type A calanchi are relict landforms developed under past climate conditions. In addition, Moretti and Rodolfi (2000) considered the Type A as calanchi developed in areas with extreme rainfall events. However, this thesis

stresses that the nature of the bedrock, the relief energy as well as the size of the basin must be considered in the Oltrepo context. The MaxEnt model was also applied in another Northern Apennine region by Maerker et al. (2020). They indicated that the elevation, slope and lithology play a fundamental role in the development of badland landforms. Moreover, they revealed that the soil type is an important environmental variable in the development of rill-interrill and calanchi erosion. Unfortunately, our study area is not covered by a complete pedological map consequently it was not possible to add this information in our study. In addition, other researchers applied different techniques to model calanchi erosion at basin scale (e.g. Vergari, 2015). Our study confirms the influence of the dominant predictors such as elevation, lithology, etc., on calanchi formation. However, the less important predictors change in different environments reported by other authors, due to the different local conditions. Finally, the study shows that MaxEnt is a robust model and can be successfully applied to study also complex landforms and hence, may be applied to other calanchi contexts. The results of the stochastic modelling approach are described in chapter III.

Finally, the fourth step of the study consists in the quantification of calanchi erosion processes in situ. Historically, studies on the quantity of eroded sediments as well as their dynamics were performed through pin measurements, turbidimeter analysis, discrete sampler, root analysis etc. However, these measurements have several disadvantages because the direct measurements of the sediments leaving the catchment are often not available. We applied a laser diffraction method to estimate the Suspended Sediment volume Concentration (SSC) and the Sauter Mean Diameter (SMD) in a small basin sited in the Oltrepo Pavese. The study reveals the sediment dynamics and their interplay with precipitation and discharge in a small watershed deeply affected by calanchi and rill-interrill erosion. The in-situ measurements were conducted with a LISST-25X instrument. The main results regard the sediment concentration as well as the sediment diameter of the sediments transported along the ephemeral drainage creek in a

representative calanco located close to Varzi town, Northern Apennines. The SSC and SMD were plotted against the precipitation (5 minutes resolutions) and discharge and the results were described in chapter IV. The study highlights that the runoff responded quickly to the precipitation with a small delay (1 hour). The SSC is directly related to the runoff even if time lapsed in respect to the precipitation. This is essentially due to the bedrock characteristics. In fact, the area is characterised by the fine-grained Brecce Argillose di Baiso that are rich in illite and montmorillonite clay minerals responsible for the formation of cracks due to swelling and shrinking phenomena. The macro structural pores may lead to an infiltration of the surface runoff and the conduction of the water along preferential pathways as quick interflow. In case of consecutive rainfall events the cracks close and surface runoff increase due to the general small infiltration rates of clay minerals. The conducted measurements indicate complex surface generation dynamics that can be explained with the soil moisture conditions and the respective development of cracks in dry phases. In the examples reported we observe a time lapse between first rain and the respective runoff generated probably due to infiltration and quick interflow phenomena especially after the dry period. Whereas, after wetting antecedent conditions soil cracks close and immediate runoff response can be observed that is also reported in the SMD and SSC values. Regarding the SMD the results show that the initial water flux comes along with small, suspended sediments and every consecutive precipitation event generically increase the diameter of the particles from fine silt to medium sand fractions. Once again, we can resume the importance of bedrock characteristics and the morphometric characteristics of the basin that guide the infiltration and saturation excess favouring the runoff and consequently erosion phenomena. Finally, the SMD and SSC curves are strictly linked to the vegetation and initial soil conditions which directly act on runoff processes and consequently on sediment dynamics.

CONCLUSION AND FUTURE RESEARCH NEEDS

This study contributed to answer some of the open research questions through a set of innovative and integrative methodologies including remote sensing, numeric modelling, advanced statistics and field survey activities. The study area shows a complex structural and tectonic setting as well as a high variability of the bedrock lithology characterized by 11 significant lithotypes. The study area is dominated by soft Plio-Pleistocene and Eocene sedimentary bedrock substrates prone to be eroded by surface runoff. Subsequently, the calanchi were classified from a morphological, morphometrical, lithological, temporal and vegetational point of view. This approach allows to have a full description of forms and features. The mapped calanchi are 263 and mainly belong to type B. The calanchi are distributed in the central and southern part of the study area following mainly certain bedrock lithologies as well as morphological settings. Their formation and morphological evolution are mainly connected with melange and landslides deposits. The temporal evolution shows a decrease of calanchi area due to land use change, population decrease and a decrease of precipitation. The observed trend in calanchi stabilization is also reported in other scientific publications. However, to have an integral vision at national scale further systematic work must be carried out covering a wide range of triggering factors. From the probabilistic analysis it appears that a significant portion of the study area is susceptible to calanchi and rill-interrill erosion. The chosen stochastic approach based on statistical mechanics (MaxEnt) is a powerful tool to model complex landforms. As documented, the model shows robust results and is able to decipher between the two types of calanchi. It was also reported that the approach is applicable in similar environments of the Northern Apennines. However, the application is obviously depending on the quality of the input data. The last chapter of the thesis discusses the quantification of the erosion processes and the related sediment dynamics at micro-basin scale. A typical A-type calanco basin was chosen for a detailed analysis using a LISST-25X that was installed at the

outlet of a basin. Thus, the sediment concentration and diameter were assessed during autumn 2018 and spring 2019. The results reveal in detail that the sediment dynamics are associated to the precipitation dynamics and the initial physical properties of soils, particularly of the soil moisture conditions. Moreover, soil cracks, micro debris flows, and hypodermic "interflow" drainage and related erosion processes may play a fundamental role regarding the sediment dynamics including the location and intensities of eroded areas and depositional zones. Based on this thesis and on suggestions reassumed from Caraballo-Arias and Ferro (2016) the necessity of future development in calanchi research can be summarized as follows:

i) A calanchi inventory in Italy and other Mediterranean areas should be created to document the morphological characteristics of calanchi where climate, vegetation and geological conditions are similar. Nevertheless, a comprehensive calanchi inventory should be compiled at national level including previous work and new morphological and morphometric characterisations. A national calanchi inventory map may be a robust base of information for future research development.

ii) I evaluated the temporal evolution of calanchi in terms of their spatial extent comparing a set of orthophotos for the Oltrepo Pavese study area. However, in the last decades several other authors have investigated the badland dynamics of different Italian regions. Nonetheless, a comprehensive morpho-climatic evaluation of the calanchi dynamics at national scale is still missing. A detailed study may contribute to enhance the spatial and temporal knowledge of calanchi which may be linked to local and global climate change processes and effects.

iii) The erosion potential as well as the denudation rate might be evaluated through shape variation and morphometric analysis at national scale. Furthermore, we have seen that vegetation is playing a key role in calanchi development. However, for example lichen communities present on calanchi deposits have only marginally been studied but may contribute

to soil stabilisation. Also, effects of specific tree species on pedogenesis and soil erosion remain still poorly studied.

iv) The Oltrepo Pavese calanchi were characterised from a morphometric point of view including also the geo-environmental predictors which induce rill-interrill and calanchi erosion. The rill-interrill and calanchi susceptibility maps were derived at regional scale for both type A and B calanchi, also highlighting the importance of land use management in the development of the above-mentioned soil erosion forms and features. However, the model might be better evaluated including a full pedological dataset, up to now not available with sufficient detail in the study area.

v) Calanchi should be investigated as micro-basins in order to understand if these landforms have a similar behaviour as fluvial systems.

vi) Calanchi areas and their connectivity to the main drainage system should be investigated through a detailed sediment transport and structural connectivity analysis. Badlands' connectivity was analysed by different authors. This thesis emphasizes the relationship between sediment dynamics and morpho-climatic conditions. Especially we point out the relation between sediment discharge dynamics and precipitation. However, a direct assessment of erosion thought the application of physical based models (e.g. Erosion 2D-3D Model) may be suitable to evaluate, plan and suggest specific land use practices in Mediterranean regions.

In conclusion this study highlights the importance of precipitation as well as the land use that may significantly contribute to the stabilisation or development of soil erosion forms and features in the study area. In an epoch deeply influenced by human actions, and in a context of local and global climate change, the importance of geo-environmental conditions that directly influence the development of calanchi and other soil erosion forms and features is highlighted. For these regions, accurate local and regional planning procedures, agricultural investments as

well as rural support strategies are significant means to control soil loss and desertification phenomena.

References

Alatorre, L.C. Beguería, S. 2009. Identification of eroded areas using remote sensing in a badlands landscape on marls in the central Spanish Pyrenees. Catena, 76, 182-190

Alexander, D.E. 1980. I Calanchi — accelerated erosion in Italy. Geography, 65, 95–100.

Alexander, D.E. 1982. Differences between "Calanchi" and "biancane" Calanchi in Italy. In: Bryan, R., Yair, A. (Eds.), Badland Geomorphology and Piping. Geo Books Norwich, 71–87.

Amici, F. 1898. I Calanchi. Riv. Geogr. It. V, Fasc. VII-VIII.

Aucelli, P.P.C., Conforti, M., Della Seta, m., Del Monte, M., D'uva. L., Rosskopf, C.M. Vergari, F. 2016. Multi-temporal digital photogrammetric analysis for quantitative assessment of soil erosion rates in the Ladola catchment of the upper Orcia valley (Tuscany, Italy). Land Degradation and Development, 27:1075-1092.

Battaglia, S., Leoni, L., Sartori, F. 2002. Mineralogical and grain size composition of clays developing Calanchi and biancane erosional landforms. Geomorphology 49, 153–170.

Battaglia, S., Leoni, L., Rapetti, F., Spagnolo M. 2011. Dynamic evolution of badlands in the Roglio basin (Tuscany, Italy). Catena, 86, 14-23.

Benito, G., Gutiérrez, M. and Sancho, C. 1992. Erosion rates in badlands areas of the Central Ebro Basin (NE-Spain). Catena, 19, 269-286.

Bianchini, S., Del Soldato, M., Solari, L., Nolesini, T., Pratesi, F., and Moretti, S. 2016. Badland susceptibility assessment in Volterra municipality (Tuscany, Italy) by means of GIS and statistical analysis. Environmental Earth Sciences, 75(10), 1–14.

Biondi, E., and Pesaresi, S. 2004. The badland vegetation of the northern-central Apennines (Italy). Fitosociologia, 41(1), 155-170.

Bollati, I., Della Seta, M., Pelfini, M., Del Monte, M., Fredi, P., Palmieri, E. L. 2012. Dendrochronological and geomorphological investigations to assess water erosion and mass wasting processes in the Apennines of Southern Tuscany (Italy). Catena, 90, 1-17.

Bombicci, 1881. L'Appennino Bolognese. Bologna, 1881.

Bordoni, M., Valentino, R., Meisina, C., Bittelli, M., Chersich, S. 2018. A Simplified Approach to Assess the Soil Saturation Degree and Stability of a Representative Slope Affected by Shallow Landslides in Oltrepò Pavese (Italy). Geosciences, 8, 472.

Brakensiek, D.L., H.B. Osborn, and W.J. Rawls. 1979. Field manual for research in agricultural hydrology. Agricultural Handbook No. 224, U.S. Department of Agriculture: Washington, DC.

Brandolini, P., Pepe, G., Capolongo, D., Cappadonia, C., Cevasco, A., Conoscenti, C., Marsico, A., Vergari, F., Del Monte, M. 2018. Hillslope degradation in representative Italian areas: just soil erosion risk or opportunity for development? Land Degrad. Dev., 29, 3050–3068.

Bruzzo, G. 1908. Nuove osservazioni sui calanchi del Bolognese. (Sesto congresso geografico). Venezia, 1908.

Bucciante, M. 1922. Sulla distribuzione geografica dei calanchi in Italia. L'Universo, 38, 585–605.

Buccolini, M., Gentili, B., Materazzi, M., Aringoli, D., Pambianchi, G., Piacentini, T. 2007. Human impact and slope dynamics evolutionary trends in the monoclinal relief of Adriatic area of central Italy. Catena, 71, 96–109.

Buccolini, M., and Coco, L. 2010. The role of the hillside in determining the morphometric characteristics of "Calanchi": The example of Adriatic central Italy. Geomorphology, 123, 200-210.

Buccolini, M., Coco, L., Cappadonia, C., Rotigliano, E. 2012. Relationship between a new slope morphometric index and calanchi erosion in northern Sicily, Italy. Geomorphology, 149-150, 41-48.

Buccolini, M., Coco, L., 2013. MSI (morphometric slope index) for analysing activation and evolution of Calanchi in Italy. Geomorphology, 191, 142-149.

Bryan, R., and Yair, A. (Eds.). 1982. Badland geomorphology and piping. Norwich: Geo Books.

Cantón, Y., Domingo, F., Solé-Benet, A., Puigdefábregas, J. 2001. Hydrological and erosion response of a Badlands system in semiarid SE Spain. Journal of Hydrology, 252, 65-84.

Cappadonia, C., Conoscenti, C., Rotigliano, E. 2011. Monitoring of erosion on two calanchi fronts – Northern Sicily (Italy). Landforms Analysis, 17, 21-25

Cappadonia, C., Coco, L., Buccolini, M., Rotigliano, E. 2016. From slope morphometry to morphogenetic processes: an integrated approach of field survey, geographic information system morphometric analysisis and statistics in italian Calanchi. Land Degrad. Develop., 27, 851-862.

Capolongo, D., Pennetta, L., Picarreta, M., Fallacara, G., Boenzi, F. 2008. Spatial and temporal variations in soil erosion and deposition due to land-levelling in a semi-arid area of Basilicata (Southern Italy). Earth Surface Processes and Landforms, 233, 364-379.

Caraballo-Arias, N.A., Conoscenti, C., Di Stefano, C., Ferro, V., 2014. Testing GIS-morphometric analysis of some Sicilian Calanchi. Catena, 113, 370-376.

Caraballo-Arias, N.A., Conoscenti, C., Di Stefano, C., Ferro, V. 2015. A new empirical model for estimating Calanchi Erosion in Sicily, Italy. Geomorphology, 231, 292-300.

Caraballo-Arias, N.A., Ferro, V., 2016. Assessing, measuring and modelling erosion in Calanchi areas: a review. Journal of Agricultural Engineering, XLVII 573, 181–190.

Caraballo-Arias, N. A., and Ferro, V. 2017. Are calanco landforms similar to river basins? Science of the Total Environment, 603-604, 244-255.

Caraballo-Arias, N.A. Di Stefano, C., Ferro, V. 2017. Morphological characterisation of calanchi (badland) hillslope connectivity. Land Degradation and Development, 29, 1190-1197.

Castaldi, F., and Chiocchini, U. 2012. Effect of land use changes on Badlands erosion in clayey drainage basin, Radicofani, Central Italy. Geomorphology, 169, 98-108.

Castaldini, D., Valdati, J., Ilies, D. C. Chiriac, C. 2005. Geo-tourist map of the natural reserve of Salse di Nirano (Modena Apennines, Northern Italy) Il Quaternario. Italian Journal of Quaternary Sciences, 18(1) 243-253.

Castiglioni, B. 1933. Osservazioni sui Calanchi appenninici. Estr. da: Boll. Della Soc. Geologica Ital. 52, 1933, fasc.2.

Ciccacci, S., Galiano, M., Roma, M.A., Salvatore, M.C. 2008. Morphological analysis and erosion rate evaluation in Badlands of Radicofani area (Southern Tuscany — Italy). Catena, 74, 87-97.

Ciccacci, S., Galiano, M., Roma, M.A., Salvatore, M.C. 2009. Morphodynamics and morphological changes of the last 50 years in a Badlands sample area of Southern Tuscany (Italy). Zeitschrift für Geomorphologie, 53(3), 273-297.

Clarke, M. L. and Rendell, H. M. 2006. Process-form relationship in Southern Italian Badlands: erosion rates and implications for landforms evolution. Earth Surface Processes and Landforms, 31, 15-29.

Cocco, S., Brecciaroli, G., Agnelli, A., Weindorf, D., Corti, G. 2015. Soil genesis and evolution on Calanchi (badland-like landform) of central Italy. Geomorphology, 248, 33-46.

Corona, C, Lopez Saez, J, Rovéra, G, Stoffel, M, Astrade, L, Berger, F. 2011. Corona, C, Lopez Saez, J, Rovéra, G, Stoffel, M, Astrade, L, Berger, F. 2011. High resolution, quantitative

reconstruction of erosion rates based on anatomical changes in exposed roots at Draix, Alpes de Haute-Provence—critical review of existing approaches and independent quality control of results. Geomorphology, 125, 433–444.

Della Seta, M., Del Monte, M., Fredi, P., Palmieri, E. L. 2009. Space-time variability of denudation rates at the catchment and hillslope scales on the Tyrrhenian side of Central Italy. Geomorphology, 107(3-4), 161-177.

De Ploey, J., Gabriels, D. 1980. Measuring soil loss and experimental studies. In Soil Erosion, Kirkby MJ, Morgan RPC (eds). Wiley: New York; 63–108

De Waele, J., Anfossi, G., Campo, B., Cavalieri, F., Chiarini, V., Emanuelli, V., Grechi, U., Nanni. P., and Savorelli F. 2012. Geomorphology of the Castel de' Britti area (Northern Apennines, Italy): an example of teaching geomorphological mapping in a traditional and practical way. Journal of Maps, 8 (3), 231-235.

Del Monte, M. 2017. The Typical Calanchi Landscape between the Tyrrhenian Sea and the Tiber River. © Springer International Publishing AG 2017 M. Soldati and M. Marchetti (eds.), Landscapes and Landforms of Italy, World Geomorphological Landscapes.

Di Stefano, C. and Ferro, V. 2019. Assessing sediment connectivity in dendritic and parallel calanchi systems. Catena, 172, 647-654.

D'Intino, J., Buccolini, M., Di Nardo, E., Esposito, G., Miccadei, E. 2002. Geomorphology of the Anversa delgi Abruzzi Badlands area (Central Apennines, Italy). Journal of Maps, 16 (2), 488-499

Dramis, F., Gentili, B., Coltorti, M., Cherubini, C. 1982. Osservazioni geomorfologiche sui calanchi marchigiani. Geografia fisica e Dinamica Quaternaria, 5, 38-45.

Farabegoli, E., and Agostini, C. 2000. Identification of calanco, a badland landform in the Northern Apennines, Italy. Earth Surf. Process. Landform, 25, 307-318.

Farifteh, J., Soeters, R. 2006. Origin of biancane and calanchi in East Aliano, southern Italy. Geomorphology, 77, 142-152.

Farabegoli, E., Agostini, C. 2000. Identification of calanco, a badland landform in the Northern Apennines, Italy. Earth Surf. Process. Landform, 25, 307-318.

Fauklner, H. 2008. Connectivity as a crucial determinant of badland morphology and evolution. Geomorphology, 100, 91-103.

Gallart, F., Solè, A., Puigdefàbregas, J., Lázaro, R. 2002. Calanchi System in the Mediterranean. -In: BULL, L.J. and M.J. Kirkby (eds): Dryland Rivers: hydrology and geomorphology of semi-arid channels. Chichester: John Wiley and Sons Ltd., 299-326.

Gallart, F., Marignani, M., Perez-Gallego N., Santi, E., Maccherini S. 2013. Thirty years of studies on badlands, from physical to vegetational approaches. A succinct review. Catena, 106 4-11.

García-Ruiz, J. M., Nadal-Romero, E., Lana-Renault, N., Beguerí, S. 2013. Erosion in Mediterranean landscapes: Changes and future challenges. Geomorphology, 198, 20-36.

Grubin, K. M. 2013. Clay mineralogy as a crucial factor in badland hillslope processes. Catena, 106, 54-67.

Grubin, K. M. Vergari, F., Troiani, F., Della Seta, M. 2018. The role of Lithology: Parent Material Control on badland Develompment. In Badland Dynamics in the Context of global Change, 61-109.

Krenz, J., Kuhn, NJ. 2018. Assessing badland sediment sources using unmanned aerial vehicles. In Badland Dynamics in the Context of Global Change, Nadal-Romero E, Martínez-Murillo JF, Kuhn NJ (eds). Elsevier: Amsterdam

Kropáček, J., Schillaci, C., Salvini, R. and Märker, M. 2016. Assessment of gully erosion in the Upper Awash, Central Ethiopian Highlands based on a comparison of archived aerial

photographs and very high resolution satellite images. Geografia Fisica e Dinamica Quaternaria, 39(2), 161-170.

Liberti, M., Simoniello, T., Carone, M.T., Coppola, R., D'Emilio, M., Macchiato, M. 2009. Mapping badland areas using LANDSAT TM/ETM satellite imagery and morphological data. Geomorphology, 106, 333-343.

Licciardello, F., Barbagallo, S., Gallart F. 2019. Hydrological and erosional response of a small catchment in Sicily. J. Hydrol. Hydromech., 67(3), 201–212.

Llena, M., Smith, M.W., Wheaton, J.M., Vericat, D. 2020. Geomorphic process signatures reshaping sub-humid Mediterranean Badlands: 2. Application to 5-year dataset. Earth Surface Processes and Landforms, 45(5), 0197-9337.

Loppi, S., Boscagli, A., De Dominicis. 2004. Ecology of Soil lichens from Pliocene clay badlands of central Italy in relation to geomorphology and vascular vegetation. Catena, 55, 1-15.

Maccherini, S., Marignani, M., Gioria, M., Renzi, M., Rocchini, D., Santi, E., Torri, D., Tundo, J., Honnay, O. 2011. Determinants of plant community composition of remnant biancane Badlands: a hierarchical approach to quantify species-environment relationships. Applied Vegetation Sciences, 14, 378–387.

Maerker, M., Bosino, A., Scopesi C., Giordani, P., Firpo, M., Rellini, I. 2020. Assessment of calanchi and rill-interrill erosion susceptibility in northern Liguria, Italy: A case study using a probabilistic modelling framework. Geoderma, 371, 114367

Maerker, M, Della Seta, M, Vergari, F, Del Monte, M. 2012. Process-based assessment of erosion dynamics in the Upper Orcia Valley (Southern Tuscany, Italy): a new semi-quantitative integrated approach. Rend Online Soc Geol It., 21:1208–1211.

Mazzanti, R., Rodolfi, G. 1988. Evoluzione del rilievo nei sedimenti argillosi e sabbiosi dei cicli neogenici e quaternari italiani. In: La Gestione delle Aree Franose, Edizioni delle Autonomie, pp. 13–60.

Meisina, C., Zizioli, D., Zucca, F. 2013. Comparison between different methods for shallow landslides susceptibility mapping: an example in Oltrepo Pavese (Northern Italy). N In book: Landslides Science and Practice. Volume 1: Landslide Inventory and Susceptibility and Hazard Zoning. Publisher: Springer, Editors: Margottini Claudio, Canuti Paolo, Sassa Kyoji.

Moretti, S., and Rodolfi, G. 2000. A typical "Calanchi" landscape on the Eastern Apennines margin (Atri, Central Italy): geomorphological features and evolution. Catena, 40, 217-228.

Nadal-Romero, E., Latron, J., Marti-Bono, C., Regüés, D. 2008. Temporal distribution of suspended sediment transport in a humid Mediterranean badland area: The Araguás catchment, Central Pyrenees. Geomorphology, 97 (3-4), 601,616.

Nadal-Romero, E., Petrlic, K., Verachterl, E., Bochet, E., and Poesen, J. 2014. Effects of slope angle and aspect on plant cover and species richness in a humid Mediterranean badland. Earth Surface Processes and Landforms, 39 (13), 1705-1716.

Phillips, C.P. 1998. The Badlands of Italy: a vanishing landscape? Applied Geography, 18, 3, 243–257.

Phillips, S.J., and Dudik, M. 2008. Modeling of species distributions with Maxent: new extensions and a comprehensive evaluation. Ecography, 31, 161-175.

Piccarreta M., Capolongo, D., Bentivenga, M., Pennetta, L. 2005. Influenza sulle precipitazioni e dei cicli umido-secco sulla morfogenesi calanchiva in un'area memi-arida della Basilicata (Italia meridionale). Geografia Fisica e Dinamica Quaternaria, 7, 281-289.

Piccarreta, M., Faulkner, H., Bentivenga, M., Capolongo, D. 2006. The influence of physico-chemical material properties on soil erosion processes in the Badlands of Basilicata, Southern Italy. Geomorphology, 81, 235-251.

Pulice, I., Di Leo., P, Robustelli, G., Scarciglia, F., Cavalcante, F., Belviso, C. 2013. Control of climate and local topography on dynamics evolution of Badlands from southern Italy (Calabria). Catena, 109, 83-95.

Pulice, I., Cappadonia, C., Scarciglia, F., Robustelli, G., Conoscenti, C., De Rose, R., Rotigliano, E., Agtnesi, V. 2012. Geomorphological and chemical-physical study of "calanchi" landforms in NW Sicily (southern Italy). Geomorphology, 153-154, 219-231.

Regüés, D. and Nadal-Romero, E. 2013. Uncertainty in the evaluation of sediment yield from badland areas: Suspended sediment transport estimated in the Araguás catchment (central Spanish Pyrenees). Catena, 106, 96-100.

Saez, J.L., Corona, C., Stoffel, M., Rovéra G., Astrade, L., Berger, F. 2011. Mapping of erosion rates in marly badlands based on a coupling of anatomical changes in exposed roots with slope maps derived from LiDAR data. Earth Surf. Process. Landforms, 36, 1162–1171.

SERVIZIO GEOLOGICO D'ITALIA. 2005. Carta Geologica d'Italia alla scala 1:50.000, Foglio 179 Ponte dell'Olio. Roma.

SERVIZIO GEOLOGICO D'ITALIA. 2010. Carta Geologica d'Italia alla scala 1:50.000, Foglio 178 Cabella Ligure. Roma.

SERVIZIO GEOLOGICO D'ITALIA. 2014. Carta Geologica d'Italia alla scala 1:50.000, Foglio 178 Voghera. Roma.

Sirvet, J. Desir, G. Gutierrez, M. Sancho, C. Benito, G. 1997. Erosion rate in badlands areas recorded by collectors, erosion pins and profilometer techniques (Ebro Basin, NE-Spain). Geomorphology, 18, 61-75.

Summa, V., Tateo, F., Medici, L., and Gianossi, M.L. 2007. The role of mineralogy, geochemistry and grain size in badland development in Pisticci (Basilicata, Southern Italy). Earth Surface Processes and Landforms, 32, 980-997.

Tarolli, P. 2014. High-resolution topography for understanding earth surface processes: opportunities and challenges. Geomorphology, 216: 295–312.

Torri, D., Santi, E., Marignani, M, Rossi, M., Borselli, L., Maccherini, S. 2013. The recurring cycles of biancana badlands: erosion, vegetation and human impact. Catena, 106, 22–30.

Tosi, M. 2007. Root tensile strength relationships and their slope stability implications of three shrub species in the Northern Apennines (Italy). Geomorphology, 87, 268-283.

Vergari, F., Della Seta, M., Del Monte, M., Barbieri, M. 2013. Badlands denudation "hot spots": The role of parental material properties on geomorphic processes in 20-years monitored sites of Southern Tuscany (Italy). Catena, 106, 31-41.

Vergari, F. 2015. Assessing soil erosion hazard in a key badland area of Central Italy. Nat Hazards, 79(S1), 71–95.

Vergari, F., Della Seta, M., Del Monte, M., Pieri, L., Ventura, F. 2015. Integrated Approach to the Evolution of Denudation Rates in an Experimental Catchment of the Northern Italian Apennines. G. Lollino et al. (eds), Engineering Geology for Society and Territory – Volume 1, Springer International Publishing Switzerland 2015.

Vergari, F., Troiani, F., Faulkner, H., Del Monte, M., Della Seta, M., Ciccacci, S., Fredi, P. 2019. The use of the slope-area function to analyse process domains in complex badland landscape. Earth Surface Processes and Landforms, 44,273-286.

Zizioli, D., Meisina, C., Valentino, R., Montrasio, L. 2013. Comparison between different approaches to modelling shallow landslide susceptibility: a case history in Oltrepo Pavese, Northern Italy. Nat. Hazards Earth Syst. Sci., 13, 559–573.

APPENDIX:

List of published and submitted manuscripts during the PhD career

2018

Bonì Roberta, **Bosino Alberto**, Meisina Claudia, Novellino Alessandro, Bateson Luke, McCormack Harry (2018). A Methodology to Detect and Characterize Uplift Phenomena in Urban Areas Using Sentinel-1 Data.

Remote Sensing, 2018, 10, 607

2019

Maerker Michael, Schillaci Calogero, Melis Rita T., Kropáček Jan, **Bosino Alberto**, Vilímek Vít, Hochschild Volker, Sommer Christian, Altamura Flavio, Mussi Margherita (2019). Geomorphological processes, forms and features in the surroundings of the Melka Kunture Palaeolithic site, Ethiopia.

Journal of Maps, 15(2), 797–806

2020

Bosino Alberto, Bernini Alice, Botha Greg A., Bonacina Greta, Pellegrini Luisa, Omran Adel, Hochschild Volker, Sommer Christian, and Maerker Michael (2020-accepted). Geomorphology of the upper Mkhomazi River basin, KwaZulu-Natal, South Africa with emphasis on late Pleistocene colluvial deposits.

Journal of Maps, https://doi.org/10.1080/17445647.2020.1790435

Bonacina Greta, Sanfilippo Alessio, Zana Simone, **Bosino Alberto**, Massara Elisabetta Previde, Viaggi Paolo, Sabato Luisa, Gallicchio Salvatore, Scotti Paolo (2020-accepted). Geochemical evidence for local variability in redox and depositional conditions in a deep-water Bonarelli equivalent section from southern tethys (Fontana Valloneto section, Southern Italy).

Ofioliti

Maeriaelena Cama, Calogero Schillaci, Jan Kropáček, Volker Hochschild, **Alberto Bosino** and Michael Maerker (2020). A probabilistic assessment of soil erosion susceptibility in a head catchment of the Jemma Basin, Ethiopian Highlands.

Geosciences, 10(7), 248

Maerker Michael, **Bosino Alberto**, Scopesi Claudia, Giordani Paolo, Firpo Marco, Rellini Ivano (2020). Assessment of calanchi and rill-interrill erosion susceptibility in northern Liguria, Italy: A case study using a probabilistic modelling framework.

Geoderma, 371, 114367

Cazzini Ferdinando Franco, Amadori Chiara, **Bosino Alberto**, Fantoni Roberto (2020). New seismic evidence of the Messinian paleomorphology beneath Lake Maggiore area (Italy).

Italian Journal of Geosciences, 139(2), 195-211

Ferdinando Franco Cazzini, **Alberto Bosino**, Giovanni Toscani, Roberto Fantoni (submitted). The back thrusts of the South Margin of the Western Southern Alps evaluated with seismic and wells data.

Schillaci C., Perego A., Valkama E., Maerker M., Sacco D., Saia S., Veronesi F., Lipani A., Lombardo L., Tadiello T., Gamper H., Tedone L., Moss C., Pareja-Serrano E., Amato G., Kuhl K., Damatirca C., Cogato A., Mzid N., Eeswaran R., Rebelo M., Spreandino G., **Alberto Bosino,** Bufalini M., Tucay T., Ding J., Fiorentini M., Tiscornia G., Conradt S., Acutis M (in prep). New pedotransfer approaches to predict soil bulk density using WoSIS soil data and 2 environmental covariates in Mediterranean agro-ecosystems.

ACKNOWLEDGEMENT

I want to thanks my parents and my wife who has supported me for all my career.

Thanks to Prof. Michael Maerker that guided me during these three years.

A sincere thanks also to all my colleagues of the University of Pavia, Tübingen, Darmstadt, Freiberg, Bydgoszcz, Genova and Milano.

Moreover, a heartfelt thanks to the Council for Geoscience (South Africa) for the unique collaboration.

Finally, I want to thank all scientist and persons which allowed me to arrive at this point.